Instituto de Biociências – Universidade de São Paulo

Caio Gueratto Coelho da Silva

Análise filogenética do gênero *Mischonyx* Bertkau, 1880, com mudanças taxonômicas e descrição de novas espécies (Opiliones: Gonylepitdae: Gonyleptinae)

Phylogenetic analysis of the genus *Mischonyx* Bertkau, 1880, with taxonomic changes and new species descriptions (Opiliones: Gonylepitdae: Gonyleptinae)

São Paulo

2020

Caio Gueratto Coelho da Silva

Análise filogenética do gênero *Mischonyx* Bertkau, 1880, com mudanças taxonômicas e descrição de novas espécies (Opiliones: Gonylepitdae: Gonyleptinae)

Phylogenetic analysis of the genus *Mischonyx* Bertkau, 1880, with taxonomic changes and new species descriptions (Opiliones: Gonylepitdae: Gonyleptinae)

Dissertação apresentada ao Instituto de Biociências da Universidade de São Paulo, para a obtenção de Título de Mestre em Ciências Biológicas, na Área de Zoologia.

Orientador(a): Prof. Dr. Ricardo Pinto-da-Rocha.

São Paulo

2020

Ficha Catalográfica

Gueratto, Caio
Análise filogenética do gênero Mischonyx Bertkau, 1880 e filogeografia de *Mischonyx squalidus* Bertkau, 1880 (Opiliones: Gonylepitdae: Gonyleptinae)
119 páginas

Dissertação (Mestrado) - Instituto de Biociências da Universidade de São Paulo. Departamento de Zoologia.

1. Opiliones 2. *Mischonyx* 3. Análise filogenética I. Universidade de São Paulo. Instituto de Biociências. Departamento de Zoologia.

Comissão Julgadora:

_____ _____

Prof(a). Dr(a). Prof(a). Dr(a).

_____

Prof. Dr. Ricardo Pinto da Rocha

Orientador

Agradecimentos

Gostaria de agradecer, em primeiro lugar, ao professor Ricardo Pinto-da-Rocha, meu orientador. Com seus conselhos e ajuda, sempre presente quando precisei, pensando não somente na minha produção acadêmica, mas também em minha sanidade mental, me auxiliou a levar este mestrado de uma maneira leve (na medida do possível).

Agradeço aos colegas do LAL, que me auxiliaram em minha formação como zoólogo e pessoa durante os 6 anos que estudei ali. Alípio, Jairo, Daniel, Daniel (estagiário), Juliana, Marília, Amanda, Avatar, França. Um agradecimento especial à Brittany, que pacientemente me auxiliou nas análises e nos meus conflitos internos. Outro agradecimento especial ao Jimmy, que opinou sobre este documento.

Deixo meus agradecimentos ao corpo técnico do departamento de Zoologia, em especial ao Manuel, pela sua paciência em ensinar as técnicas do Laboratório de Evolução Molecular (LEM) e a me ajudar sempre que precisei; à Bia e à Sabrina, também do LEM; ao Ênio e ao Phillip, sempre muito solícitos para operar o MEV; ao Mauro, sempre disposto à ajudar na coleção do Museu de Zoologia.

Também agradeço às pessoas que, nos bastidores, me ajudaram a tornar esses anos de mestrado mais leves. Aos meus pais, que sempre me incentivaram a cursar, estudar e trabalhar com que eu gostasse e hoje, por isso, me sinto realizado. À Ana Lara, sempre disposta a ajudar, me compreendendo, ouvindo minhas crises e sendo minha companheira durante uma boa parte deste trajeto e espero que por muitos anos mais. À galera (Vanessa, Lekão, Taly, Evelyn, Emily, Zé, Karine, Tonho, Luisão, Flora, Tamara, Rafa, Mauro e Hashi), pelas conversas infinitas nos bares. Às amigas da EMEF Dilermando (Carol, Claudia, Fátima, Liliane, Ivanise, Marina, Renata, e Samanta), por serem compreensivas quando eu pulava um bar para me dedicar ao mestrado e por ajudarem a segurar a onda nesses anos difíceis que passamos juntas. Sem vocês este mestrado não teria saído, de verdade!

Finalmente, agradeço à CAPES, por ter financiado os primeiros meses de meu mestrado.

Resumo

Bertkau descreveu o gênero *Mischonyx*, baseando-se em um indivíduo juvenil, em 1880. O holótipo está perdido, restando apenas a imagem e a descrição original. Kury, em 2003, considerou vários gêneros como sinônimos juniores de *Mischonyx* (e.g. *Ilhaia* e *Xundarava*). O gênero, até o presente trabalho, possuía 11 espécies, de acordo com trabalhos de revisão publicados anteiormente. No entanto, até o momento, não há nenhuma proposta filogenética para o gênero, afim de saber se ele seria válido ou não e se todas as espécies descritas como *Mischonyx* representam um agrupamento natural.

Os objetivos desta pesquisa foram propor uma hipótese filogenética para *Mischonyx*, baseado em análise de Evidência Total (TE) e propor mudanças taxonômicas embasadas na filogenia. Estudei 54 indivíduos, 15 de grupo externo e 39 de grupo interno, sequenciei sete marcadores (28S, 12S, 16S, COI, CAD, ITS e H3), totalizando 3742 bp. Levantei 124 caracteres morfológicos e de genitália. Analisei os dados sob dois critérios de otimalidade: Máxima verossimilhança (ML) e Máxima Parcimônia (MP).

A hipótese com mais embasamento biogeográfico e morfológico foi a de TE com ML. Descrevi três espécies novas: *Mischonyx minimus* **sp. nov.** (localidade-tipo: Petrópolis, Rio de Janeiro), *Mischonyx intervalensis* **sp. nov.** (localidade-tipo: Ribeirão Grande, São Paulo), e *Mischonyx petroleiros* **sp. nov.** (localidade-tipo: Nova Iguaçu, Rio de Janeiro). O gênero *Urodiabunus* é aqui considerado sinônimo júnior de *Mischonyx*. *Geraercormobius bresslaui* Roewer, 1927, *Geraecormobius clavifemur* Mello-Leitão, 1927 e *Geraecormobius reitzi* Vasconcelos, 2005 foram transferidos para *Mischonyx*. *M. cuspidatus* Roewer, 1913 é sinônimo júnior de *M. squalidus* Bertkau, 1880. Pelo relacionamento das hipóteses filogenéticas, *Gonyleptes antiquus* Mello-Leitão, 1934 (antigo *Mischonyx antiquus*) não pode ser considerado uma espécie pertencente ao gênero, portanto eu reestabeleci a composição original. *Mischonyx* tem uma composição nova de 17 espécies, 7 delas com novas combinações. Discuto acerca das transformações de caráteres ao longo da filogenia, sobre as diferentes hipóteses filogenéticas com diferentes *datasets* e a respeito da congruência dos clados com as hipóteses biogeográficas de áreas de endemismo na Mata Atlântica.

Abstract

Bertkau described *Mischonyx* genus based on a juvenile, in 1880. This holotype is lost, and we can analyze now only the original drawing and the description. Kury, in 2003, considered other genus junior synonyms of *Mischonyx* (e.g. *Ilhaia* and *Xundarava*). Due to revision publications, the genus contained 11 species. However, until this moment, none proposed a phylogenetic hypothesis for the genus to analyze whether it is valid or not and if all described species as *Mischonyx* represent a natural clade.

The objectives of this research are: to propose a phylogenetic hypothesis for *Mischonyx* based on Total Evidence (TE), to propose taxonomic changes based on the phylogeny and analyse the phylogenetic hypothesis biogeographically as well. I studied 54 individuals, 15 of external group and 39 of internal group. I sequenced seven genes (28S, 12S, 16S, COI, CAD, ITS e H3), totalizing 3742 bp. I raised 124 morphological and genitalic characters. I analysed the dataset under two optimality criteria: Maximum likelihood (ML) and Maximum parsimony (MP).

The hypothesis with better biogeographic and morphological background is the TE with ML. I described Three new species: *Mischonyx minimus* **sp. nov.** (type locality: Petrópolis, Rio de Janeiro), *Mischonyx intervalensis* **sp. nov.** (type locality: Ribeirão Grande, São Paulo) and *Mischonyx petroleiros* **sp. nov** (type locality: Nova Iguaçu, Rio de Janeiro). The genus *Urodiabunus* is junior synonym of *Mischonyx*. *Geraercormobius bresslaui* Roewer, 1927, *Geraecormobius clavifemur* Mello-Leitão, 1927 and *Geraecormobius reitzi* Vasconcelos, 2005 were transferred to *Mischonyx*. *M. cuspidatus* Roewer, 1913 is junior synonym of *M. squalidus* Bertkau, 1880. By the phylogenetic hypothesis of relationship, *Gonyleptes antiquus* Mello-Leitão, 1934 (former *Mischonyx antiquus*) cannot be considered a *Mischonyx* species, therefore I reestablish the original composition. The new composition for *Mischonyx* comprises 17 species, with 7 new combinations. I discuss the transformation of character states throughout the phylogeny, the different phylogenetic hypothesis using different datasets and the congruence of evidence between the clades in the phylogenetic hypothesis with the biogeographical hypothesis on Atlantic Forest areas of endemism.

Summary

General Introduction

Since the first molecular work applied to phylogenetics, this field has gained much more confidence, thanks to technological advances and to cheaper and more reliable methods arising (Wendel & Doyle, 1998). These advances help us to understand better the evolutionary relationships among clades in any taxonomic level, from the great three domains, published by Woese et al. (1990), to populational relationships within a species (Boyer et al., 2007).

First studies that applied molecules to infer phylogenetic relationships became reality in the end of the 1980's decade (Wheeler, 2012), 30 years after Hennig's works which built the term “Phylogenetics” (Hennig, 1965). First authors used typically one or two genes to infer the evolutionary relationships and applied some rudimentary analysis methods, as the Wagner (Farris, 1972) or the neighbor-joining methods (Saitou & Nei, 1987). As researchers improved techniques for sequencing and analyzing molecular data, phylogenetic trees with more genes and using more complex search algorithms arose (e.g. Li et al., 1990; Kim et al., 1990; Woese et al., 1990).

Afterwards, due to the raise of dynamic homology and total evidence analysis, scientists began using morphological and molecular data together to propose phylogenetic hypothesis. Page (1996), Wheeler (1998), Grant & Kluge (2005), Wheeler (2012) and other specialists in this field believe that combined data analysis create more complete datasets and, therefore, more powerful inferences regarding relationships among groups, besides more reliable hypothesis about their evolutionary history.

For Opiliones order, strictly molecular and Total Evidence phylogenetic inferences arrived later than for other clades. First total evidence hypothesis for the order came from Giribet et al. (1999) followed by Giribet et al. (2002). Although these publications used both molecular and morphological evidence, most phylogenetic works for harvestmen published in 2000's used whether molecular (Bragagnolo, 2015; Clouse et al., 2010; Giribet et al., 2010; Pinto-da-Rocha et al., 2014; Sharma & Giribet, 2009, 2011) or morphology (Bragagnolo & Pinto-da-Rocha, 2009; Da Silva & Gnaspini, 2010; Mendes, 2011; Da Silva & Pinto-da-Rocha, 2010; Pinto-da-Rocha & Bragagnolo, 2011) to support relationship hypothesis. Specifically for Gonyleptidae family, there are few phylogenetic hypothesis using molecular data (Bragagnolo, 2015; Peres et al., 2019; Pinto-da-Rocha et al., 2014) and they are restricted to subfamilies or less inclusive clades.

Despite the fact that molecular techniques arrived later for harvestmen than for other groups, their use changed significantly the view of Opiliones phylogeny, improving the evidence to some phylogenetic hypothesis previously proposed (e.g. Pinto-da-Rocha et al., 2014 supported many Gonyleptidae subfamilies, as Heteropachylinae, Sodreaninae, Caelopyginae) or creating new ones (e.g. Pinto-da-Rocha et al., 2014 evidenced that Gonyleptinae is not monophyletic; Sharma & Giribet, 2011 proposed two new harvestmen families).

Beyond the phylogenetic field, in the 1980's, very important authors (e.g. Avise et al., 1979a-b, Laerm et al., 1982, Avise et al., 1983) gathered information from population genetics, genetic demography, biogeography, ethology and paleontology to infer other evolutionary patterns using molecular data, in a field called Phylogeography. With this field, scientists could answer questions about estimating genetic structure within and among populations, divergence time among clades, haplotype networks related to the area in which populations are, genetic flow among populations, and many other ones (Avise, 2000).

Regarding specifically the Atlantic Rainforest, an important Neotropical biome which covers almost the entire eastern Brazilian coast, recent phylogeographic studies are elucidating its evolutionary history. Several works point out the evidence that there are some biotic disjunctions related to a latitudinal gradient (e.g. Doce and São Francisco Rivers, Todos os Santos Bay and south of São Paulo state) (Cabanne, Santos, & Miyaki, 2007; Calderón, D'Horta, & Miyaki, 2014; Carnaval et al., 2009; D'Horta et al., 2011) and these researchers agree with biogeographic studies, which uses morphological data (Cavarzere et al. 2014; DaSilva, Pinto-da-Rocha, & DeSouza, 2016; Silva et al., 2012). Besides this spatial congruence of evidence, the temporal evidence is not the same among different studies. Some authors show that Pleistocene climatic fluctuations may be responsible for the diversification of their studied groups (e.g. Brunes et al., 2010; Carnaval et al., 2009). On the other hand, other scientists point out to older events shaping the lineages diversification (e.g. Amaro et al., 2012; Thomé et al., 2014). Due to these differences, Cabanne et al. (2016) suggest that the evolutionary diversification of a specific group of study depends on its particular tolerance and behaviour. Therefore, to understand the whole evolutionary history of this biome, it is important to investigate a broad variety of biological groups (Peres et al., 2017).

Therefore, in this dissertation, I will use molecular and morphological data to propose total evidence phylogenetic hypothesis for *Mischonyx*'s species, a genus lacking relationship studies yet.

Phylogenetic relationships of the genus *Mischonyx* Bertkau, 1880, with taxonomic changes (Opiliones: Gonyleptidae).

Introduction

The order Opiliones Sundevall, 1833 comprises more than 6,600 valid species (Kury, 2019) and it represents one of the most ancient arachnid orders, with the first fossils dating from the Devonian (Dunlop, 2007). The main morphological synapomorphies for the group are: the stretching of the second pair of legs, which has mainly tactile and chemosensorial function; a typical trochanter - femur junction; paired tracheal stigmas present on the genital segment; and a pair of odoriferous glands in the cephalothorax (Schultz, 1990).

Four suborders hold all the extant harvestmen species: Cyphophthalmi Simon, 1879, with six families and 202 species; Eupnoi, Hansen & Sørensen, 1904, comprising five families and 1825 species; Dyspnoi, Hansen & Sørensen, 1904, with eight families and 377 species; and Laniatores Thorell, 1876, with 32 families and 4212 species (Kury, 2019). Therefore, the whole order has 51 families in total (Bragagnolo et al., 2015; Kury, 2003; Pinto-da-Rocha et al., 2014; Acosta, 2019). Besides them, there is the extinct suborder Tetraophthalmi, Garwood *et al.*, 2014.

Laniatores is the most diverse suborder within Opiliones and from its more than 3,900 species, at least 2,400 are from the Neotropical region (Kury, 2003). Taxonomists are trying to organize families and less inclusive groups based on the cladistics paradigm (e.g. Bragagnolo & Pinto-da-Rocha, 2009; Da Silva & Gnaspini, 2009; Pinto-da-Rocha, 2002; Pinto-da-Rocha & Bragagnolo, 2010), including recently molecular data to understand some clade's evolution (e.g. Bragagnolo et al., 2015; Pinto-da-Rocha et al., 2014). However, most families and genera within Laniatores lack evolutionary studies yet.

Even though researchers have done progress in phylogenetic systematics and taxonomy recently in Laniatores, there still is a strong influence of Carl F. Roewer's (1881- 1963) classification system. Roewer based his nomenclature and groupings on a few arbitrary characters. As a result, he created a lot of monotypic genera and placed close related species in distinct clades (Pinto-da-Rocha et al., 2012). Another issue of roewerian's classification system is supra-generic groupings not reflecting phylogenetic relationships. This happens because Roewer proposed these groups based on their

differences and not their similarities, rendering artificial groups (Pinto-da-Rocha, 2002).

Gonyleptidae Sundevall, 1833 is one of the families within Laniatores that had many monotypic genera and many artificial groups as well. According to Kury (1990), the literature for the family showed that there were many species cited only once and this fact pointed to the possibility of high degree of synonymies within Gonyleptidae. However, recently researchers studied many subfamilies of Gonyleptidae in the light of phylogenetic systematics and there are cladistics evidences to support these groups (Benedetti & Pinto-da-Rocha, 2019; Bragagnolo & Pinto-da-Rocha, 2012; Da Silva & Gnaspini, 2009; Da Silva & Pinto-da-Rocha, 2010; Pinto-da-Rocha & Bragagnolo, 2010). Besides that, with the use of molecular data in phylogenetic inference, Giribet et al. (2010), Pinto-da-Rocha et al. (2014) and Benedetti et al. (in prep.) proposed new relationships among most subfamilies of Gonyleptidae.

Although researchers studied many gonyleptid subfamilies, Gonyleptinae Sundevall, 1833, is one that needs more phylogenetic research, once its 39 genera (140 species in total) have uncertain phylogenetic relationships (Kury, 2003). Moreover, the diagnosis for this subfamily is based on the number of areas in the dorsal scutum and the absence of characteristics from other subfamilies (Pinto-da-Rocha et al., 2014). Thus, probably Gonyleptinae is polyphyletic and, to become monophyletic, some genera must be transferred to other clades.

Mischonyx background

Bertkau (1880) described *Mischonyx squalidus*. This species was the type of this new genus, by monotypy. In his work, he presented drawings from a sub-adult, evidenced by the incomplete tarsal segmentation, which is typical from harvestmen nymphs. The type species of the genus came from Copacabana, Rio de Janeiro. After Bertkau (1880), it remained monotypic until Kury (2003), which synonymized other genus within *Mischonyx*.

Roewer (1913) described the genus *Ilhaia*, type species being *Ilhaia cuspidata*, by monotypy, originally from Ilha Grande, Rio de Janeiro. In this same publication, he described the genus *Weyhia*, which had *Weyhia armata* as its type species, from Paranaguá, Paraná state. Afterwards, Roewer (1917) described *Weyhia parva*, from Santos, São Paulo. The same author, in 1923, referred to *Mischonyx squalidus* as a non-recognizable Gonyleptinae, because the described individual was an immature (Roewer,

1923).

Candido Firmino de Mello Leitão [1886—1948], an important arachnologist, described several species of interest in his career. In 1922, he described *Ilhaia fluminensis*, from Ilha do Pinheiro, Rio de Janeiro. In 1923, he considers *Ilhaia* as presenting two species and *Weyhia* composed by the type species and three other (*W. curvicornis*, *W. salebrosa* and *W. spinifrons*). In 1927, the same author described a new genus, type species *Xundarava holacantha*, originally from Niterói, Rio de Janeiro (Mello-Leitão, 1927). Beyond that, he described *Weyhia clavifemur* and *Ilhaia meridionalis*, from Blumenau, Santa Catarina, the first based on a male individual and the last based on a female. In 1931, he described the two genera: *Eduardoius*, for *E. fidelis* as the type species and *E. granulosus*, and monotypic *Geraecormobiella* (*G. convexa)*. In the same work, he described *Weyhia anomala*, a species that resembles the type species of *Weyhia*, according to the author. The same naturalist, in 1932 described a new monotypic genus, *Giltaya* (its species being *Giltaya solitaria*) and *Weyhia absconsa*. In 1934, he described *Gonyleptes antiquus* and *Ilhaia intermedia*, both from Minas Gerais state. In 1935, he described *Arleius incisus*, as the first species of this genus. He states in this work that *A. incisus* could be a synonym of *Mischonyx squalidus*. However, as he could not analyze precisely that last species, he preferred to leave *A. incisus* as a separated species. In 1936, Mello-Leitão described *Xundarava anomala* and a new monotypic genus, that contained *Ziltaia nigrifemur*. In 1940, he described *Geraecormobius cheloides* among other species from this genus and recognized *Weyhia* as a synonym of *Geraecormobius*.

After Mello-Leitão, B. Soares (1943) synonymized *Ilhaia* with *Eduardoius* and *I. fluminensis* with *I. cuspidata.* In 1944, the same author synonymized *Eduardoius granulosus* with *Ilhaia cuspidata* and *Penygorna infuscata* with *Ilhaia intermedia*. As *P. infuscata* was the type species of the genus, it became junior synonym of *Ilhaia*. Soares (1945) synonymized *Geraecormobiella* with *Geraecormobius* and transferred *G. antiquus* to *Paragonyleptes*, remaining the new combination *P. antiquus*. Soares & Soares (1946) added *Arleius* and *Ziltaia* to *Ilhaia* synonyms list and, in 1947, the same authors described *Ilhaia sulina*. Soares & Soares (1970) described *Ilhaia processigera* and state that *E. lutecens* is synonym of *I. cuspidata*. Helia Soares (1972) described *Ilhaia insulana*, which she believed to be related to *I. cuspidata*. Soares & Soares (1987) published several Gonyleptidae synonymic remarks. They considered *G. cheloides* as junior synonym of *G. convexus*, *A. incisus* and *Cryptomeloleptes spinosus* as synonyms of *Ilhaia parva* and

Xundrava a synonym of *Ilhaia*.

Kury (2003), in his "Annotated Catalogue of the Laniatores of the New World" synonymized *Ilhaia* and *Giltaya* with the almost forgotten genus *Mischonyx.* Besides that, he transferred *P. antiquus* to *Mischonyx*. Apparently, *Mischonyx squalidus* holotype is lost and the author based his conclusions on Roewer's drawings and description.

Finally, in Vasconcelos (2004, 2005) the two last *Mischonyx* species were described: *Mischonyx kaisara*, from the coast of São Paulo state, and *Mischonyx poeta*, from the north of Rio de Janeiro state. Besides these two publications, Vasconcelos has an unpublished dissertation regarding *Mischonyx* taxonomy (Vasconcelos, 2003).

The last published research containing taxonomical remarks regarding the genus, Pinto-da-rocha *et al.* (2012) considered 11 valid species within *Mischonyx*: *M. anomalus* (Mello-Leitão, 1936); *M. antiquus* (Mello-Leitão, 1934); *M. cuspidatus* (Roewer, 1913); *M. fidelis* (Mello-Leitão, 1931); *M. insulanus* (Soares, 1972); *M. intermedius* (Mello-Leitão, 1935); *M. kaisara* Vasconcelos, 2004; *M. poeta* Vasconcelos, 2005; *M. processigerus* (Soares & Soares, 1970); *M. squalidus* Bertkau, 1880 and *M. sulinus* (Soares & Soares, 1947).

Beyond the taxonomic part, *Mischonyx cuspidatus* is one of the most studied harvestmen species regarding its biology. There are publications regarding its odoriferous glands chemical composition (Rocha et al., 2013), defensive behavior (Dias & Willermart, 2013; Dias et al., 2014; Willemart & Pellegatti-Franco, 2003), odor sensitivity (Dias, 2017) and synanthropic behaviour (Mestre & Pinto-da-Rocha, 2004). As it is possible to see from the historical background, although there was a lot of discussion about *Mischonyx* taxonomy, there is no phylogenetic hypothesis for this genus until the present.

Objectives

The main goal of this work is to propose a phylogenetic hypothesis for *Mischonyx*, based on a Total Evidence approach, using seven genes and morphological characters, from external morphology and genitalia. Besides that, this work intends to propose taxonomical changes and biogeographical remarks for the genus based on the phylogenetic hypothesis created.

Material and Methods

Type and analyzed ingroup specimens

The analyzed types are in the table 01. To choose these type specimens, I analyzed at least one specimen from each *Mischonyx* species present in Kury (2003). Moreover, some specimens were selected according to previews pictures that we have of type harvestmen species in our databank at USP Arachnology Lab (LAL-USP).

With these specimens in hand, I looked through the tissue collection present at LAL-USP to compare the specimens at our collection with the types and determine them correctly. I analyzed them through a stereomicroscope (Zeiss Stemi DV4). Afterwards, as there were some species lacking individuals in LAL's collection, I did collection expeditions to have material to extract DNA from as much species as possible. Individuals that resembled *Mischonyx* species and did not match with any the existing species were included in the analysis. The ingroup for this work is presented in Table 02, with their register number of the tissue collection.

Outgroup selection

All outgroup species are Gonyleptidae. I chose species from different gonyleptid subfamilies to have a broader representativeness of this family. Species from Caelopyginae Sørensen, 1884, Gonyleptinae, Hernandariinae Sørensen, 1884, Mitobatinae Simon, 1879, Pachylinae Sørensen, 1884, Progonyleptoidellinae Soares & Soares, 1985, Sodreaninae Soares & Soares, 1985 are included as outgroup. I have chosen at most two species of each subfamily in order to reduce the total possibilities of the number of trees. This strategy reduces the computational demand, as I used dynamic homology search algorithms. All information regarding the specimens used as outgroup is present in Table 02, along with ingroup information.

Molecular data acquirement

All specimens which had their tissues extracted are in the tissues collection of LAL-USP. We keep all the collected specimens in 92-98% ethanol and at -20°C. Some specimens from target species had their DNA extracted for other works and have already had some target genes sequenced, so I used these data in my analysis. For those species

which did not have the DNA extracted, I extracted muscular tissue from the coxa IV of individuals (Pinto-da-Rocha, 2014). Alternatively, when the individual was small, I used tissues from chelicerae and pedipalps. I used the kit Agencourt® DNAdvance System (Beckman Coulter, California, EUA) for extractions and modified the protocols according to Pinto-da-Rocha *et al*. (2014).

From the extracted DNA, I amplified seven molecular *loci*: the ribosomal nuclear gene 28S; the ribosomal mitochondrial genes 12S and 16S; the nuclear Internal Transcribed Spacer subunit II (ITS2), carbamoylphosphate synthetase 2 (CAD) and the coding histone H3 gene (H3); and the mitochondrial Cytochrome Oxidase subunit I coding gene (COI). For polymerase chain reactions (PCRs), I used Thermo-fisher Taq kit, following the concentration present in Pinto-da-Rocha (2014).

The primers used to amplify the genes were:

- 28S: sobreposition of two primer sets: 28SRDIAF – 28SRD4B (Arango & Wheeler, 2007 and Edgecombe & Giribet, 2006, respectively) and 28SD3AP – 28SB (Reyda & Olson, 2003 and De Ley *et al.*, 1999, respectively);

- 16S: 16SpotFN – 16SBR (Pinto-da-Rocha et al., 2014 and Palumbi, 1996, respectively);

- 12S: 12SAIN – 12SOP2RN (Pinto-da-Rocha *et al.*, 2014);

- COI: dgLCO1490 – dgHCO2198 (Meyer 2003). Alternatively, LCO1490 – HCO2198 (Folmer *et al.*, 1994) and LCO1490 – HCOout (Folmer *et al.*, 1994 and Prendini *et al.*, 2005, respectively);

- H3: H3AF – H3AR (Colgan *et al.*, 1998). Alternatively, H3AF_edit (5'-GCVMGVAAGTCYACVGGMGG-3') – H3AR_edit (5'-ATGGTSACTCTCTTGGCGTGR-3'), made at the Molecular Systematics Laboratory of IBUSP;

- ITS: 5.8SF – CAS28Sb1d (Ji *et al.*, 2003);

- CAD: op_cad_F1 – op_cad_R1 (Peres *et al.*, 2018).

I conducted PCR reactions in an Eppendorf Mastercycler® gradient thermal cycler and the cycles and temperature used in this work are the same present in Pinto-da-Rocha (2014).

Afterwards, I inspected the PCR products using agarose gel electrophoresis (2% agarose), purified the products using Agencourt Ampure XP (Beckman Coulter) and

quantified the products using a Thermo Scientific NanoDrop spectrophotometer. In order to prepare the products for sequencing, I used the BigDye® Terminator v3.1 Cycle Sequencing Kit (Applied Biosystems). The precipitation was with sodium acetate and the sequencing process was in an ABI PRISM® 3100 Genetic Analyser/HITACHI (Applied Biosystems).

Following to that, I assembled the contiguous sequences using Consed/PhredPhrap package (Ewing & Green, 1998; Ewing *et al.*, 1998; Gordon *et al.*, 1998, 2001). After assembling, I queried the contigs against the online NCBI BLAST database to check for contamination from other external sources. I aligned the sequences using MS AFFT (Katoh *et al.*, 2002), visualized, and edited the results in Aliview (Larson, 2014). After aligning, I searched for stop codons in the coding genes (COI, CAD and H3) in Aliview. I trimmed the coding genes sequences to match the first base of the sequences with the first codon position.

Morphological data acquisition, terminology and new species drawings

I analyzed all the type material in table 01 and matched with individuals present in the tissue collection from LAL-USP and in the Arachnology collection from MZSP. I obtained the external morphological characters analyzing both the type material and other individuals from the species under a Zeiss Stemi DV4 stereomicroscope. I used Scanning Electron Microscopy (SEM) to obtain males' genitalia characters. I followed Pinto-da-Rocha (1997) to dissect and prepare the genitalia for SEM. The Scanning Electron Microscope used was a Zeiss DSM940, from Instituto de Biociências, Universidade de São Paulo. Scale bars and in micrometers.

I used Mesquite 3.51 (Maddison & Maddison, 2011) to build the character matrix and I codified the characters treating them preferentially as binary, in order to avoid the redundancy and to assure the principle of characters independence (Strong & Lipscomb, 1999). Nonetheless, to avoid building non-comparable characters, in some cases, I used multistate characters and I treated them as unordered. The character description follows Sereno (2007). The complete character matrix is available online, at MorphoBank (http://morphobank.org/permalink/?P3599 – for reviers, the password is Squalidus).

The terminology used follows DaSilva & Gnaspini (2010). Granules refers to minute elevations, concentrated in a particular region or article. Tubercles are elevations which are clearly distinguishable from granules by its height and width and can present

blunt or acuminated apex. Spines are those acuminated elevations present on the ocularium. Apophyses are those armatures present on coxa IV, free tergites, anterior and posterior margins and can present several shapes. The terminology for dorsal scutum shapes follows Kury & Medrano (2016). The terminology for penis macrosetae follows Kury & Villareal (2015).

To make the new species drawings, I used a stereomicroscope with *camara lucida.* Afterwards, I digitalized them and used Adobe Photoshop Lightroom 6.0® to remove background inconsistencies. All the scale bars in the drawings are in millimeters.

Phylogenetic inferences

To analyze the dataset, I ran three analysis: using morphological data only, using molecular data only and using combined evidence (Total Evidence Analysis). For all of them, I used two optimality criteria: Maximum parsimony (MP) and maximum likelihood (ML).

Maximum likelihood. For morphological analysis (ML1), I inserted the dataset as input in IQ-TREE, using the best model found by the program, which uses BIC to analyse which model is the best for that specific dataset. The analysis displayed by the program is the same described for the molecular data below. To analyse characters change, I inserted the phylogeny output from iqtree on Winclada 1.61 (Nixon, 2002).

For molecular (ML2) and TE (ML3) analysis, I aligned the sequences on MS MAFFT and analyzed them on Aliview. I built a FASTA file with all the sequences concatenated using SequenceMatrix 1.8 (Vaidya *et al.*, 2011). I ran the analysis on IQ-TREE version 1.6.10 (Nguyen *et. al.*, 2015). All the partitions coming from the seven different genes present in the concatenated FASTA file (and the morphological dataset for TE) were first analyzed on IQ-TREE through the partition model (Chernomor *et al.*, 2016), using the "-spp" command. The program selected the best substitution model for each partition under the BIC (*Bayesian information crtiterion*) (Schwarz, 1978), using the program ModelFinder (Kalyaanamoorthy *et al.*, 2017), through the command "-m TESTNEWMS ERGE". I ran the likelihood analysis with 10000 search iterations, through the command "-s -n 10000". Afterwards, the program ran a bootstrap analysis as a support measure for the nodes. Through the command "-bb 1000", the program ran 1000 iterations of ultrafast bootstrap (Minh *et al.*, 2013). Finally, I analyzed the output using

FigTree 1.4.4 (Rambaut, 2010) and the character changes through the phylogeny using parsimony on Winclada 1.61. I used a parsimony method to analyse character change because, as pointed by Cheng & Kuntner (2014), the aim is to "understand the evolutionary changes of characters rather than the probability of particular ancestral states on the phylogeny".

Maximum parsimony. I carried out the analysis using morphological characters only (MP1) on TNT (Goloboff *et al.*, 2008), through the heuristic search, with the TBR algorithm, making 10000 replicates and retaining 100 trees per replicate. I used the command "collapse branches after search" to eliminate non-supported nodes. The program also did searches using Ratchet (Nixon, 1999) and Tree Fusing (Goloboff, 1999). The characters were treated as unordered and unweighted. To analyse character change throughout the phylogeny, I used Winclada 1.61.

The molecular only (MP2) and TE (MP3) analysis were implemented using the program POY 5.1.1 (Varón *et al.*, 2010), which did the searches for most parsimonious trees using direct optimization (hereafter DO) of unaligned sequences (Wheeler, 1996). This search strategy is also referred as Dynamic Homology (Wheeler 2001 a,b). This strategy differs from traditional static homology search because the former integrates both alignment and tree searches, while the last treats them as two separated searches. DO is able to insert in a static matrix the tests of possible homology hypothesis for unaligned nucleotides dynamically, optimizing these sequences directly on the available trees and, concomitantly, converts of the transformation series of pre-aligned sequences (Kluge & Grant, 2006; Grant & Kluge, 2009; Sánchez-Pacheco et al., 2017).

At first, I ran DO analysis for five searches, specifying search time (from two hour to ten hours, totalizing 30 hours search). This was an exploratory search and allowed me to check which one of these five search times presented the lowest tree scores as outputs and, consequently, the optimal search time for DO ("max_time" parameter). The best tree scores for my dataset was with maximum search time of 2 hours. After this initial search, I submitted the dataset to the analysis, treating H3, COI and CAD sequences as pre-aligned and 28S, 12S, 16S and ITS to be aligned using dynamic homology methods ("transform" command in POY). I treated morphological characters as unordered and transformations as equally weighted. The program performed five rounds of searches using the "max_time" (with "search" command). In POY each "search" round

implements Tree Bisection and Reconnection (TBR), Wagner tree building, Subtree Pruning and Regrafting (SPR), Branch Swapping (RAS+swapping, as in Goloboff, 1999), Tree fusing (Goloboff, 1999) and Parsimony Ratchet (Nixon, 1999). I used the final trees from this previous analysis in an exact iterative pass (IP) analysis (Wheeler, 2003a). Costs for all the previous optimal trees were calculated and POY generated the implied alignment of this final analysis (Wheeler, 2003b). Finally, I used TNT 1.5 (Goloboff & Catalano, 2016) to calculate Bootstrap, with "hold" command of 10000000 trees, "mult" command of 1000 replicates, holding 10 trees per replicate.

Species distribution

To analyze the records of geographical distribution of the *Mischonyx* species, I inserted the geographical coordinates of individuals from different locations of all the species available at Museu de Zoologia da Universidade de São Paulo (MZSP) and from LAL tissue collection into a spreadsheet and used DIVA-GIS to plot the localities on the map. I analyzed the type localities and records present in Kury (2003) as well. The only published works in which there are information regarding the distribution of *Mischonyx* species are Kury (2003) and Pinto-da-Rocha *et al.* (2012). Both present the distribution of the species because they are taxonomic researches of broader groups. However, none of them presented a distribution map of species.

Results

Molecular data

In total, I have sequenced 54 individuals, including ingroup and outgroup. I could not obtain fresh tissue two species, namely, *Urodiabunus arlei* and *Mischonyx holacanthus*. The fragments sequenced have the following lengths: 28S has 972 bp, 16S has 386 bp, 12S has 408 bp, CAD has 639 bp, COI has 570 bp, H3 has 309 bp and ITS has 456 bp, totalizing 3742 bp for all the sequences. From all the 54 individuals, I could sequence 88% of all the fragments. I included in the analysis terminals that had at least five of the seven fragments sequenced. The information regarding sequenced genes per taxon is in Table 02.

Morphological data

For morphological data, I coded 124 characters. The ones taken from literature are properly acknowledge. I included 45 characters from dorsal scutum, 44 characters from appendages, 6 characters from free tergites, 27 characters from male genitalia and two characters from general aspect.

List of Morphological Characters and States

1. Dorsal scutum, shape (males)
    0 Gamma P
    1 Gamma R
    2 Gamma
    3 Gamma T
    4 Non-Gamma

2. Dorsal scutum, shape (females)
    0 Alfa
    1 Gamma
    2 Gamma T
    3 Gamma P
    4 Non-Gamma

3. Coda (males)
    0 Conspicuous
    1 Hardly seeing or totally absent

4. Coda (females)
    0 Conspicuous
    1 Hardly seeing or totally absent

5. Coda in comparison to mid-bulge (males), separation
    0 Clearly separated
    1 Not separated

6. Pedipalp, length

0 Short (shorter than the dorsal scutum)

1 Long (longer than the dorsal scutum)

7. Pedipalp, tibia and tarsus, expansion

0 Same thickness of femur

1 Clearly more expanded than femur

8. Dorsal scutum, anterior margin, lateral tubercles, number

0 3 in each lateral

1 2 in each lateral

2 4 or more in each lateral

3 Absent

9. Dorsal scutum, anterior margin, lateral tubercles, size

0 All with the same size

1 One of the tubercles clearly more developed than the others

2 Absence

10. Dorsal scutum, frontal hump, elevation

0 Low

1 Elevated (Figs. 15 — 23)

11. Dorsal scutum, frontal hump, tubercles

0 Absent

1 Present

12. Dorsal scutum, frontal hump, tubercles, number

0 0 (Absence)

1 1 (single armature)

2 2 (one pair) (Fig. 19C)

3 4 (2 pairs)

13. Dorsal scutum, number of areas

0 3

1 4

14. Dorsal scutum, ocularium, median armature, number

0 1

1 2 (one pair) (Figs. 15 — 23)

2 3 pairs

3 Absent

15. Dorsal scutum, ocularium, median armature, size

0 Tubercle (smaller than the ocularium height) (Fig. 15D)

1 Spine (longer than the ocularium height) (Fig. 19C)

2 Absence

16. Dorsal scutum, ocularium, median armature, merge

0 Not merged (Figs. 15— 23)

1 Apex merged

17. Dorsal scutum, ocularium, anterior armature

0 Absent (Fig. 17D)

1 Present (Fig. 15C)

18. Dorsal scutum, ocularium, posterior armature

0 Absent (Fig. 17C)

1 Present (Fig. 18C)

19. Dorsal scutum, prosoma, lateral tubercles

0 Absent

1 Present (Fig. 12A)

20. Dorsal scutum, prosoma, posterior armature

0 Absent

1 Present (1 pair of tubercles) (Figs. 15 — 23)

2 Several tubercles

21. Dorsal scutum, mid-bulge, lateral margin, armature

0 Absent

1 Present in the whole extension (Fig. 17A)

2 Present on the posterior half only (Fig. 18B)

22. Dorsal scutum, mid-bulge, lateral margin, armature, size

0 Large tubercles (Fig. 22A)

1 Small tubercles (Fig. 16D)

2 Absence of armature

23. Dorsal scutum, mid-bulge, lateral margin, armature, shape

0 Rounded (Figs. 15 — 23)

1 Pointed

2 Absence of armature

24. Dorsal scutum, mid-bulge, lateral margin, armature, color (in ethanol)

0 Clearer than the rest of the body (Fig. 22A)

1 Darker than the rest of the body (Fig. 23A)

2 Same color of the rest of the body (Fig. 15B)

25. Dorsal scutum, mid-bulge, lateral margin, posterior armature, merge

0 Merged, forming large tubercles (Fig. 16A)

1 Not merged (Fig. 17A)

2 Absence of armature

26. Dorsal scutum, area I, longitudinal groove

0 Absent

1 Present

27. Dorsal scutum, area I, paired median armature

0 Absent

1 Present

28. Dorsal scutum, area I, paired median armature, size

0 Small tubercles (Fig. 17A)

1 Conspicuous tubercles (Fig. 15B)

29. Dorsal scutum, area I, paired median armature, color (in ethanol)

0 Clearer than the rest of the body (Fig. 15B)

1 Darker than the rest of the body (Fig. 15A)

2 Same color of the rest of the body

30. Dorsal scutum, area I, paired median armature, length in comparison median armatures of other dorsal scutum areas

0 Larger than the median armatures from other areas (Fig. 15B)

1 Smaller than the median armatures from other areas (Fig. 15A)

2 Same size of the median armatures from other areas

31. Dorsal scutum, area II, paired median armature

0 Absent

1 Present

32. Dorsal scutum, area II, other armatures

0 Absent (Fig. 21B)

1 Present (Fig. 18A)

33. Dorsal scutum, area II, paired median armature, color (in ethanol)

0 Lighter than the rest of the body (Fig. 20A)

1 Darker than the rest of the body (Fig. 19A)

2 Same color of the rest of the body

34. Dorsal scutum, area II, paired median armature, size in comparison median armatures of other dorsal scutum areas

0 Larger than the median armatures from other areas (Fig. 20A)

1 Smaller than the median armatures from other areas (Fig. 19A)

2 Same size of the median armatures from other areas

35. Dorsal scutum, area III, armature

0 Absent

1 Present

36. Dorsal scutum, area III, median armature, number

0 pair

1 single

37. Dorsal scutum, area III, paired median armature, color (in ethanol)

0 Lighter than the rest of the body (Fig. 21A)

1 Darker than the rest of the body (Fig. 20B)

2 Same color of the rest of the body

38. Dorsal scutum, area III, paired median armature, size

0 Tubercles (Fig. 20B)

1 Apophysis (Fig. 15D)

39. Dorsal scutum, area III, paired median armature, form

0 Rounded

1 Elliptic (Fig. 20B)

2 Strongly compressed laterally (Fig. 16A)

3 Sharp (Fig. 15D)

40. Dorsal scutum, area III, other armature

0 Absent

1 Present (Fig. 16A)

41. Dorsal scutum, area III, other armature, size

0 Small tubercles (Fig. 18A)

1 Well-developed tubercles (Fig. 16A)

42. Dorsal scutum, area III, other armature, color (in ethanol)

0 Clearer than the rest of the body (Fig. 21B)

1 Darker than the rest of the body (Fig. 16A)

2 Same color of the rest of the body (Fig. 15B)

43. Dorsal scutum, area III, other armature, form

0 Rounded (Fig. 18A)

1 Ellipse (Fig. 20B)

2 Strongly compressed laterally (Fig. 16A)

44. Dorsal scutum, posterior margin, armature

0 Absent

1 Present

45. Dorsal scutum, posterior margin, armature, size

0 Small tubercles (Fig. 15A)

1 Presence of central apophysis

2 Presence of central tubercle more developed than the others (Fig. 22C)

3 All tubercles well-developed

46. Dorsal scutum, granulation, density (DaSilva & Pinto-da-Rocha, 2010)

0 Low (scattered granules, some regions of dorsal scute smooth)

1 Median (granules scattered throughout dorsal scute)

2 High

47. Dorsal scutum, region of maximum width

0 Area II

1 Posterior to Area II

48. Free tergite I, armature

0 Absente

1 Present

49. Free tergite I, armature, size

0 Small tubercles (Fig. 15A)

1 Presence of central apophysis (Fig. 22C)

2 Presence of central tubercle more developed than the others

3 All tubercles well-developed

50. Free tergite II, armature

0 Absent

1 Present

51. Free tergite II, armature, size

0 Small tubercles (Fig. 15A)

1 Presence of central apophysis (Fig. 21B)

2 Presence of central tubercle more developed than the others (Fig. 19D)

3 All tubercles well-developed

52. Free tergite III, armature

0 Absent

1 Present

53. Free tergite III, armature, size

0 Small tubercles (Fig. 15A)

1 Presence of central apophysis (Fig. 21B)

2 Presence of central tubercle more developed than the others (Fig. 19A)

3 All tubercles well-developed

54. Leg II, basitarsus, segmentation, number

0 6

1 7

2 8

3 9

4 11 or more

55. Leg III, trochanter, armature

0 Absence of armature

1 Trochanter with many tubercles

2 Prolateral basal apophysis

56. Leg IV, coxa, apical width of males in ventral view (compared to coxa III)

0 Coxa III and IV with the same width

1 Coxa IV 2 times larger than coxa III

2 Coxa IV 4 times larger than coxa III

57. Leg IV, coxa, apical prolateral apophysis

0 Absent

1 Present

58. Leg IV, coxa, apical prolateral apophysis, length (compared to trochanter IV)

0 Shorter than trochanter IV (Fig. 18B)

1 Similar size of trochanter IV (Fig. 18A)

2 Longer than trochanter IV

3 Tubercle

59. Leg IV, coxa, apical prolateral apophysis, basal tubercle

0 Absent

1 Present (Fig. 17A)

60. Leg IV, coxa, apical prolateral apophysis, secondary subdistal lobe

0 Absent

1 Present (Fig. 19A)

61. Leg IV, coxa, apical prolateral apophysis, direction in dorsal view

0 Slightly inclined relative to the axis of the base of coxa IV (Fig. 19A)

1 Transversal

2 Oblique (Fig. 18B)

62. Leg IV, coxa, apical prolateral apophysis, apex width

0 Base more than 4 times larger than the apex (Fig. 17A)

1 Base 2 times larger than the apex (Fig. 22C)

2 Base as large as the apex

63. Leg IV, coxa, apical prolateral apophysis, thickness

0 Robust (Fig. 20B)

1 Sharp (Fig. 20A)

2 Tubercle only

64. Leg IV, coxa, apical prolateral apophysis in females

0 Absent

1 Smaller than the male

2 Similar to the male

65. Leg IV, coxa, apical retrolateral apophysis

0 Absent

1 Present (Fig. 22B)

66. Leg IV, coxa, apical retrolateral apophysis, size

0 Tubercle

1 Apophysis

67. Leg IV, coxa, apical retrolateral apophysis, ramifications

0 1

1 2

68. Leg IV, trochanter, length

0 Short

1 Long

69. Leg IV, trochanter, prolateral armature

0 Absent

1 Present

70. Leg IV, trochanter, retrolateral apical armature

0 Absent

1 Tubercle

2 Apophysis (Fig. 15B)

71. Leg IV, trochanter, retrolateral armature, number

0 Absent

1 One (Fig. 22A)

2 Two (Fig. 17B)

3 Three or more (forming a line)

72. Leg IV, femur, thickness

0 Short and robust (Fig. 20B)

1 Long and thin (Fig. 18B)

73. Leg IV, femur, prolateral curvature

0 Straight (not curved) (Fig. 18B)

1 Curved (Fig. 21B)

74. Leg IV, femur, retrolateral basal apophysis

0 Absent

1 Present (Fig. 17C)

75. Leg IV, femur, dorso-basal apophysis (DBA)

0 Absent

1 Present (Fig. 17C)

76. Leg IV, femur, dorso-basal apophysis, size

0 Small (Fig. 22D)

1 large (longer than larger) (Fig. 17C)

2 Tubercle (Fig. 15D)

3 Absent

77. Leg IV, femur, dorso-basal apophysis, number of ramifications

0 1 (Fig. 15C)

1 2 (Fig. 22C)

2 Absence of armature

78. Leg IV, femur, dorso-basal apophysis, apex direction

0 Apex anteriorly directed (Fig. 22C)

1 Apex dorsally directed (Fig. 20D)

2 Apex retrolaterally directed (Fig. 21B)

3 Apex prolaterally directed

4 Absence of armature

79. Leg IV, femur, dorso-basal apophysis, apex width

0 Base more than 4 times wider than apex (Fig. 17C)

1 Base 2 times wider than apex (Fig. 22C)

2 Base as wide as apex (Fig. 22D)

80. Leg IV, femur, dorso-basal apophysis, shape

0 Digitiform (Fig. 21C)

1 Falciform (Fig. 17D)

2 Blunt

3 Branched (Fig. 22C)

4 Conic (Fig. 17C)

81. Leg IV, femur, branched dorso-basal apophysis, bigger branch

0 Retrolateral (Fig. 21B)

1 Dorsal (Fig. 19C)

2 Unbranched

82. Leg IV, femur, prolateral row of tubercles

0 Absent

1 Present

83. Leg IV, femur, prolateral row of tubercles, development

0 Equally developed (Fig. 22A)

1 Median larger (Fig. 21B)

2 Apical larger (Fig. 21A)

3 Absent

84. Leg IV, femur, prolateral row of tubercles, single apical apophysis

0 Absent

1 Present (Fig. 18B)

85. Leg IV, femur, dorsal row of tubercles

0 Absent (dorsally smooth) (Fig. 18D)

1 Present (Fig. 16D)

86. Leg IV, femur, dorsal row of tubercles, apophysis after DBA

0 Absent (Fig. 17C)

1 Present (Fig. 16D)

87. Leg IV, femur, dorsal row of tubercles, apophysis after DBA, number

0 1 (Fig. 20D)

1 2 (Fig. 19C)

2 3 - 6 (Fig. 16D)

3 More than 6

88. Leg IV, femur, row of tubercles between the dorsal and retrolateral lines

0 Absent

1 Present

89. Leg IV, femur, retrolateral row of tubercles

0 Absent

1 Present

90. Leg IV, femur, retrolateral row of tubercles, position of the larger apophysis

0 Basal third

1 Medial third (Fig. 16A)

2 Apical Third (Fig. 20B)

3 Several large apophysis on the row

91. Leg IV, femur, retrolateral row of tubercles, number of apophysis on the basal half

0 0 (absence of apophysis on the basal half) (Fig. 18B)

1 1 (one) (Fig. 18A)

2 2 (two) (Fig. 19A)

3 3 - 6 (Fig. 21A)

4 More than 6

92. Leg IV, femur, retrolateral row of tubercles, median apophysis

0 Absent (Fig. 21B)

1 Present (Fig. 16A)

93. Leg IV, femur, retrolateral row of tubercles, number of apophysis on the apical half

0 0 (absence of apophysis on the apical half)

1 1 (one) (Fig. 17D)

2 2 (two) (Fig. 15A)

3 3 - 6 (Fig 18B)

4 More than 6

94. Leg IV, femur, retrolateral row of tubercles, more developed apical tubercle

0 Absent

1 Present (Fig. 15B)

95. Color (in ethanol)

0 Brownish

1 Black

2 Yellowish

3 Reddish

96. Body totally or partially covered with sediment

0 Absent

1 Present

97. Penis, *truncus*, form in lateral view

0 Globose (Fig. 25E)

1 Thin (Fig. 26E)

98. Penis, ventral plate, form

0 As long as large (Fig. 25A)

1 Longer than larger (thin) (Fig. 26D)

2 Larger than longer (developed lateral expansions) (Fig. 26A)

99. Penis, ventral plate, ventral side, T1 microsetae

0 Absence

1 Sparse or present in regions (Fig. 25F)

2 Presence in the whole extension (Fig. 27C)

100. Penis, ventral plate, ventral side, medio-apical excavation

0 Not excavated (Fig. 25C)

1 Slightly excavated (Fig. 25I)

2 Very excavated (Fig. 27F)

101. Penis, ventral plate, apical groove

0 Absent

1 Small groove (in dorsal view, reaches at most the line of the first MS C) (Fig. 26D)

2 Median groove (in dorsal view, reaches the line of the second and third MS C) (Fig. 24A)

3 Prominent groove (in dorsal view it is more basal than the MS C) (Fig. 24G)

102. Penis, ventral plate, apical groove, format

0 Edges slightly sloped (Fig. 24A)

1 Edges very sloped (Fig. 24G)

103. Penis, ventral plate, Macrosetae C (MS C), number

0 2

1 3 (Fig. 26D)

2 4

104. Penis, ventral plate, Macrosetae C (MS C), shape

0 Straight

1 Helicoidal (Fig. 25G)

2 Curved (Fig. 26D)

105. Penis, ventral plate, Macrosetae C (MS C), position

0 Distal (Fig. 24A)

1 Sub-distal (Fig. 26D)

2 Medial

106. Penis, ventral plate, Macrosetae A (MS A), number

0 2 (Fig. 24D)

1 3 (Fig. 14G)

2 4 (Fig. 24A)

107. Penis, ventral plate, Macrosetae A (MS A), position on the ventral plate

0 Linear in dorso-ventral direction (Fig. 25A)

1 Triangle shaped (Fig. 27D)

2 Parable shaped (Fig. 25H)

3 Linear in baso-apical direction

108. Penis, ventral plate, Macrosetae B (MS B), size

0 Small (clearly smaller than the MS A) (Fig. 14B)

1 Big (same size of the MS A) (Fig 14G)

109. Penis, ventral plate, Macrosetae D (MS D)

0 Absent (Fig. 24E)

1 Present (Fig. 24H)

110. Penis, ventral plate, Macrosetae D (MS D), number

0 1 (Fig. 24H)

1 2

2 3

3 Absent

111. Penis, ventral plate, Macrosetae D (MS D), size

0 Small (Fig. 24H)

1 Large (Fig. 14B)

2 Absent

112. Penis, ventral plate, Macrosetae D (MS D), position in lateral view

0 Aligned with MS C (Fig. 27G)

1 Ventral to the MS C (Fig. 25A)

2 Dorsal to the MS C

3 Absent

113. Penis, ventral plate, Macrosetae E (MS E)

0 Absent

1 Present

114. Penis, ventral plate, Macrosetae E (MS E), number

0 1

1 2

115. Penis, ventral plate, Macrosetae E (MS E), position of the most basal MS E

0 Ventral and aligned to the MS C (Fig. 26B)

1 Ventral and medial to the MS C (Fig. 24H)

116. Penis, ventral plate, well-developed lateral lobes

0 Absent (Fig. 26D)

1 Present (Fig. 26A)

117. Penis, ventral plate, lateral lobes, position

0 Medial (Fig. 26A)

1 Basal (Fig. 26D)

118. Penis, ventral process

0 Absent

1 Present

119. Penis, ventral process, flabellum

0 Absent

1 Present

120. Penis, ventral process, flabellum, shape

0 As long as large (Fig. 27A)

1 Longer than wide (thin) (Fig. 27D)

121. Penis, ventral process, flabellum, lateral parts

0 Serrated, with the apex of the processes pointed to the penis base (Fig. 25A)

1 Smooth (Fig. 24G)

2 Serrated, with the apex of the processes pointed to the penis apex

122. Penis, ventral process, flabellum, apex

0 Without a longer central terminal

1 With a longer central terminal (Fig. 25H)

123. Penis, stylus, apex, microsetae

0 Absence (Fig. 27G)

1 Presence (Fig. 27B)

124. Penis, stylus, apex, format

0 Inclined relative to the penis axis, keeled

1 Inclined relative to the penis axis, without keel

2 Straight

3 Absent

Phylogenetic analysis

Morphological data analysis.

Likelihood (Figure 01). The maximum likelihood analysis (hereon, ML) recovered one tree with the value of Log-likelihood -2618.689, with Mk+F as the best model, according to the Bayesian Information Criterion (BIC). In ML, *Mischonyx* is monophyletic if *Gonyleptes antiquus* is considered a member of the genus. Inside

Mischonyx, clade (*Mischonyx arlei* + *Mischonyx minimus* sp. nov.) is sister to the other species. Followed by this divergence, *Mischonyx intermedius* branches off as sister to the remaining species. In this clade, *G. antiquus* is sister to a clade which holds two lineages. In one of them, *M. poeta* diverges first as sister to the others inside the clade and (*M. holacanthus* + *M. fidelis*) diverge from (*M. insulanus* + (*M. kaisara* + *M. squalidus*)). The other clade holds *M. processigerus* as sister species to the clade with the other species. Inside this clade, *M. petroleiros* sp. nov. is the most basal. *M. bresslaui* branches off as sister to the clade which holds *M. intervalensis* sp. nov. as sister species to a less inclusive clade, presenting *M. reitzi* as sister to (*M. parvus* (*M. clavifemur* + *M. anomalus*). The minimum bootstrap support value inside *Mischonyx* genus is 29 (Fig. 1), followed by 52. Bootstrap value for *Mischonyx* clade is 94.

Parsimony (Figure 02). The maximum parsimony analysis (hereon, MP) retained three most parsimonious tree, with 645 steps. The only terminals that change in both trees are specimens from the same species, which present few differences among the analyzed individuals, namely *M. bresslaui*, *M. anomalus* and *M. insulanus*. The Strict Consensus of trees is presented in Figure 02. In this Consensus, *Mischonyx* is monophyletic with all the analyzed species and *Gonyleptes antiquus is excluded from the genus*. The clade (*M. arlei* + *M. minumu* sp. nov.) is sister to the clade holding the remaining species. Inside this clade, *M. intermedius* is sister to the other species. The clade ((*M. holacanthus* + *M. poeta*) + *M. kaisara* + *M. squalidus*)) branches off as sister species of the group containing the rest of the species. Inside this group, (*M. processigerus* + *Gonyleptes antiquus*) diverge as the sister species of the others, followed by *M. insulanus*, *M. fidelis* and *M. petroleiros* sp. nov.. The clade with the other species has (*M. reitz* + *M. intervalensis* sp. nov.) diverging from the rest. *M. bresslaui* diverges from the other three species, which form the clade (*M. parvus* (*M. clavifemur* + *M. anomalus*). Most part of the nodes present very low bootstrap values, which are presented in Figure 02. Consistency and Retention indexes are 26 and 66, respectively.

Molecular data analysis.

Likelihood (Figure 03). *Mischonyx* is monophyletic if *G. antiquus* is removed, once it groups with *Ampheres leucopheus*, not related the genus. In *Mischonyx* clade, there are two major lineages. In one of them, *M. insulanus* + *M. kaisara* is sister to another clade, in which *M. intervalensis* **sp. nov.** is sister species of the group containing

M. anomalus as the sister species of *M. reitzi* + *M. clavifemur*. In the other lineage, *M. intermedius* diverges from the species from Rio de Janeiro state. In this clade, *M. minimus* **sp. nov.** is the species sister to the other. The rest of the species form a clade in which *M. processigerus* diverges from the remaining, followed by *M. poeta*, which is sister species to the lineage with the five other species. In this lineage, *M. bresslaui* is the sister species of the clade holding *M. petroleiros* **sp. nov.** as sister species of a monophyletic group with *M. fidelis* as sister of *M. parvus* + *M. squalidus*.

Parsimony (Figure 04). *Mischonyx* is monophyletic if *G. antiquus* is removed, once it diverges far from the genus. Besides that, inside the genus topology, there are three inner clades. The lineage that diverges first is composed strictly of species from the northern coast of São Paulo (*M. kaisara* + *M. insulanus*) and is sister group to the other two clades. One of them holds *M. intermedius*, only the species from Minas Gerais, as sister species to the species of south of São Paulo (*M. intervalensis* **sp. nov.**), Parana and Santa Catarina states. *M. intervalensis* **sp. nov.**, is sister species to the group holding *M. anomalus* as the sister species to *M. clavifemur* + *M. reitzi*. In the other lineage, there are only species from Rio de Janeiro state and the widely distributed *M. squalidus*. *M. minimus* **sp. nov.** is the species that diverges first, followed by *M. processigerus*, which is sister group to the clade holding two lineages: one with *M. poeta* as sister species of *M. bresslaui* and *M. petroleiros* **sp. nov.**, and the other holding *M. fidelis* as sister species of the clade with *M. squalidus* + *M. parvus*. Bootstrap values are on the nodes of Figure 04.

Total Evidence analysis.

As in molecular data, the Total Evidence (TE) analysis from both parsimony and likelihood analyses retrieved *Mischonyx* as monophyletic. In MP, the phylogeny retained after Iterative Pass presents 6267 of cost, while in ML, the phylogeny presents -19758.819 score. There are some differences in the topology of both analyses.

Likelihood (Figure 05-07). *Mischonyx* is monophyletic if *G. antiquus* is removed. The *Multumbo* lineage is sister to the *Mischonyx* clade. There are two major lineages inside *Mischonyx* clade. In one of them, the clade with from northern coast of São Paulo state (clade *M. kaisara* + *M. insulanus*) is sister to another clade, holding species from the south of São Paulo (M. intervalensis **sp. nov.**), which is sister to the group containing species from Parana (*M. anomalus*) and Santa Catarina (*M. clavifemur*, *M. reitzi*) states. The other clade holds the species from Minas Gerais (*M. intermedius*) and Rio de Janeiro

(*M. arlei, M. bresslaui, M. fidelis, M. holacanthus, M. minimus* **sp. nov.**, *M. parvus, M. poeta, M. processigerus, M. petroleiros* **sp. nov.**) states. Besides these species, *M. squalidus*, the only species of the genus that occur in both south and southeastern regions of the Atlantic Forest, belong to this second clade (called hereon as RJMG clade). In RJMG, there is one clade with *M. intermedius* as sister group of *M. arlei* + *M. minimus* **sp. nov.** and another clade with all the rest of the species from Rio de Janeiro state. In this last lineage, *M. processigerus* is the first lineage that branches off, followed by *M. poeta*, *M. bresslaui* and *M. petroleiros* **sp. nov.**. The remaining species form two small lineages: *M. fidelis* + *M. holacanthus* and *M. parvus* + *M. squalidus*. The minimum bootstrap support value is 60, which is from the RJMG branching. When analyzing the character change plotted in the topology (Fig. 6), the Consistency and Retention indexes are 30 and 64 respectively.

Parsimony (Figures 08-10). As in ML, in MP *Mischonyx* remain monophyletic only if *G. antiquus* is removed from the genus. It forms a clade with *Ampheres leucopheus* (Caelopyginae) and *Gonyleptes horridus* (Gonyleptinae). Besides that, there are three inner clades within *Mischonyx*. The lineage that diverges first is composed strictly of species from the northern coast of São Paulo (*M. kaisara* + *M. insulanus*) and they are sister to the other two clades. One of them contains the species from Minas Gerais, south of São Paulo, Parana and Santa Catarina states. In this clade, *M. intermedius* branches off first, being the sister species of the clade in which *M. intervalensis* **sp. nov.** is sister species of the group holding *M. anomalus* as sister species of *M. clavifemur* + *M. reitzi*. In the other lineage, there are only species from Rio de Janeiro state and the widely distributed *M. squalidus*. The clade that diverges first is composed of *M. arlei* + *M. minimus* **sp. nov.**, which is sister to the remaining species. *M. processigerus* branches off as the sister species of the lineage containing the rest of the species, which holds two clades: one with *M. bresslaui* + *M. poeta* and the other with two clades (*M. holacanthus* + *M. fidelis* as sister to *M. squalidus* + *M. parvus*). Regarding the bootstrap support, the minimum value is 33 for the clade *M. holacanthus* + *M. fidelis*, followed by the value 51 of (*M. holacanthus* + *M. fidelis*) + (*M. parvus* + *M. squalidus*) clade. Besides these two values, all the other nodes present values higher than 70. When analyzing the character change plotted on the topology (Fig. 10), the Consistency and Retention indexes are 28 and 61 respectively.

Taxonomic changes

Mischonyx new combinations and diagnosis

Before this publication, *Mischonyx* had the following 11 species, present in Kury (2003) and Pinto-da-Rocha *et al.* (2012): *M. anomalus* (Mello-Leitão, 1936); *M. antiquus* (Mello-Leitão, 1934); *M. cuspidatus* (Roewer, 1913); *M. fidelis* (Mello-Leitão, 1931); *M. holacanthus* (Mello-Leitão, 1927); *M. insulanus* (Soares, 1972); *M. intermedius* (Mello-Leitão, 1935); *M. kaisara* (Vasconcelos, 2004); *M. poeta* (Vasconcelos, 2005); *M. processigerus* (Soares & Soares, 1970); *M. squalidus* Bertkau, 1880 and *M. sulinus* (Soares & Soares, 1947).

With the phylogenetic analysis present on this work, I propose a new combination, composition and diagnosis for this genus:

***Mischonyx* Bertkau, 1880**

Mischonyx Bertkau, 1880: 106; Kury, 2003: 132 (type species: *Mischonyx squalidus* Bertkau, 1880, by monotypy).
Urodiabunus Mello-Leitão, 1935b: 396. (type species: *Urodiabunus arlei* Mello-Leitão, 1935, by original designation). **Syn.nov.**

Composition: *Mischonyx. anomalus* (Mello-Leitão, 1936) **comb. nov.**; *Mischonyx arlei* (Mello-Leitão, 1935b) **comb.nov.**, *Mischonyx bresslaui* (Roewer, 1927) **comb.nov.**, *Mischonyx clavifemur*, (Mello-Leitão, 1927a) **comb.nov.**,; *Mischonyx fidelis* (Mello-Leitão, 1931b); *Mischonyx holacanthus* (Mello-Leitão, 1927); *Mischonyx insulanus* (H. Soares, 1972); *Mischonyx intermedius* (Mello-Leitão, 1935b); *Mischonyx intervalensis* **sp. nov.**; *Mischonyx kaisara* (Vasconcelos, 2004); *Mischonyx minimus* **sp. nov.**; *Mischonyx parvus* (Roewer, 1917) **comb. nov.**; *Mischonyx poeta* (Vasconcelos, 2005); *Mischonyx processigerus* (Soares & Soares, 1970); *Mischonyx petroleiros* **sp. nov.**; *Mischonyx reitzi* (Vasconcelos, 2005) **comb.nov.**; *Mischonyx squalidus* Bertkau, 1880 **comb. nov.**.

Taxonomic remarks: I transferred *Mischonyx arlei* **comb. nov.**, *Mischonyx bresslaui* **comb**. **nov**., *Mischonyx clavifemur* **comb**. **nov**., *Mischonyx parvus* **comb**. **nov**.

and *Mischonyx reitzi* **comb. nov.** based on the phylogenetic analysis present in this paper (molecular and morphological) and by analysis the types from these species. Other new combinations I have proposed based on the morphological analysis of the types as well. The only exception is *M. squalidus* **comb**. **nov**., which I had to analyze original figures and description from Bertkau to propose this new combination. Vasconcelos (2003), in his master's dissertation, and Benedetti (2017), in his PhD thesis, have already proposed most of these new combinations. However, they have not published their works and, according to ICZN (1999), nomenclatural acts in thesis or dissertations are not valid if they are not officially published.

Besides that, by this new phylogenetic analysis, I restablish here the original combination of *Gonyleptes antiquus* Mello-Leitão, 1934, removing the species from *Mischonyx* genus. This species was considered a member of *Mischonyx* by Kury (2003) and Pinto-da-Rocha (2012). Now it returns to the genus in which it was originally described.

Diagnosis. Small size Gonyleptinae (3-6 mm of dorsal scutum length). Dorsal scutum outline γP in males, with coda involved by the mid-bulge, which is very distinct. Females have dorsal scutum outline α, with coda long and clearly separated from mid-bulge. Anterior margin with lateral armature, normally two or three tubercles on each side. Frontal hump is high and narrow, with a pair of median tubercles (except in *M. processigerus*, which has two pairs). Lateral margin of prosoma with several granules, posterior to the ozopore. *Ocularium* is narrow and not very high, armed with median spines or tubercles. Some species have small tubercles anterior or posterior to the eye (or both). Posterior margin of prosoma with a pair of tubercles. Dorsal scutum with three areas. Mesotergal Area I divided by a longitudinal groove. Areas I and II armed with median tubercles (which are big and whitish in *M. arlei* and *M. minimus* **sp. nov.**). Area III with a pair of median elliptic tubercles (except in *M. arlei* and *M. minimus* **sp. nov.**), which can vary in size and lateral compression. Some species have other elliptic tubercles besides the median ones (e.g. *M. bresslaui*). Lateral margin of dorsal scutum (mid-bulge) with rounded tubercles, which can be fused in some species (e.g. *M. bresslaui*). Distitarsi of all legs with three segments. Basitarsus of leg I with three or four segments. Basitarsus of leg II variable from 4 – 8 segments). Basitarsus of legs III and IV with four or five segments. Ventral face of coxae I generally with more developed tubercles than the ones on the other coxa. Coxa IV with apical prolateral apophysis, generally robust and can

present ventral process and a basal tubercle. Trochanter IV short and robust, with a blunt prolateral apophysis and with at least one retrolateral armature. Femur IV with DBA, which can be small (as in *M. arlei* and *M. minimus* **sp. nov.**), or large large in most species. DBA can be branched or not and varies in shape and size in every species. Retrolateral row of tubercles generally with some large apophysis. Penis with ventral plate trapezoidal, presenting an apical parabolic groove; three pairs of MS A and one pair of MS B on the lateral projections; three pairs of helicoidal MS C, two pairs of reduced MS E, one pair of MS D, venter of ventral plate with microsetae type T1 covering its whole extension or the basal half. Glans with ventral process, which present *flabellum,* which can be serrated or smooth. Stylus with microsetae, inclined in relation to the penis axis and presenting a ventral groove.

Species new combinations

Besides the combinations and synonyms present in Kury (2003) and Pinto-da-Rocha (2012), the following new combinations are here proposed:

***Mischonyx. anomalus* (Mello-Leitão, 1936) comb. nov. (Figs. 15A, 15C, 24A-C)**

Xundarava anomala Mello-Leitão, 1936: 13, fig 10; B. Soares, 1945d: 192; 1945h: 366; H. Soares, 1945a: 210; Soares & Soares, 1949b: 220 (syntype, MNRJ 42282).

Ilhaia anomala: Soares & Soares, 1987: 7.

Mischonyx anomalus: Kury, 2003: 133.

Ilhaia sulina Soares & Soares, 1947: 215 (lectotype, MHNCI 3618).

Mischonyx sulinus: Kury, 2003: 134.

Diagnosis. *Mischonyx anomalus* **comb. nov.** resembles *M. clavifemur* **comb. nov.** by: prolateral apophysis of coxa IV with its apex directed posteriorly; prolateral apophysis of trochanter IV small when compared to other species; retolateral row of femur IV with median apophysis larger than the other armatures of this row; ventral plate of the penis with MS A forming a baso-apical, reduced MS B, MS E slightly medial when compared to the MS C, ventral side entirely covered with microsetae, lateral lobes basal. It differs from *M. clavifemur* by: its reduced size (4 – 4.5 mm of dorsal scutum length) (5 – 6 mm in *M. clavifemur*); Dorsal scutum is narrower than in *M. clavifemur*; Mesotergal Area III

with a pair of large median tubercles (reduced in *M. clavifemur*); retrolateral side of trochanter IV with a row of small tubercles (two tubercles in *M. clavifemur*, with the apical more developed than the other); ventral plate longer than wider (as wide as long in *M. clavifemur*) dorsal row of femur IV with small tubercles only after DBA (three big tubercles after DBA in *M. clavifemur*) apical groove reaching the line of the second MS C (reaching deeper than the MS C in *M. clavifemur*).

***Mischonyx arlei* (Mello-Leitão, 1935b) comb.nov. (Fig. 15B, 15D, 27G-I)**

Urodiabunus arlei Mello-Leitão, 1935: 397, fig 22 (syntype, MNRJ 42476).

Diagnosis. *Mischonyx arlei* **comb. nov.** resembles ***M. minimus* sp. nov.** by the combinations of following characters: Mesotergal Area I with a pair of well-developed median tubercles, which are clearer (whitish) than the rest of the body's color (dark brown); median armatures on Mesotergal Area III are spines; lateral margin of dorsal scutum with several small tubercles; Free Tergite II with a well-developed median apophysis; prolateral apophysis on coxa IV small and pointing posteriorly; retrolateral side of trochanter IV with two armatures; femur IV with several small apophysis on dorsal and retrolateral row of tubercles; femur IV with a well-developed terminal tubercle on pro and retrolateral rows of tubercles; ventral plate with three subdistal MS C on each side; MS B smaller than MS A; *flabellum* with serrated ends. It differs from ***M. minimus* sp. nov.** by: its size (7 – 8 mm) (3 – 3.5 mm in ***M. minimus* sp. nov.**); Mesotergal Area II with median tubercles small and darker than the rest of the body (median tubercles whitish and as big as the median tubercles on Mesotergal Area I in ***M. minimus* sp. nov**); basitarsus II with seven segments (four in ***M. minimus* sp. nov**); leg IV curved in dorsal view (straight in ***M. minimus* sp. nov**); MS D reduced (well-developed in ***M. minimus* sp. nov**).

***Mischonyx bresslaui* (Roewer, 1927) comb.nov. (Figs. 16A, 16C, 24D-F)**

Weyhia bresslaui Roewer, 1927: 344; 1930: 356, pl. 6, fig. 1; Mello-Leitão, 1931d: 127; 1932: 285, fig. 178; 1933b: 143 (syntype SMF 1420).

Geraecormobius bresslaui: Soares & Soares, 1949: 168.

Geraecomorbiella convexa Mello-Leitão, 1931d: 128, fig 16 (type MNRJ 18203, % lectotype, 5 paralectotypes).

Geraecormobius convexus: Soares & Soares, 1949b: 169

Geraecormobius cheloides Mello-Leitão, 1940b: 19, fig 23 (type MNRJ 58236) Synonymy established by Soares & Soares, 1987a.

Diagnosis. *Mischonyx bresslaui* **comb. nov.** resembles ***Mischonyx petroleiros* sp. nov.** by the combinations of following characters: anterior margin of dorsal scutum with two tubercles on each side; tubercles on Mesotergal Area III, besides the median ones, elliptic; lateral margin of dorsal scutum with the most posterior lateral tubercles fused (forming bigger tubercles); all free tergites with small tubercles; retrolateral apophysis on coxa IV apparent on dorsal view; dorsal row on leg IV with a tubercle anterior to the DBA; retrolateral row on leg IV with a large median apophysis; ventral plate with three pairs of apical MS C. It differs from ***Mischonyx petroleiros* sp. nov.** by: median tubercles on Mesotergal Area III strongly compressed (elliptic but not strongly compressed laterally in ***Mischonyx petroleiros* sp. nov**); lateral margin of dorsal scutum with small tubercles (big in ***Mischonyx petroleiros* sp. nov**); prolateral apophysis on coxa IV smaller than trochanter IV (approximately with the same length in ***Mischonyx petroleiros* sp. nov**); DBA not branched (branched in ***Mischonyx petroleiros* sp. nov**); dorsal row of tubercles of leg IV with three big tubercles after DBA (without big tubercles after DBA in ***Mischonyx petroleiros* sp. nov**); retrolateral row of leg IV with big tubercles (small in ***Mischonyx petroleiros* sp. nov**); MS B reduced much smaller than MS A (as big as the the MS A in ***Mischonyx petroleiros* sp. nov**); MS A forming a triangle and hidden behind the ventral process (forming a dorso-ventral line and apparent in ***Mischonyx petroleiros* sp. nov.**); *flabelum* with smooth ends (serrated in ***Mischonyx petroleiros* sp. nov**).

***Mischonyx clavifemur* (Mello-Leitão, 1927a) comb.nov. (Figs. 16B, 16D, 24G-I)**

Weyhia clavifemur Mello-Leitão, 1927: 416; Roewer, 1930: 356; Mello-Leitão, 1932: 286, fig 177 (holotype, MNRJ 1496).

Geraecormobius clavifemur: Mello-Leitão, 1940b: 22; B. Soares, 1945h: 354; Soares & Soares, 1949b: 169.

Ilhaia meridionalis Mello-Leitão, 1927a: 417 (type MNRJ 1474, &holotype).

Jlhaia meridionalis: Roewer, 1930: 363.

Mischonyx meridionalis: Kury, 2003: 133-134.

Diagnosis. *Mischonyx clavifemur* **comb. nov.** resembles *M. anomalus* **comb. nov.** by the

combinations of following characters: prolateral apophysis of coxa IV with its apex directed posteriorly; prolateral apophysis of trochanter IV small when compared to other species; retolateral row of femur IV with median apophysis larger than the other armatures of this row; ventral plate of the penis with MS A forming a baso-apical, reduced MS B, MS E slightly medial when compared to the MS C, ventral side entirely covered with microsetae, lateral lobes basal. It differs from *M. anomalus* by: its size (5 – 6 mm of dorsal scutum) (4 – 4.5 mm in *M. anomalus*); Mesotergal Area III with small median tubercles (more developed in *M. anomalus*); retrolateral side of trochanter IV with two tubercles, with the apical more developed than the other (a row of small tubercles in *M. anomalus*); ventral plate of the penis as wide as long (longer than wider in *M. anomalus*) dorsal row of femur IV with three large tubercles after DBA (small tubercles only after DBA in *M. anomalus*), apical groove reaching deeper than the line of the last MS C (reaching the line of the second MS C in *M. anomalus*).

***Mischonyx fidelis* (Mello-Leitão, 1931b) (Figs. 17A, 17C, 25A-C)**

Eduardoius fidelis Mello-Leitão, 1931a: 95; 1932: 344 (type MNRJ 1408, 2 syntypes).

Ilhaia fidelis: B. Soares, 1943f: 56 [by implication]; 1945h: 358; Soares & Soares, 1946a: 76; 1949b: 186.

Mischonyx fidelis: Kury, 2003: 133.

Diagnosis. *M. fidelis* resembles *M. parvus* **comb. nov.** by the combinations of following characters: pair of tubercles on the frontal hump and lateral margins of the dorsal scutum whitish (in ethanol); median tubercles on Mesotergal Area III big and elliptic; prolateral apophysis of trochanter IV big, when compared to other species (e.g. *M. bresslaui*); DBA conic and the tallest of the genus (almost as tall as the whole body), with a tubercle on the anterior side of the apophysis; prolateral row of femur IV with median tubercles more developed than the others on this row; retrolateral row of femur IV with the largest tubercle on the distal third; penis truncus apex not globose in lateral view; ventral plate with microsetae only on the basal half; apical groove shallow, reaching the line of the most apical MS C; lateral projections basal; MS A forming a dorso-ventral line; MS E basal when compared to the MS C; flabellum with the median large projection. It differs from *M. parvus* **comb. nov.** by: prolateral apophysis on coxa IV with small ventral lobe (ventral lobe as developed as the main projection in *M. parvus*); retrolateral side of

trochanter IV with three small tubercles (two big tubercles in *M. parvus*); dorsal row of femur IV with an elevation basal to the DBA (absence of an elevation basal to the DBA in *M. parvus*); dorsal row of femur IV with small tubercles only after DBA (one big tubercle after DBA in *M. parvus*); retrolateral row of femur IV with three big tubercles on the basal half (without big tubercles tubercles on the basal half in *M. parvus*); ventral plate of the penis as large as wide (larger than wider in *M. parvus*); lateral lobes projected (not projected in *M. parvus*); MS B ventral to MS A (MS B apical to the MS A in *M. parvus*); MS C more distal than in *M. parvus.*

***Mischonyx holacanthus* (Mello-Leitão, 1927) (Figs. 17B, 17D)**

Weyhia vellardi Mello-Leitão in litteris: Soares & Soares, 1987a: 7.

Xundarava holacantha Mello-Leitão, 1927b: 20 (type MNRJ 1469 [and not 469 as in B. Soares, 1945h], & holotype).

Ilhaia holacantha: Soares & Soares, 1987a: 7, figs 27-28.

Weyhia absconsa Mello-Leitão, 1932: 284, fig 175 (type MNRJ 1501, % holotype). Synonymy established by Soares & Soares, 1987a.

Geraecormobius absconsa: Mello-Leitão, 1940b: 22.

Geraecormobius absconsus: B. Soares, 1945h: 354; Soares & Soares, 1949b: 167.

Geraecormobius carioca Mello-Leitão, 1940b: 18, fig 22; Soares & Soares, 1949b: 168 (types MNRJ 53927, lost % & syntypes). Synonymy established by Soares & Soares, 1987a.

Mischonyx holacanthus: Kury, 2003: 133.

Diagnosis. *M. holacanthus* resembles *M. fidelis* by the combinations of following characters: median tubercles on frontal hump whitish when compared to the rest of the body (in ethanol); lateral margin of dorsal scutum with whitish tubercles when compared to the rest of the body (in ethanol); dorsal row of tubercles with an elevation before DBA; DBA with its apex directed anteriorly; no apophysis after DBA on the dorsal row of femur IV; prolateral row with median tubercles bigger than the others in this row; retrolateral row with the biggest apophysis on the apical third. It differs from *M. fidelis* by: lateral margin of dorsal scutum with smaller tubercles when compared to *M. fidelis*; prolateral apophysis on coxa IV with its apex directed dorsally (Fig. D) (prolateral apophysis with apex directed posteriorly in *M. fidelis*); retrolateral apophysis on coxa IV visible in dorsal view (not visible in *M. fidelis*); prolateral apophysis on trochanter IV small when

compared to *M. fidelis*; retrolateral side of trochanter IV with three big tubercles (small tubercles in *M. fidelis*); DBA small, much smaller than the body height (almost as big as the body height in *M. fidelis*); retrolateral row with tubercles increasing in size from the base to the middle of the row (small tubercles only in *M. fidelis*); after the apophysis on the retrolateral row, there is no big tubercles (two big tubercles in *M. fidelis*).

***Mischonyx insulanus* (H. Soares, 1972) (Figs. 18A, 18C, 25D-F)**

Ilhaia insulana H. Soares, 1972: 65, figs 1-4 (types HSPC 361, % holotype, 1 & paratype).

Mischonyx insulanus: Kury, 2003: 133.

Diagnosis. *M. insulanus* resembles *M. processigerus* by the combinations of following characters: median tubercles on ocularium smaller than the ocularium height; ocularium with small tubercles on the anterior and posterior sides; Mesotergal Area III with small median tubercles when compared to other species (e.g. *M. fidelis*); Free Tergites II and III with median apophysis; prolateral row of femur IV with median tubercles bigger than the others in this row; dorsal row of femur IV with small tubercles after DBA; retrolateral row of femur IV with the biggest apophysis on the distal third; ventral side of the ventral plate of the penis with microsetae only on the laterals; lateral lobes well-developed; apical groove of the ventral plate reaching the line of the second MS C; MS A forming a dorso-ventral line; reduced MS B. It differs from *M. processigerus* by: prolateral apophysis of coxa IV with ventral lobe as big as the main projection and close to each other (ventral lobe smaller and more separated from the main projection of the apophysis in *M. processigerus*); retrolateral apophysis of coxa IV not visible on dorsal view; (visible in *M. processigerus*); DBA not branched (branched in *M. processigerus*); retrolateral row of femur IV with two big apophysis (one in *M. processigerus*); retrolateral row of femur IV with small tubercles besides the two apophysis (several big tubercles in *M. processigerus*); *flabellum* with smooth apex (serrated in *M. processigeus*); stylus without microsetae (stylus with microsetae in *M. processigerus*); MS B closer to MS E when compared to *M. processigerus*.

***Mischonyx intermedius* (Mello-Leitão, 1935) (Figs. 18B, 18D, 25G-I)**

Ilhaia intermedia Mello-Leitão, 1935e: 401, fig 25; 1935b: 107 (type IBSP 46, %holotype).

Penygorna infuscata Mello-Leitão, 1936b: 31, fig 26 (type MNRJ 42695, 1 % 2 & syntypes). Synonymy established by B. Soares, 1944i.

Mischonyx intermedius: Kury, 2003: 133.

Diagnosis. *M. intermedius* resembles *M. arlei* **comb. nov.** by the combinations of following characters: lateral margin of dorsal scutum with several small tubercles; Mesotergal Area III with median tubercles that are not elliptic; prolateral apophysis of coxa IV smaller than trochanter IV, blunt and oblique to the body axis; femur IV thin and long; retrolateral row of femur IV with an apical sharp tubercle; MS B reduced; MS E in the same dorso-basal line of the MS C; *flabellum* with serrated ends. It differs from *M. arlei* by: median tubercles on Mesotergal Area I smaller than the median tubercle of the other Mesotergal Areas and darker than the rest of the body color (in ethanol) (bigger and whitish in *M. arlei*); Free Tergite II with small tubercles only (big median apophysis in *M. arlei*); retrolateral apophysis of coxa IV not visible in dorsal view (visible in *M. arlei*) prolateral apophysis of trochanter IV big (reduced in *M. arlei*); retrolateral side of trochanter IV with a line of three tubercles (two n *M. arlei*); DBA big in relation to the other armature on the dorsal row and with its apex directed anteriorly (DBA almost with the same size of other tubercles on the row and with its apex directed dorsally in *M. arlei*); prolateral ros of femur IV with a large number of tubercles when compared to other species (e.g. *M. bresslaui* and *M. arlei*); retrolateral row of femur IV with tubercles increasing in size apically (retrolateral row with minute armature in *M. arlei*); ventral side of the ventral plate of the penis with microsetae on the basal half (ventral side entirely covered with microsetae in *M. arlei*); apical groove of the ventral plate of the penis reaches the line of the most basal MS C (apical groove reaches the line of the median MS C in *M. arlei*); MS A forming a parable (MS A forming a diagonal baso-apical line in *M. arlei*); MS D more apical, when compared to *M. arlei*, that has the MS D medial on the ventral plate;

***Mischonyx kaisara* (Vasconcelos, 2004) (Figs. 19B, 19D, 26A-C)**

As *M. kaisara* was recently described and there is no new combination for the species, Vasconcelos (2004) diagnosis for the species remains unaltered and with no necessity to add information.

***Mischonyx parvus* (Roewer, 1917) comb. nov. (Figs. 20B, 20D, 26D-F)**

Weyhia parva Roewer, 1917: 133 (holotype, SMF 1331).

Geraecormobius parva: Mello-Leitão, 1940b: 22.

Geraecormobius parvus: B. Soares, 1945: 355; Soares & Soares, 1949b: 171.

Ilhaia parva: Soares & Soares, 1987a: 6.

Cryptomeloleptes spinosus Mello-Leitão, 1931d: 138 (holotype MNRJ 11392). Synonymy established by Soares & Soares, 1987a.

Arleius incisus Mello-Leitão, 1935a: 22 (holotype MNRJ 41759).

Ilhaia incisa: Soares & Soares, 1946a: 76. [= *Bunoleptes armatus* Mello-Leitão, 1935e; = *Geraecormobius cervicornis* Mello-Leitão, 1940b].

Bunoleptes armatus Mello-Leitão, 1935e: 398. Synonymy established by Soares & Soares, 1987a.

Geraecormobius cervicornis Mello-Leitão, 1940b: 17 (holotype MNRJ 53924). Synonymy established by Soares & Soares, 1987a.

Diagnosis. *M. parvus* **comb. nov.** resembles *M. fidelis* by the combinations of following characters: pair of tubercles on the frontal hump and lateral margins of the dorsal scutum whitish (in ethanol); median tubercles on Mesotergal Area III big and elliptic; prolateral apophysis of trochanter IV big, when compared to other species (e.g. *M. bresslaui*); DBA conic and the tallest of the genus (almost as tall as the whole body), with a tubercle on the anterior side of the apophysis; prolateral row of femur IV with median tubercles more developed than the others on this row; retrolateral row of femur IV with the biggest tubercle on the distal third; penis not globose in lateral view; ventral plate with microsetae only on the basal half; apical groove shallow, reaching the line of the most apical MS C; lateral projections basal; MS A forming a dorso-ventral line; MS E basal when compared to the MS C; flabellum with the median projection big. It differs from *M. fidelis* by: prolateral apophysis on coxa IV with ventral lobe as developed as the main projection (ventral lobe reduced in *M. fidelis*); retrolateral side of trochanter IV with two big tubercles (small in *M. fidelis*); dorsal row of femur IV without an elevation basal to the DBA (presence of an elevation basal to the DBA in *M. fidelis*); dorsal row of femur IV with a big tubercle after DBA (small tubercles only after DBA in *M. fidelis*); retrolateral row of femur IV without big tubercles on the basal half (three big tubercles on the basal half in *M. fidelis*); ventral plate of the penis larger than wider (as large as wide in *M. fidelis*); lateral lobes not very projected, with the MS A and MS B close to the penis base

(projected in *M. fidelis*); MS B apical to MS A (MS B ventral to the MS A in *M. fidelis*); MS C more median than in *M. fidelis.*

Taxonomic remarks: Kury (2003) synonymized this species with *M. squalidus*. However, the distribution of *M. parvus* does not match with the original location of the described individual in Bertkau (1880). In this last work, the location of the specimen is "Copacabana, Rio de Janeiro". By the distribution map in the Figs. 29 and 30, the registers from this species are from Mangaratiba and Angra dos Reis, which are to the south of Rio de Janeiro state. For this reason, I removed this species from the synonymy created by Kury (2003).

***Mischonyx poeta* (Vasconcelos, 2005) (Figs. 21A, 21C, 26G-I)**

As *M. poeta* was recently described and there is no new combination for the species, Vasconcelos (2005) diagnosis for the species remains unaltered and with no necessity to add information.

***Mischonyx processigerus* (Soares & Soares, 1970) (Figs. 21B, 21D, 27A-C)**

Ilhaia processigera Soares & Soares, 1970: 340, figs 1-3 (types MZUSP 4501, % holotype, 1 & paratype).

Mischonyx processigerus: Kury, 2003: 134.

Diagnosis. *M. processigerus* resembles *M. insulanus* by the combinations of following characters: median tubercles on ocularium smaller than the ocularium height; ocularium with small tubercles on the anterior and posterior sides; Mesotergal Area III with small median tubercles when compared to other species (e.g. *M. fidelis*); Free Tergites II and III with median apophysis; prolateral row of femur IV with median tubercles bigger than the others in this row; dorsal row of femur IV with small tubercles after DBA; retrolateral row of femur IV with the biggest apophysis on the distal third; ventral side of the ventral plate of the penis with microsetae only on the laterals; lateral lobes well-developed; apical groove of the ventral plate reaching the line of the second MS C; MS A forming a dorso-ventral line; reduced MS B. It differs from *M. insulanus* by: prolateral apophysis of coxa IV with ventral lobe small and separated from the main projection (ventral lobe as big as the main projection and close to each other in *M. insulanus*); retrolateral apophysis of

coxa IV visible on dorsal view; (not visible in *M. insulanus*); DBA branched (not branched in *M. insulanus*); retrolateral row of femur IV with one big apophysis (two in *M. insulanus*); retrolateral row of femur IV with big tubercles besides the apophysis (small tubercles in *M. insulanus*); *flabellum* with serrated apex (smooth in *M. insulanus*); stylus with microsetae (stylus without microsetae in *M. insulanus*); MS B distant from MS E when compared to *M. insulanus*.

***Mischonyx reitzi* (Vasconcelos, 2005) comb.nov. (Figs. 23A-B, 28A-C)**

Geraecormobius reitzi Vasconcelos, 2005: 6, figs. 10— 19.

Diagnosis. *M. reitzi* **comb. nov.** resembles ***M. petroleiros* sp. nov.** by the combinations of following characters: Median armature on Mesotergal Area III small when compared to other species (e.g. *M. bresslaui*) and elliptic; no median armature on Free Tergites I — III; prolateral apophysis on coxa IV with its apex directed laterally, as big as the trochanter IV and with ventral lobe; a small tubercles basal to DBA on the dorsal row; DBA branched; dorsal row of femur IV with small tubercles only; prolateral row with tubercles of the same size; apical groove on ventral plate of the penis reaching the line of the most basal MS C; MS A forming a baso-apical line; stylus with microsetae. It differs from ***M. petroleiros* sp. nov.** by: lateral margin of dorsal scutum with small tubercles which have the same color of the rest of the body (whitish than the rest of the body in ***M. petroleiros* sp. nov.**); median armature on ocularium smaller than the ocularium height (bigger in ***M. petroleiros* sp. nov.**); trochanter IV with two retrolateral tubercles (three in ***M. petroleiros* sp. nov.**); median apophysis on retrolateral row of femur IV is the biggest on this row (biggest apophysis is on the apical third in ***M. petroleiros* sp. nov.**); MS B reduced (as big as MS A in ***M. petroleiros* sp. nov.**)

***Mischonyx squalidus* (Bertkau, 1880) comb. nov. (Figs. 22B, 22D, 27D-F)**

Ilhaia cuspidata Roewer, 1913: 221 (holotype, SMF 900).

Jlhaia cuspidata: Roewer, 1930: 363 *lapsus calami).*

Mischonyx cuspidatus: Kury 2003: 133.

Ilhaia fluminensis Mello-Leitão, 1922: 334 (syntype, MZUSP 503).

Jlhaia fluminensis: Roewer, 1930: 363, fig 4*(lapsus calami).*

Eduardoius granulosus Mello-Leitão, 1931a: 95 (holotype MNRJ 1479).

Ilhaia granulosa: B. Soares, 1943f: 56.

Giltaya solitaria Mello-Leitão, 1932: 467 (holotype MNRJ 1473).
Eduardoius lutescens Roewer, 1943: 44 (syntypes SMF 5392/58).
Ilhaia lutescens: B. Soares, 1943f: 56.

Taxonomic remarks: Vasconcelos (2003) proposed this new combination in his dissertation. In this research, I have analyzed Bertkau's original drawing (Bertkau, 1880, fig. 38) and the original description for *M. squalidus*. I could not analyze the holotype because it is lost. The collection in which it was deposited is at the Institut Royal des Sciences Naturelles de Belgique. Part of the description translated from German is presented below:

"... The first abdominal dorsal segment is almost fused with the thorax, and in general the articulation skin between each segment is not very flexible. **The first three [abdominal] segments have in their superior part a line of "dots", of which the median ones stand out in height, like little spines**." (Bertkau, 1880, pp. 107)

By this excerpt, it is possible to conclude that possibly the only species which has one median armature on each free tergite in females in the region Roewer collected the specimen (Copacabana, Rio de Janeiro) is the traditionally called *M. cuspidatus*. Therefore, I propose that *Mischonyx cuspidatus* is a junior synonym of *M. squalidus.*

Diagnosis. *M. squalidus* **comb. nov.** resembles *M. bresslaui* **comb. nov.** by the combinations of following characters: lateral margin of dorsal scutum with whitish tubercles (in ethanol); posterior tubercles on lateral margin of dorsal scutum fused; retrolateral apophysis of coxa IV visible on dorsal view; DBA with apex directed anteriorly; dorsal row on femur IV with three tubercles after DBA, on the distal half; retrolateral row on femur IV with median apophysis more developed than the others in this row; ventral side of ventral plate without microsetae on the distal half; lateral projections of ventral plate projected dorsally and behind the ventral projection of the glans; MS A forming a triangle; MS B reduced; apical groove of ventral plate reaching the line of the most basal MS C. It differs from *M. bresslaui* by: median tubercles on Mesotergal Area III strongly compressed and big (small and elliptic but not strongly compressed laterally in *M. bresslaui*); prolateral apophysis on coxa IV approximately with the same length of trochanter IV (smaller in *M. bresslaui*); Free Tergites I — III with

median apophysis (without median apophysis in *M. bresslaui*); prolateral row with median tubercles bigger than the others in this row (all tubercles with the same size in *M. bresslaui*); retrolateral row on femur IV with several (7 — 8) big tubercles basal to the median apophysis (three tubercles basal, followed by a gap and one tubercle after this gap in *M. bresslaui*).

New Species Description

***Mischonyx minimus* sp. nov.**
(Figures: 11, 14A— C, 20A and 20C)

Type material. BRAZIL. Rio de Janeiro: Teresópolis (Parque Nacional da Serra dos Órgãos, Barragem Beija-flor, 22°26'16.4"S 43°36'35.4"W), C. Gueratto & M. Abrão leg., 29.VII.2017, male holotype (MZSP XXXX); same data, X males and X females paratypes, (IBSP XXXXX); same data, , A. Benedetti et al. leg., 30.IV.2014.
Etymology. From the Latin *minimus*, meaning small, little. This is due to its reduced size when compared to other *Mischonyx* species, specially *Mischonyx arlei*, sister species of ***M. minimus* sp. nov.**.
Diagnosis. ***Mischonyx minimus* sp. nov.** resembles *M. arlei* **comb. nov.** by the combinations of following characters: Mesotergal Area I with a pair of well-developed median tubercles, which are clearer (whitish) than the rest of the body (dark brown); median armatures on mesotergal area III are spines; lateral margin of dorsal scutum with several small tubercles; free tergite II with a well-developed median apophysis; prolateral apophysis on coxa IV small and pointing posteriorly; retrolateral side of trochanter IV with two tubercles; femur IV with several small apophyses on dorsal and retrolateral row of tubercles; femur IV with a well-developed apical tubercle on prolateral and retrolateral rows of tubercles; ventral plate of penis with three subdistal MS C on each side; MS B smaller than MS A; *flabellum* with serrated ends. It differs from *M. arlei* **comb. nov.** by: its reduced size (3 – 3.5 mm) (7 – 8 mm in *M. arlei* **comb. nov.**); mesotergal area II with median tubercles whitish and as large as the median tubercles on mesotergal area I (dark brown and smaller than the ones on mesotergal area I in *M. arlei* **comb. nov.**); basitarsus II with four segments (seven in *M. arlei* **comb. nov.**); leg IV not curved (straight) in dorsal view (curved in *M. arlei* **comb. nov.**); MS D well-developed (reduced in *M. arlei*).
Description. Male holotype: *Dorsum* (Figs. 11, 20A, 20C): Measurements: Dorsal

scutum: L: 3.2; W:2.9; Prosoma: L:1.3; W: 1.6. Femur IV: 4.4. Scutum outline γP, widest at Mesotergal Area II. Anterior margin of carapace with three tubercles on each side, with approximately the same size. Frontal hump high, with two spines of the same color from the rest of the body (in ethanol), curved one to the other. Anterior regionof the ocularium smooth, ocularium with one pair of median tubercles (as tall as the ocularium height). Posterior region of the ocularium with one pair of small tubercles, right behind the median tubercles. Lateral margin of prosoma with numerous small tubercles. Posterior part of prosoma with a pair of tubercles. Besides these tubercles, prosoma has a low density of granules. Dorsal scutum divided into three mesotergal areas, with low density of granules (DaSilva & Pinto-da-Rocha, 2010). Areas; Area I divided by a median longitudinal groove, with a pair of whitish big median tubercles and no granules; area II with a pair of large whitish median tubercles, with the same size of the tubercles on Area I without granules; Area III with a pair of dark median sharp spines, smaller than the other armatures on other mesotergal areas, a pair of tubercles posterior to the median spines. Lateral margins of dorsal scutum with a row of small tubercles, with the same approximate size, extending from the middle of area I until the posterior margin of Area III; no fusion of tubercles. Posterior margin of dorsal scutum with a line of small tubercles. Free tergite I with a line of small tubercles of the same approximate size. Free tergite II with a big sharp median apophysis and two large tubercles, lateral to the median apophysis; free tergite III with a line of small tubercles. Dorsal anal operculum with small sparse tubercles. *Venter*. Coxa I with several sparse tubercles, larger than the ones in other coxa. Coxa II with sparse numerous granules. Coxa III with an anterior and a posterior basal-apical row of tubercles; coxa IV with sparse numerous granules. Ventral anal operculum with granules. *Chelicerae*. Segment II with several setae, mainly in the apical part. Fix and movable fingers with seven teeth each. *Pedipalps*. Venter of trochanter with few sparse tubercles; tibia setation: prolateral IIi, retrolateral IiIi. Tarsal setation: prolateral IiI, retrolateral III, ventral side with two baso-apical lines of setae. *Legs*. Leg I: trochanter with several ventral tubercles, femur, patella and tibia with granules. Leg II: Trochanter II with several ventral tubercles; femur, patella and tibia with granules. Leg III: trochanter with several ventral tubercles; femur, patella and tibia with granules; Leg IV: Coxa IV: robust apical oblique prolateral apophysis, smaller than the trochanter size; large retrolateral apophysis, visible in dorsal view. Trochanter IV: prolateral small blunt apophysis; retrolateral side with a line of three big tubercles, two slightly more ventral. Femur IV: long, thin and straight; all tubercles on prolateral row with approximately the

same size; DBA small, unbranched, conic, sharp, pointing upwards; dorsal row with several small tubercles after DBA; retrolateral row of with several small tubercles and two more developed tubercles on the apical half; all tubercles on the ventral row small. Tarsal formula: 6(3)-6(3)-4-5. *Male genitalia* (Figs. 14A— C). Ventral plate: Ventral face with microsetae on its whole extension; pronounced apical groove (reaching the line of the first basal MS C); lateral lobes basal when compared to other species (e.g. *Mischonyx intervalensis* **sp. nov.**); three sub-apical helicoidal MS C on each side; two MS E, ventral and in the same baso-apical orientation of MS C; long MS D when compared to other species (e.g. *Mischonyx intervalensis* **sp. nov.**), basal relative to MS C and in the same dorso-ventral orientation of MS C; three spatular MS A, forming a diagonal baso-apical line; one reduce MS B, much smaller than MS A. Glans: Small dorsal process; flabelum triangular, with serrated apex; stylus with subapical microsetae, with the apex inclined relative to the penis axis and keeled. *Color*. Dark brown; pedipalps and trochanters I—III yellow.

Female. Unknown.

***Mischonyx intervalensis* sp. nov.**

(Figs. 12, 14D— F, 19A and 19C)

Type material. BRAZIL. São Paulo: Ribeirão Grande (Parque Estadual Intervales, 24°15'27.1"S 48°16'23.0"W), C. Gueratto *et al.* leg., 25.III.2017, male hololtype (MZSP XXXXXX); same data, X malles and X females paratypes (IBSP XXXX); ditto X males and X females paratypes (MNRJ XXXX); same data, Ribeirão Grande (Parque Estadual Intervales, 24°15'27.1"S 48°16'23.0"W), F. Carbayo *et al*. Leg., 12 – 14.XII.2008, X males and X females paratyes (SMF XXXX).

Etymology. The epithet is due to its first collecting locality, Parque Estadual Intervales, type and only locality registered for this species.

Diagnosis. It resembles *Mischonyx anomalus* by the combinations of following characters: Anterior margin of dorsal scutum with two tubercles on each side; Areas I and II with small median tubercles; area III with well-developed and elliptic median tubercles; other tubercles on area III are rounded; all free tergites with small tubercles; retrolateral row of leg IV with a big median apophysis; retrolateral row of leg IV with several well-developed tubercles. It differs from *M. anomalus* by: prolateral apophysis of coxa IV with ventral process and basal tubercle (not present in *M. anomalus*); retrolateral

side of trochanter IV with three tubercles (one in *M. anomalus*); DBA of leg IV branched and the dorsal branch is the biggest (not branched in *M. anomalus*); one apophysis on the dorsal row of tubercles of leg IV after DBA (three in *M. anomalus*); tubercles on prolateral row of tubercles on leg IV small and with the same size (median tubercles bigger in *M. anomalus*); ventral plate with the same approximate height and width (square-shaped) (higher than wider in *M. anomalus*); lateral processes of the ventral plate medial (basal in *M. anomalus*).

Description. Male holotype: *Dorsum* (Figs. 12, 19A and 19C): Measurements: Dorsal scutum: L: 4.5; W:4.6; Prosoma: L:1.8; W: 2.4. Femur IV: 3.9. Scutum outline γP, widest at area II. Anterior margin of carapace with two tubercles on each side, with approximately the same size. Frontal hump high, with two tubercles of the same color from the rest of the body (in ethanol). Anterior face of the ocularium with one pair of tubercles, one pair of median tubercles/spines (taller than the ocularium height). Anterior face of the ocularium with one pair of small tubercles, right before the eyes. Lateral margin of prosoma with numerous small tubercles. Posterior part of prosoma with a pair of tubercles. Besides these tubercles, prosoma has a low density of granules. Dorsal scutum; Area I divided by a median longitudinal groove, with a pair of dark median tubercles and few sparse granules; Area II with a pair of dark median tubercles slightly larger than the tubercles on Area I and few sparse granules; Area III with a pair of dark median elliptic tubercles, largerthan the ones on the other mesotergal areas, a pair of rounded tubercles posterior to the median elliptic ones and few sparse granules. Lateral margins of dorsal scutum with a row of small tubercles, increasing in size posteriorly and from sulcus I to the posterior margin of area III; no fusion of tubercles. Posterior margin of dorsal scutum with a line of small tubercles, with the median ones slightly larger than the rest. Dorsal scutum with medium density of granules. Free tergites I—II with a line of small tubercles of the same approximate size. Free tergite III with a row of tubercles larger than the ones on the other free tergites and the central tubercle slightly bigger than the others. Dorsal anal operculum with small sparse tubercles. *Venter*. Coxa I with several sparse tubercles, bigger than the ones in other coxae. Coxae II—IV with sparse numerous granules. Ventral anal operculum with granules. *Chelicerae*. segment II with several setae, mainly in the apical part. Fixed finger with eight and movable finger with 12 teeth. *Pedipalps*. Ventral side of trochanter with few sparse tubercles; tibia setation: prolateral IiIi, retrolateral IiI. Tarsal setation: prolateral IiI, retrolateral II, ventral side with two baso-apical lines of setae. *Legs*. Leg I: trochanter, femur, patellae and tibia with granules.

Leg II: Trochanter II with two retrolateral tubercles; femur, patella and tibia with granules. Leg III: trochanter, femur, patella and tibia with granules. Leg IV: coxa IV: robust apical prolateral apophysis, slightly inclined relative to the axis of the base of coxa IV, with ventral process and basal tubercle, with the approximate trochanter size; retrolateral apophysis small, not visible in dorsal view. Trochanter IV: prolateral small blunt apophysis; retrolateral side with a line of three big tubercles, two slightly more ventral. Femur IV: short and robust; all tubercles on prolateral row with approximately the same size; dorsal row of tubercles with a large tubercle before the DBA, DBA branched with the largest branch pointing upwards, one large tubercle after DBA; retrolateral row of with a big median apophysis, eight large tubercles before, three large (yet smaller than the ones anterior to the median apophysis) and three small tubercles posterior to the median apophysis, intercalated; all tubercles on the ventral row small. Tarsal formula: 3(3)-7(3)-4-5. *Male genitalia* (Fig. 14D— F). Ventral plate: Ventral face with microsetae on the whole extension; pronounced apical groove (reaching the line of the most basal MS C); lateral process median when compared to other species (e.g. ***Mischonyx petroleiros* sp. nov.**); three apical helicoidal MS C on each side; two MS E, ventral and in the same baso-apical orientation of MS C; one small MS D, basal relative to MS C and in the same dorso-ventral orientation of MS C; three spatular MS A, forming a parable line; one spatular MS B, smaller than MS A. Glans: Small dorsal process; flabellum triangular, with serrated margin; stylus with subapical microsetae, with the apex inclined relative to the penis axis and keeled. *Color*. Brown; dorsal scutum with yellowish tones; pedipalps and trochanters I— III yellow.

Female. (paratype; MZSP XXXXX): Measurements: Dorsal scutum: L: 4.2; W: 4.0. Prosoma: L: 1.3; W: 2.0; Femur IV: L: 3.9. Dorsal scutum outline α, with a constriction at the area III and evident *coda*; small median tubercles on each area; median tubercles on area III rounded; lateral tubercles of the dorsal scutum small and the most posterior are not fused; absence of prolateral and retrolateral apophysis on coxa IV; trochanter and femur IV unarmed.

***Mischonyx petroleiros* sp. nov.**

(Figs. 13, 14G— I, 22A, 22C)

Type material. BRAZIL. Rio de Janeiro: Nova Iguaçu, (Reserva Biológica Tinguá/ RPPN Petroleiros, 22°35'23.9"S 43°26'25.7"W), C. Sampaio, F. Uemori & C. T. Olivares

leg., 04-06.IV.2012, male holotype (MZSP XXXXX).

Etymology. From Latin language, *petroleiros* means “tankers”. The only individual collected is from a natural reserve which was from the Oil Tankers Union from Rio de Janeiro (RPPN Petroleiros). The epithet is due to this preserved area.

Diagnosis. It resembles *Mischonyx bresslaui* by the combinations of following characters: anterior margin of dorsal scutum with two tubercles on each side; several tubercles on area III elliptical; lateral margin of dorsal scutum with the most posterior lateral tubercles fused (forming bigger tubercles); all free tergites with small tubercles; retrolateral apophysis on coxa IV apparent on dorsal view; dorsal row on leg IV with a tubercle anterior to the DBA; retrolateral row on leg IV with a big median apophysis; ventral plate with three pairs of apical MS C. It differs from *M. bresslaui* by: median tubercles on area III elliptic but not strongly compressed laterally (strongly compressed in *M. bresslaui*); large tubercles on lateral margin of dorsal scutum (small in *M. bressslaui*); prolateral apophysis on coxa IV approximately with the same length of trochanter IV (smaller in *M. bresslaui*); DBA branched (not branched in *M. bresslaui*); dorsal row of tubercles of leg IV without large tubercles after DBA (three large tubercles after DBA in *M. bresslaui*); tubercles on the basal half of the retrolateral row of leg IV small (some are big in *M. bresslaui*); MS B as large as the MS A (reduced in *M. bresslaui*); MS A forming a dorso-ventral line and apparent (forming a triangle and hidden behind the ventral process); *flabellum* with serrated on margin (smooth in *M. bresslaui*).

Description. Male holotype: *Dorsum* (Figs. 13, 22A, 22C): Measurements: Dorsal scutum: L: 4.1; W:4.2; Prosoma: L:1.6; W: 2.1. Femur IV: 4.0. Scutum outline γP, widest at Mesotergal Area II. Anterior margin of carapace with two tubercles on each side, with approximately the same size. Frontal hump high, with two whitish tubercles (in ethanol). Anterior face of the ocularium with one pair of tubercles, one pair of median tubercles (as tall as the ocularium height). Lateral margin of prosoma with numerous small tubercles. Posterior part of prosoma with a pair of tubercles. Besides these tubercles, prosoma has a low density of granules (DaSilva & Pinto-da-Rocha, 2010). Dorsal scutum: area I divided by a median longitudinal groove, with a pair of dark median tubercles; area II with a pair of dark median tubercles slightly larger than the tubercles on area I; area III with a pair of dark median elliptic tubercles, larger than the ones on the other areas, and some sparse elliptic tubercles. Lateral margins of dorsal scutum with a row of whitish (in ethanol) big tubercles, reaching the posterior margin of area III; most posterior tubercles fused, forming large tubercles. Posterior margin of dorsal scutum with a line of white (in

ethanol) small tubercles of similar size. Dorsal scutum with low density of granules. All free tergites with a line of small tubercles of the same approximate size. Dorsal anal operculum with small sparse tubercles. *Venter*. Coxa I with several sparse tubercles, larger than the one in other coxa. Coxa II with sparse tubercles; the apical are larger. Coxae III and IV with granules. Ventral anal operculum with granules. *Chelicerae*. Middle segment with several setae, mainly in the apical part. Fixed and movable fingers with nine teeth each. *Pedipalps*. Tibia setation: prolateral IiIi, retrolateral IiI. Tarsal setation: prolateral II, retrolateral II, ventral side with two baso-apical lines of setae. *Legs*. Leg I: trochanter, femur, patella and tibia with granules. Leg II: Trochanter II with two retrolateral tubercles; femur, patella and tibia with granules. Leg III: trochanter, femur, patella and tibia with granules. Leg IV: Coxa IV: robust apical transversal prolateral apophysis, with ventral process, with the approximate trochanter size; retrolateral apophysis visible in dorsal view. Trochanter IV: prolateral small blunt apophysis; retrolateral side with small tubercles. Femur IV: short and robust; all tubercles on prolateral row with approximately the same size; dorsal row of tubercles with a large tubercle before the DBA, DBA branched with the largest branch pointing upwards, small tubercles after DBA; retrolateral row of with a big median apophysis, four big tubercles before and three large tubercles posterior to the median apophysis; all tubercles on the ventral row small. Tarsal formula: 4(3)-8(3)-8-5. *Male genitalia* (Fig. 14G—I). Ventral plate: Ventral face with microsetae on basal 2/3; pronounced apical groove (reaching the line of MS B); lateral process basal when compared to other species (e.g. *Mischonyx intervalensis* **sp. nov.**); three apical helicoidal MS C on each side; two MS E, ventral and slightly basal relative to MS C; small MS D, basal relative to MS C and between MS E and MS C; four spatular MS A, forming a diagonal baso-apical line; one spatular MS B, with the same size of MS A. Glans: Small dorsal process; flabellum triangular with serrated margin; no information regarding stylus (broken in the analyzed specimen). *Color*. Brown; dorsal scutum with tones of yellow; pedipalps and trochanters I— III yellow. *Female*. (paratype; MZSP XXXXX): Measurements: Dorsal scutum: L: 3.9; W: 3.4. Prosoma: L: 1.5; W: 2.0; Femur IV: L: 3.8. Dorsal scutum outline α, with a constriction at the chelicerae, area III and evident *coda*; small median tubercles on each area; median tubercles on Area III rounded; lateral tubercles of the dorsal scutum small and the most posterior are not fused; absence of prolateral apophysis on coxa IV, but with a small retrolateral apophysis; trochanter and femur IV unarmed.

Identification key for Mischonyx males

1. Median armature on Area I larger and lighter (in ethanol) than those on a area III (clearer than the general body color) 2

Median armature on area II smaller and with the same color (in ethanol) of those on area III (clearer than the general body color) …..... 3

2. Small individuals (3-3.5 mm of dorsal scutum); median armature on area II with same color (in ethanol) those on area I (lighter than general body color) ..…..... ***Mischonyx minimus* sp. n.**

Large individuals (7 – 8 mm); Median armature on area II with same color (in ethanol) those on area III (darker than the body color) ……..... *Mischonyx arlei* **comb. nov.**

3. More posterior lateral mid-bulge tubercles fused, forming larger tubercles, clearer than the rest of the body color 4

Lateral mid-bulge tubercles not fused …….... 6

4. Ellipsed tubercles on Mesotergal Area III strongly laterally compressed; only one clearly more developed apophysis on leg IV retrolateral row of tubercles …..... *Mischonyx bresslaui* **comb. nov.**

Ellipsed tubercles on area III not strongly compressed laterally; more than one developed aphophysis on leg IV, with retrolateral row of tubercles 5

5. DBA digitiform and uniramous ..... *Mischonyx poeta*

DBA birramous ..... ***Mischonyx petroleiros* sp. n.**

6. At least one mesotergal area with well-developed median armature 7

Mesotergal Areas with small tubercles with the same size 9

7. All mesotergal areas and posterior part of dorsal scutum with well-developed median armature ..... *Mischonyx squalidus* **comb. nov.**

Mesotergal areas II-III only with well-developed median armature 8

8. DBA branched, retrolateral branch being the largest; prolateral row of tubercles on leg IV with medial tubercles more developed ..... *Mischonyx processigerus*

DBA falciform, not branched and; prolateral row of tubercles on leg IV with tubercles of the same size …..... *Mischonyx insulanus*

9. Median tubercles on mesotergal area III small …..... 10

Median tubercles on mesotergal area III well-developed 11

10. Leg IV robust, with well-developed armature; DBA well-developed; dorsal row

of tubercles from leg IV with four well-developed tubercles after DBA; registers from Santa Catarina state ..... *Mischonyx clavifemur* **comb. nov.**

Leg IV long and thin, with few well-developed armatures located terminally; DBA small and sharp; without dorsal row of tubercles after DBA .... *Mischonyx intermedius*

11. DBA branched 12

DBA not branched 13

12. Retrolateral branch of DBA evidently larger than other branch; two apophysis on the leg IV dorsal row of tubercles, after DBA; prolateral apophysis of coxa IV with a prominent ventral process ..... ***Mischonyx intervalensis* sp. n.**

Both branches of DBA of the same size; two well-developed apophysis on leg IV retrolateral row of tubercles .....…..... *Mischonyx reitzi* **comb. nov.**

13. DBA robust and sharp, with a tubercle emerging from its median part and almost as high as the whole body 14

DBA smaller than the body height 15

14. DBA pointing upwards; after DBA, only one well-developed tubercle on the dorsal row ..... *Mischonyx parvus* **comb. nov.**

DBA pointing anteriorly; no well-developed tubercles on the dorsal row, after the DBA; lateral mid-bulge tubercles clearer than the general body color (in ethanol) …..... *Mischonyx fidelis*

15. DBA with the same approximate size of the other tubercles on the dorsal row …. ..... *Mischonyx kaisara*

DBA more developed than the tubercles on the dorsal row ..... *Mischonyx anomalus* **comb. nov.**

One extra row of tubercles between dorsal and prolateral rows; median tubercles on Leg IV prolateral row of tubercles more developed; one apophysis on the leg IV terminal third of the retrolateral row of tubercles ..... *Mischonyx holacanthus*

Mischonyx geographical distribution

The geographical distribution of all *Mischonyx* species is depicted at Figures 29 - 31. All species occurring from Santa Catarina until Espirito Santo states, throughout the Atlantic Forest and in some cerrado areas (Minas Gerais state). In general, all the species are restricted to specific localities, with exception of *M. anomalus*, which occur in the

whole Parana state, and *M. squalidus* **comb. nov.** which is a widespread species. This species occurs throughout the genus distribution and even in some regions which other species of the genus do not occur, such as Espírito Santo state. Moreover, this species present synanthropic behavior (Mestre & Pinto-da-Rocha, 2004) and can be found in degraded areas, such as regions with *Pinus* plantation and even in some pasture areas.

Discussion

Phylogenetic inference approaches

The phylogenetic hypothesis recovered in this research show some differences depending on which approach and dataset used.

Morphological data analysis (Figs. 1 and 2). Analysing the phylogenies strictly morphological, both of them present *Mischonyx arlei* and *Mischonyx minimus* **sp. nov.** as the first clade diverging inside the genus, followed by *M. intermedius*. Beyond these similarities, both analyses present the clade (*M. parvus* + (*M. clavifemur* + *M. anomalus*). Another similarity is *G. antiquus* as a member of *Mischonyx* genus. While the morphological analysis place it inside the genus, the other phylogenies, using molecular and TE, show it as unrelated to the genus. Therefore, it is not surprising that other authors placed this species in the genus by morphological similarity (Kury, 2003; Pinto-da-Rocha, 2012), once they share morphological characteristics, such as dorsal scutum outline γP, well-developed median tubercles on Area III, darker than the body general color, prolateral apophysis of coxa IV robust, with the approximate same size of trochanter IV. However, this shows the importance of using molecular evidence to infer phylogenetic hypothesis, once it presents a larger number of informative and independent characters, when we compare to the search for morphological characters (Hillis, 1996, 1998; Wiens, 2004).

Despite these agreements, some differences are clear between the trees. In ML1, *G. antiquus* diverges after *M. intermedius* branches off, while in MP1, it forms a clade with *M. processigerus*. Another difference is that, in ML1, after the divergence of *G. antiquus*, the clade sister to it branches into two major clades, while in MP1, after divergence of *M. intermedius*, there is a clade branching off holding *M. holacanthus*, *M. kaisara*, *M. poeta* and *M. squalidus*. Besides that, in ML1, *M. bresslaui* is sister to the clade containing *M. anomalus*, *M. clavifemur*, *M. intervalensis* **sp. nov.** and *M. parvus*. A clade with the first three species is recovered by molecular and TE analysis. In MP1,

M. bresslaui is separating this clade. In ML1, *M. fidelis* and *M. holacanthus* form a clade. This clade is recovered by molecular and TE analysis as well. In MP1 they are far from each other.

These differences show that ML1 presents more congruence of evidences with the analysis using molecular dataset. Puttick *et al.* (2017) suggest that using ML to infer morphological phylogenies can be less precise, when comparing to MP. Opposed to that, Lewis (2001) and Wright & Hillis (2014) expose that likelihood analysis conditional on morphological characters being variable and using MK model outperforms parsimony analysis. This research agrees with these two authors, once there are clades in ML1 which agree with molecular and TE analysis, such as (*M. clavifemur* + *M. anomalus*) and the proximity of (*M. intervalensis* **sp nov. +** *M. reitzi*) with this former clade, (*M. fidelis* + *M. holacanthus*), the proximity of *M. insulanus* and *M. kaisara*. Beyond that, ML1 present much higher general bootstrap support than MP1. This can be a signal of more favorable evidence for the hypothesis presented in ML1 when compared to MP1.

Molecular and TE analysis (Figs. 3-10). In MP2 and MP3, the topologies and relationships are the same. In ML3, after the inclusion of *M. arlei* (morphological data only), *Mischonyx intermedius* is recovered as sister of (*M. arlei* + *M. minimus* **sp. nov.**), different from in ML2, in which *M. intermedius* is sister to all the species from Rio de Janeiro State. This single change evidences that the 124 morphological characters do not change significantly the relationship hypothesis. This happens because there are much more informative characters in the 3742 bp than in the morphological dataset. In the complete TE dataset, morphological characters represent less than 3.2% of the analysed characters. Wiens (2004) and Baker & Gatesy (2002) support the hypothesis that morphological data in the framework is important especially in cases that there are some problematic or unresolved relationships in molecular data. The research of De Sá *et al.* (2014) support this hypothesis by showing that, in their target group, there were problematic relationships among species, which were better elucidated by the use of morphological and behavioural characters from both the larvae and adults of the studied frog species. Besides having some problematic relationships, in their work, De Sá *et al.* (2014) had more morphological data in proportion to molecular than in this research. Here, relationships between species seems to make sense when analyzing the morphological characters supporting groups and the biogeographical distribution of the clades. Hence, this change in *M. intermedius relationships* when adding morphological characters agrees with De Sá *et al.* (2014) and Wiens (2004) and suggests that *M.*

intermedius shares both morphological and molecular traits with *M. arlei* and *M. minimus* **sp. nov.** and the morphological dataset helped to understand the relationship in this clade.

Between the two approaches on TE analysis, topologies do not change significantly. ML3 and MP3 recover *M. arlei* and *M. minimus* **sp. nov.** as members of the genus and place *G. antiquus* outside *Mischonyx* clade, diverging in a lineage with *Ampheres leucopheus* (Caelopyginae). Both analyses support the existence of a clade that holds *M. insulanus* and *M. kaisara*, both species from the northern coast of São Paulo state (Serra do Mar region). However, in ML3, this clade is sister to the clade holding species from southern coast of São Paulo state, Paraná and Santa Catarina states, while in MP3, it is sister group to the lineage which holds all the other species. Another difference between the two TE phylogenies is that, in ML3, *M. intermedius*, the only known *Mischonyx* species from Minas Gerais state, is sister lineage to (*M. arlei* + *M. minimus* **sp. nov.**) clade, while in MP3, this species is sister lineage to the clade holding *M. anomalus*, *M. clavifemur*, *M. intervalensis* **sp. nov.** and *M. reitzi*. The third difference between both hypotheses is that, in ML3, *M. petroleiros* **sp. nov.** is sister species to the lineage containing *M. fidelis*, *M. holacanthus*, *M. parvus* and *M. squalidus*, while in MP3, it is sister species of *M. bresslaui*. And the last difference is that *M. poeta*, in ML3, is the sister species to the clade (*M. bresslaui* (*M. petroleiros* **sp. nov.** (*M. fidelis* + *M. holacanthus*) (*M. parvus* + *M. squalidus*))), while in MP3, it is sister to (*M. bresslaui* + *M. petroleiros* **sp. nov.**).

Therefore, by the analysis of both TE hypothesis, I will discuss from now on the hypothesis ML3.

The hypothesis of TE under maximum likelihood as the optimality criteria (ML3).

I have chosen to discuss ML3 grounded in the following arguments.

In ML3 hypothesis, *M. intermedius*, a species from Viçosa (Minas Gerais state), groups with (*M. arlei* + *M. minimus* **sp. nov.**) in a clade with all species from Rio de Janeiro state. In contrast, in MP3 it groups with (*M. intervalensis* **sp. nov.** (*M. anomalus* (*M. reitzi* + *M. clavifemur*), a clade with species from south of São Paulo, Paraná and Santa Catarina states. Harvestmen have low dispersion capacity and a high degree of endemism (Pinto-da-Rocha *et al.*, 2005). So, it makes more sense the hypothesis that diversification of lineages happens in areas close to each other. ML3 presents closer species diversifying in a clade than MP3, therefore, it is biogeographically (and

historically) more reliable. Heddin *et al.* (2012) support that biogeography is better than taxonomy to infer phylogenetic relationships in sclerosomatids harvestmen. This could be a hypothesis to work with in *Mischonyx* as well. This pattern could be an artifact due to poor sampling between areas, because there would be information lacking regarding species that occur in localities between the ones discussed here (Heath *et al.*, 2008; Hillis, 1998; Rosenberg & Kumar, 2001; Wheeler, 2004). Nonetheless, these areas are well-sampled in the records of Museu de Zoologia da Universidade de São Paulo and Instituto Butantan and there is no record of new species in the sampled area between Viçosa and Parque Estadual de Intervales. In order to gather more evidence on the subject, biogeographical analysis and estimates of divergence time of the nodes should be done, given that, with these new analysis, it would be possible to confront the data from vicariant events suggested by Pinto-da-Rocha *et al.* (2005) and Da Silva *et al.* (2017) with the divergence time of *Mischonyx* lineages.

Another reason is that the likelihood analysis points to a high degree of morphological similarity between *M. intermedius, M. arlei* and *M. minimus* **sp. nov.** (Figs 11, 15B, 15D, 18B, 18D). In ML3, when adding morphological characters and the terminal *M. arlei*, the analysis proposes the hypothesis of a clade with these species. The unambiguous morphological characteristics supporting this clade are: Area III with granules as armatures besides the median ones (#41-0), apical prolateral apophysis of coxa IV shorter than trochanter IV (#58-0), apical prolateral apophysis of coxa IV without secondary lobe (#60-0), apical prolateral apophysis oblique (#61-2) and femur IV thin and long (#71-1). These are characteristics that only these species share in the genus, therefore, it makes morphological sense to group them in a single clade.

Adding to that, in MP3, *M. petroleiros* **sp. nov.** presents more than 30 apomorphies. This represents almost a third of all characters. Given the number of morphological changes in the other branches and even looking at morphological changes in other harvestmen research (Bragagnolo & Pinto-da-Rocha, 2012; Da Silva & Gnaspini, 2009; Da Silva & Pinto-da-Rocha, 2010; Pinto-da-Rocha & Bragagnolo, 2010), it seems unlikely that this single species has passed through genetic drift or selection that would have changed the lineage that much. Therefore, the hypothesis of ML3 seems less improbable.

Finally, in MP3, there are nodes which are not supported by any morphological character (Fig. 10). Wipfler *et al.* (2015) support the idea that, in the field of phylogenetics, morphology is still important even with phylogenomic datasets, once “it

provides independent data for checking the plausibility of molecular phylogenies and is the only source of information for placing extinct taxa. It is the necessary basis for reconstructing character evolution on the phenotypic level and for developing complex evolutionary scenarios.". This is supported by Lee & Palci (2015) and Giribet (2015) as well. Hence, due to the lack of morphological character states supporting the nodes of interest in the MP3 analysis, the alternative hypothesis in ML3 is preferred, because its additional support in the form of morphology characters for the placement of *M. intermedius* with species from Rio de Janeiro. This convergence in data types, molecular and morphological, shows that the ML3 hypothesis should take priority.

Morphological character changes through ML3 phylogeny and bootstrap support

Mischonyx clade is supported by four morphological characters (Fig. 07): 9(0), lateral tubercles on anterior margin with the approximate same size (e.g. Fig. 17A); 46(1), median granulation density; 93(3), retrolateral row on femur IV with 3-6 apophysis on apical half (e.g. Fig. 18B) and 101(2), apical groove of ventral plate reaching the line of the second and third MS C (e.g. Fig. 25D). From these characters, only the 9(0) remains unaltered inside the genus. Character 46 changes in the clade *M. anomalus* (*M. clavifemur* + *M. reitzi*) to 46(2), high granulation density, and as apomorphy in *M. petroleiros* **sp. nov.** and *M. fidelis* to 46(0), low density. Character 93 changes into 91(1), two apophysis on the apical half, as apomorphy in *M. poeta*. Character 101 changes to 101(3), groove bottom is more basal than the MS C, as apomorphy in *M. insulanus* and *M. clavifemur*. The bootstrap value for *Mischonyx* in this analysis is 87 (Fig. 05).

This lineage splits into two major clades, both of them with only one characteristic supporting each one. The clade with species from São Paulo, Paraná and Santa Catarina (hereon SP-SC) is supported by character 92(1), the presence of a median apophysis on retrolateral row of tubercles. This character state supports two other lineages in the other major clade. It changes to 92(0), absence of central apophysis on retrolateral row, as apomorphy in *M. insulanus*. The bootstrap value is 98 for this node (Fig. 05). The clade (*M. kaisara* + *M. insulanus*), inside SP-SC, is also supported by a unique morphological synapomorphy: 43(1), median elliptic tubercles on area III. This clade has 100 as bootstrap value (Fig. 05), a high support as well, given the number of morphological synapomorphies. The other clade within SP-SC, *M. intervalensis* **sp. nov.** (*M. anomalus* (*M. clavifemur* + *M. reitzi*)) is supported by: character 15(1), spines as median armature

on ocularium; 76(1), DBA longer than larger; 112(0), MS D aligned with MS C in lateral view. Bootstrap value for this clade is 100. The inner clade, *M. anomalus* (*M. clavifemur* + *M. reitzi*), is supported by characters: 24(1), tubercles on the lateral margin darker than the rest of the body, 46(2), high granulation density (cited above), 70(2), apophysis on retrolateral side of trochanter IV, 71(1), single armature on the retrolateral side of trochanter IV, 93(2), two tubercles on the apical half of retrolateral row (cited above) and 94(0), retrolateral row without more developed apical tubercle. From all these characters, only 71 changes to 71(3), a line of three or more tubercles on retrolateral side of trochanter IV, as apomorphy of *M. reitzi*. Bootstrap value is also 100. The inner clade (*M. clavifemur* + *M. reitzi*) is supported only by the character 115(1), most basal MS E ventral and aligned to MS C and the bootstrap value is also 100. The high support values for SP-SC nodes in general, even when presenting a single morphological character supporting the clade suggests that there are molecular traits strongly supporting it.

The clade with species from Minas Gerais and Rio de Janeiro (MG-RJ) is supported by the character 121 (0), *flabellum* with serrated apex pointing to the base of the penis. Bootstrap value is 60 for this clade. The clade diverging more basally inside this clade is (*M. intermedius* (*M. arlei* + *M. minimus* **sp. nov.**), which is supported by characters: 41(0), area III with small tubercles besides the median ones; 58(0), apical prolateral apophysis on coxa IV smaller than trochanter IV; 60(0), absence of secondary distal lobe on apical prolateral apophysis on coxa IV; apical prolateral apophysis on coxa IV oblique; and 72(1) femur IV long and thin. The bootstrap value of this node is 61. The clade (*M. arlei* + *M. minimus* **sp. nov.**) is supported by characters: 24(2), lateral margin of dorsal scutum with tubercles with the same color of the rest of the body; 28(1), 29(0) and 30(0), median tubercles on area I lighterthan the rest of the body and bigger than the median tubercles on other areas; 33(0) and 34(0), median tubercles on area II clearer than the rest of the body and bigger than the median tubercles on other areas; 39(3) median tubercles on area III sharp; 51(1), central apophysis on free tergite II; 105(1), MS C sub-distal on the ventral plate; and 115(0), MS E ventral and aligned to the MS C. Bootstrap value of this node is 100.

The sister clade of (*M. intermedius* (*M. arlei* + *M. minimus* **sp. nov.**) is supported by characters: 32(0) other armatures besides the median ones in area II and 80(3), branched DBA. Character 80 is very variable throughout the entire phylogeny. Inside this clade, it changes to 80(0), digitiform DBA, as apomorphy of *M. poeta*, and 80(1), falciform DBA, in the clade ((*M. holacanthus* + *M. fidelis*) + (*M. squalidus* + *M. parvus*)).

Bootstrap value for the clade is 99. Inside this clade, diverges *M. processigerus* and its sister clade is supported by characters: 25(0), fused posterior tubercles on lateral margin of dorsal scutum; 59(1), basal tubercle on prolateral apophysis of coxa IV; 94(0), retrolateral row of tubercles without more developed apical tubercle; 99(1), sparse microsetae on the ventral part of ventral plate; 105(1), MS C sub-distal on ventral plate. Bootstrap value is 100. Only the character 78(0), DBA apex anteriorly directed, supports the sister clade of *M. processigerus*. There are two changes of this character inside this same clade: 78(2), DBA apex retrolaterally directed, as *M. petroleiros* **sp. nov.** apomorphy, and 78(1), DBA apex dorsally directed as *M. parvus* apomorphy. Bootstrap value for this branch is 94. Inside this clade, *M. bresslaui* diverges from the other species, which are in a lineage supported by characters: 64(0), prolateral apophysis on coxa IV absent in females; 100(0), ventral side of ventral plate not excavated; 108(1), MS B with the same size of MS A; and 115(1), MS E ventral and medial relative to MS C. All these characters changes inside the clade. Character 64 changes to 64(1), prolateral apophysis on coxa IV smaller in females than in males, as *M. parvus* apomorphy. The other characters change as apomorphy of *M. squalidus* to: 100(2), ventral side of ventral plate excavated; 108(0), MS B smaller than MS A; 115(0), MS E ventral and aligned to MS C. Bootstrap value for this branch is 96. From this node, branches *M. petroleiros* **sp. nov.**. Its sister clade is supported by characters: 80(1), DBA falciform and 121(1), *flabellum* with smooth ends. Character 80 changes as *M. parvus* apomorphy to 80(4), DBA conic. Bootstrap value for this branch is 100. Clade (*M. holacanthus* + *M. fidelis*) is supported by characters 62(0), prolateral apophysis on coxa IV with the base more than 4 times larger than the apex; 83(1), prolateral row of tubercles with medians larger; and 84(1), apical apophysis on prolateral row. Bootstrap value is 100. Finally, characters 51(1), free tergite II with central apophysis, 53(1) free tergite III with central apophysis; and 86 (1), presence of apophysis after DBA, support the clade (*M. squalidus* + *M. parvus*). Bootstrap value for this clade is 100.

By this section, it is clear that in both SP-SC and MG-RJ clades bootstrap values are considerably high for most of the groups. This suggests high degree of confidence in both clades and in the internal relationships inside them. Even though few morphological characters support some clades, if bootstrap value is high, this indicates that there are strong molecular evidence to support the lineages. Moreover, the supports specifically of SP-SC clade (all of them 100) indicates that is unlikely that *M. intermedius* could be inside this clade, otherwise its support would decrease. In other words, the maximum

bootstrap result means that the analysis recovered the clades in every one of the different samples it performed (Ramírez, 2005) and, thus, probably there is no other better hypothesis to explain the data better than this specific one. Therefore, it reinforces the idea that, *M. intermedius* do not belong to the clade SP-SC as MP3 indicates, once this analysis present lower bootstrap values within this clade.

Biogeographical remarks

In general, harvestmen present a high degree of endemism in the Atlantic Forest (Pinto-da-Rocha *et al.*, 2005). Species distributions throughout the order are restricted to specific areas of few thousands of square kilometers, with few exceptions (Pinto-da-Rocha *et al.*, 2005). One of these exceptions is *M. squalidus*. There are recordsof this species from Espirito Santo until Rio Grande do Sul states, occurring not only in Atlantic Rainforest but also in cerrado areas (Figs. 29-31), which are considerably drier than the Atlantic Rain Forest (Resende *et al.*, 2012). Mestre & Pinto-da-Rocha (2004) demonstrated that this species presents anthropic behavior, being found, for example, in residential areas and planting sites. Probably this anthropic behavior helps the species to disperse and colonize new areas more efficiently than most of harvestmen species. However, more studies regarding this species biology (and more comparative studies as well) are needed in order to understand what are the differences (behavioral, physiological, etc) between *M. squalidus* and other species that can explain this high dispersion and capacity to live in habitats that close related species are not able to live in.

Analyzing the biogeographical researches on harvestmen in Atlantic rainforest, the diversification of *Mischonyx* species follow roughly the same pattern of the vicariant events of the Areas of Endemism in this biome. Pinto-da-Rocha *et al.* (2005) suggest that there are eleven areas of endemism in the Atlantic Forest, from Bahia Santo to Santa Catarina states. First vicariant event splitted Bahia and Serra do Espinhaço areas from the remaining. Another, more recent other vicariant event, splitted Espirito Santo area from the others, followed by another vicariant event which splitted Serra dos Órgãos, Serra da Mantiqueira, South coast of Rio de Janeiro and Serra da Bocaina areas of endemism from Serra do Mar de São Paulo, South coast of São Paulo, Paraná and Santa Catarina areas (Pinto-da-Rocha *et al.*, 2005). Besides this research, Da Silva & Gnaspini (2010) present a phylogenetic hypothesis for Goniosomatinae with biogeographical remarks. At this subfamily level, the cladogenesis events of the six genus agrees with the biogeographical

breaks present in Pinto-da-Rocha *et al.* (2005). Moreover, in Peres *et al.* (2019), a phylogeographic work, authors agree with this same divergence pattern of clades inside Sodreaniinae. In the present work, the same pattern happens. *M. intermedius* is the only species from Serra do Espinhaço area of endemism. Given that there is no known *Mischonyx* species originally from Espirito Santo until now, this species appears on ML1 as sister group of species from Serra dos Órgãos area of endemism (*M. arlei* and *M. minimus* **sp. nov.**). The other species forming the Rio de Janeiro clade are located at this former area (*M. bresslaui*, *M. poeta*, *M. petroleiros* **sp. nov.**), Serra da Mantiqueira (*M. processigerus*) and south coast of Rio de Janeiro (*M. fidelis*, *M. parvus*, *M. holacanthus*) areas of endemism. The other clade has species from Serra do Mar of São Paulo (*M. insulanus* and *M. kaisara*), which forms the first clade to diverge, and the other clade holds the species from South of São Paulo (*M. intervalensis* **sp. nov.**), Paraná (*M. anomalus*) and Santa Catarina (*M. clavifemur* and *M. reitzi*) areas of endemism. This hypothesis agrees with the pattern found in biogeographical and phylogeographical research cited above.

To gather more evidence towards the relationships within *Mischonyx*, phylogeographical analysis can be performed in the future. This analysis could help to understand the variation of haplotypes of different species, estimate divergence time of clades and check whether the node ages agree with vicariant events in the past and access information regarding populational expansion and dispersion capacity of species. The dataset presented in this work presents the main genes used in previous phylogeographic work with Opiliones of Atlantic Forest: Internal Transcribed Spacer subunit II (Bragagnolo *et al.*, 2015; Peres *et al.*, 2017; Peres *et al.*, 2019), carbamoylphosphate synthetase 2 (Peres *et al.*, 2017; Peres *et al.*, 2019) histone H3 gene (Peres *et al.*, 2017; Peres *et al.*, 2019) Cytochrome Oxidase subunit I coding gene (Bragagnolo *et al.*, 2015; Peres *et al.*, 2017; Peres *et al.*, 2019). Therefore, making phylogeographyic analysis in the future is facilitated.

Finally, looking at the distribution area of each species, it is clear that most of *Mischonyx* species have their records restricted to only one or few points, close to each other. Apparently, most of its species present a high degree of endemism, as other harvestmen (Da Silva *et al.*, 2017). Serra do Órgãos, Mantiqueira, south coast of Rio de Janeiro and Serra do Mar areas of endemism hold 11 from the 16 species of the genus. According to Pinto-da-Rocha *et al.* (2005) and Da Silva *et al.* (2017), south coast of Rio de Janeiro and Serra dos Órgãos areas are the most species rich, which agrees with the

data found in this research. This is important information for conservational matters, once the few remaining harvestmen habitats that still exist are suffering by anthropic pressure (Morellato & Haddad, 2000) and, to maintain the diversity of the whole group, these areas deserve better attention regarding the creation of new protected areas (Da Silva *et al.*, 2017).

Conclusions

1- *Mischonyx* is monophyletic by both Total Evidence analysis (Maximum Likelihood and Maximum Parsimony), if adding *Michonyx arlei* **comb. nov** and removing *Gonyleptes antiquus*;

2- *Gonyleptes antiquus* returns to its former genus;

3- *Urodiabunus* is junior synonym of *Mischonyx*;

4- Three new species are described: *Mischonyx minimus* **sp. nov.**, *Mischonyx intervalensis* **sp. nov.** and *Mischonyx petroleiros* **sp. nov.**;

5- *Gerarcormobius bresslaui, Geraecormobius clavifemur, Geraecormobius reitzi* were transferred to *Mischonyx* and *M. cuspidatus* is junior synonym of *M. squalidus*;

6- The new composition of the genus is: *Mischonyx. anomalus* (Mello-Leitão, 1936) **comb. nov.**; *Mischonyx arlei* (Mello-Leitão, 1935b) **comb.nov.**, *Mischonyx bresslaui* (Roewer, 1927) **comb.nov.**, *Mischonyx clavifemur*, (Mello-Leitão, 1927a) **comb.nov.**,; *Mischonyx fidelis* (Mello-Leitão, 1931b); *M. holacanthus* (Mello-Leitão, 1927); *Mischonyx insulanus* (H. Soares, 1972); *Mischonyx intermedius* (Mello-Leitão, 1935b); *Mischonyx intervalensis* **sp. nov.**; *Mischonyx kaisara* (Vasconcelos, 2004); *Mischonyx minimus* **sp. nov.**; *Mischonyx parvus* (Roewer, 1917) **comb. nov.**; *Mischonyx poeta* (Vasconcelos, 2005); *Mischonyx processigerus* (Soares & Soares, 1970); *Mischonyx petroleiros* **sp. nov.**; *Mischonyx reitzi* (Vasconcelos, 2005) **comb.nov.**; *Mischonyx squalidus* Bertkau, 1880 **comb. nov.**;

7- The most plausible phylogenetic hypothesis was recovered using Total Evidence under Maximum Likelihood optimality criteria, due to morphological similarity of the clade holding *M. arlei*, *M. intermedius* and *M. minimus* **sp. nov.**, biogeographical traits of the clades, less apomorphies of *M. petroleiros* **sp. nov.**, high bootstrap supports inside *Mischonyx* and absence of morphological characters supporting clades in the other Total Evidence hypothesis (under maximum parsimony optimality criteria);

8- *Mischonyx* clade is supported by lateral tubercles on anterior margin with the approximate same size, median granulation density, retrolateral row on femur IV with 3-6 apophysis on apical half and apical groove of ventral plate reaching the line of the second and third MS C;

9- There are two major clade inside *Mischonyx*: one holding species from Rio de Janeiro (Serra dos Órgãos, Mantiqueira and south coast of Rio de Janeiro areas of endemism) and

Minas Gerais (Serra do Espinhaço area of endemism), and the other species from north coast of São Paulo (Serra do Mar area of endemism), south coast of São Paulo (South of São Paulo area of endemism), Paraná and Santa Catarina (Paraná and Santa Catarina area of endemism).

References

Acosta, L.E. 2019. A relictual troglomorphic harvestman discovered in a volcanic cave of western Argentina: *Otilioleptes marcelae*, new genus, new species, and Otilioleptidae, new family (Arachnida, Opiliones, Gonyleptoidea). PLoS ONE 14(10): e0223828. https://doi.org/10.1371/journal.pone.0223828

Arango, C.P. & Wheeler, W.C. 2007. Phylogeny of the sea spiders (Arthropoda, Pycnogonida) based on direct optimization of six loci and morphology. Cladistics 23: 255–293.

Baker R.H., Gatesy J. 2002. Is morphology still relevant? In: DeSalle R., Wheeler W., Giribet G. (eds) Molecular Systematics and Evolution: Theory and Practice. Vol 92: 163-174. Birkhäuser, Basel.

Benedetti, A. R. & Pinto-da-Rocha, R. 2019. Description of two new species of *Progonyleptoidellus* (Opiliones: Gonyleptidae), with a cladistic analysis of the genus, an overview of relationships in the K92 group, and taxonomic notes on *Deltaspidium*. Zootaxa, 4691(5), 461–490. doi:10.11646/zootaxa.4691.5.3.

Bertkau, P. 1880. Verzeichnis der von Prof. Ed. von Beneden auf seiner im Auftrage der Belgischen regierung untemommenen wissenschaftlichen Reise nach Brasilien und La Plata i. J. 1 872- 1 875 gesammelten Arachniden. Mém. cour. Acad. Belgique, 43 : 1 - 1 20.

Boyer, S. L., Baker, J. M. and Giribet, G. (2007), Deep genetic divergences in *Aoraki denticulata* (Arachnida, Opiliones, Cyphophthalmi): a widespread 'mite harvestman' defies DNA taxonomy. Molecular Ecology, 16: 4999-5016. doi:10.1111/j.1365-294X.2007.03555.x

Bragagnolo, C. & Pinto-da-Rocha, R. (2012). Systematic review of *Promitobates* Roewer, 1913 and cladistic analysis of Mitobatinae Simon, 1879 (Arachnida: Opiliones:Gonyleptidae). Zootaxa. 3308: 1-48.

Bragagnolo, C., Pinto-da-Rocha Ricardo, Antunes Manuel, Clouse Ronald M. (2015) Phylogenetics and phylogeography of a long-legged harvestman (Arachnida: Opiliones) in the Brazilian Atlantic Rain Forest reveals poor dispersal, low diversity

and extensive mitochondrial introgression. Invertebrate Systematics, 29: 386-404. https://doi.org/10.1071/IS15009

Cheng, R.-C. and Kuntner, M. (2014), Phylogeny suggests nondirectional and isometric evolution of sexual size dimorphism in argiopine spiders. Evolution, 68: 2861-2872. doi:10.1111/evo.12504

Chernomor, O., von Haeseler, A. & Minh, B.Q. 2016. Terrace aware data structure for phylogenomic inference from supermatrices. Systematic Biology. 65:997-1008.

Clouse R. M., de Bivort B. L., Giribet G. 2010. A phylogenetic analysis for the South-east Asian mite harvestman family Stylocellidae (Opiliones: Cyphophthalmi) – a combined analysis using morphometric and molecular data. Invertebrate Systematics 23, 515-529. https://doi.org/10.1071/IS09044

Colgan, D.J., McLauchlan, A., Wilson, G.D.F., Livingston, S.P., Edgecombe, G.D., Macaranas, J., Cassis, G. & Gray, M. R. 1998. Histone H3 and U2 snRNA DNA sequences and arthropod molecular evolution. Australian Journal of Zoology. 46: 419-437.

Farris, J. S. 1972. Estimating phylogenetic trees from distance matrices. Am. Nat. 106:645- 668.

Folmer O, Black M, Hoeh W, Lutz R, Vrijenhoek R. 1994. DNA primers for amplification of mitochondrial cytochrome C oxidase subunit I from diverse metazoan invertebrates. Mol Mar Biol Biotechnol. 3: 294–299.

DaSilva, M.B. & Gnaspini, P. 2010. Systematic revision of Goniosomatinae (Arachnida: Opiliones: Gonyleptidae), with a cladistic analysis and biogeographical notes. Invertebrate Systematics. 23(6): 530–624.

DaSilva, M.B. & Pinto-da-Rocha, R. 2010. Systematic review and cladistic analysis of the Hernandariinae (Opiliones: Gonyleptidae). Zoologia. 27(4): 577-642.

DaSilva, M.B., Pinto-da-Rocha, R., Morrone, J.J. 2017. Historical relationships of areas of endemism of the Brazilian Atlantic rainforest: a cladistic biogeographic analysis of harvestman taxa (Arachnida: Opiliones), Current Zoology, 63(5): 525–535,

https://doi.org/10.1093/cz/zow092

De Ley, P., Félix, M.A., Frisse, L.M., Nadler, S.A., Sternberg, P.W. & Thomas, W.K.. 1999. Molecular and morphological characterization of two reproductively isolated species with mirror image anatomy (Nematoda: Cephalobidae). Nematology. 2: 591–612.

De Sá, R.O., Grant, T., Camargo, A.W., Heyer, R., Ponssa, M.L. & Stanley, E. 2014. Systematics of the Neotropical Genus *Leptodactylus* Fitzinger, 1826 (Anura: Leptodactylidae): Phylogeny, the Relevance of Non-molecular Evidence, and Species Accounts. South American Journal of Herpetology 9(1). https://doi.org/10.2994/SAJH-D-13-00022.1

Dias, B.C.; Souza, E. S.; Hara, M.R.; Willemart, R.H. 2014. Intense leg tapping behavior by the harvestman *Mischonyx cuspidatus* (Gonyleptidae): an undescribed defensive behavior in Opiliones? The Journal of Arachnology 42(1), 123-125. https://doi.org/10.1636/Hi12-06.1

Dias, B.C.; Willemart, R.H. 2013. The effectiveness of post-contact defenses in a prey with no pre-contact detection. Zoology, Volume 116, Issue 3, Pages 168-174, ISSN 0944-2006, https://doi.org/10.1016/j.zool.2012.12.001.

Dunlop, J.A. 2007. Paleontology. In: Pinto-da-Rocha, R.; Machado, G. & Giribet, G. (Eds). Harvestmen. The Biology of Opiliones. Harvard University Press, Massachusetts. 595 pp.

Edgecombe, G.D. & Giribet, G. 2006. A century later – a total evidence re-evaluation of the phylogeny of scutigeromorpha centipedes (Myriapoda: Chilopoda). Invertebrates Systematics. 20: 503–525.

Ewing, B. & Green, P. 1998. Base-calling of automated sequencer traces using Phred. II, Error probabilities. Genome Research. 8: 186 -194.

Ewing, B., Hillier, L., Wendl, M.C. & Green, P. 1998. Base-calling of automated sequencer traces using Phred I. Accuracy assessment Genome Research. 8, 175–185.

Felsenstein, J. 1985. Phylogenies and the comparative method. The American Naturalist.

125: 1-15.

Folmer, O., Black, M., Hoeh, W., Lutz, R. & Vrijenhoek, R. 1994. DNA primers for amplification of mitochondrial cytochrome c oxidase subunit I from diverse metazoan invertebrates. Molecular Marine Biology and Biotechnology. 3: 294–299.

Kluge, A. & Grant, T. 2006. From conviction to antisuperfluity: old and new justifications of parsimony in phylogenetic inference. Cladistics. 22: 276-288.

Garwood, R. J., Sharma, P. P., Dunlop, J. A.; Giribet, G. 2014. A Paleozoic Stem Group to Mite Harvestmen Revealed through Integration of Phylogenetics and Development. Current Biology. Volume 24, Issue 9: 1017-1023. https://doi.org/10.1016/j.cub.2014.03.039.

Giribet G: Morphology should not be forgotten in the era of genomics — a phylogenetic perspective. Zool Anz 2015, 256:96-103.

Giribet, G., Rambla, M., Carranza, S., Baguñà,J., Riutort, M., Ribera, C. 1999. Phylogeny of the Arachnid Order Opiliones (Arthropoda) Inferred from a Combined Approach of Complete 18S and Partial 28S Ribosomal DNA Sequences and Morphology. Molecular Phylogenetics and Evolution, Volume 11, Issue 2, 296-307. https://doi.org/10.1006/mpev.1998.0583

Goloboff, P.A. 1999. Analyzing large data sets in reasonable times: solutions for composite optima. Cladistics 15: 415–428.

Goloboff, P. A. and Catalano, S. A. (2016), TNT version 1.5, including a full implementation of phylogenetic morphometrics. Cladistics, 32: 221-238. doi:10.1111/cla.12160.

Goloboff, P., Farris, J. & Nixon, K.C. 2008. TNT, a free program for phylogenetic analysis. Cladistics 24: 774–786.

Gordon, D., Abajian, C. & Green, P. 1998. Consed: a graphical tool for sequence finishing. Genome Research 8: 195–202.

Gordon, D., Desmarais, C. & Green, P., 2001. Automated finishing with autofinish. Genome Research 11: 614–625.

Grant, T. & Kluge, A. 2009. Parsimony, explanatory power, and dynamic homology testing. Systematics and Biodiversity. 7: 357-363.

Heath, T. A., Hedtke, S. M., & Hillis, D. M. (2008). Taxon sampling and the accuracy of phylogenetic analyses. *Journal of Systematics and Evolution*, *46*(3), 239-257. https://doi.org/10.3724/SP.J.1002.2008.08016

Hedin M, N Tsurusaki, R Macías-Ordóñez & JW Shultz (2012) Molecular systematics of sclerosomatid harvestmen (Opiliones, Phalangioidea, Sclerosomatidae): geography is better than taxonomy in predicting phylogeny. Molecular Phylogenetics and Evolution, 62, 224–236. https://doi.org/10.1016/j.ympev.2011.09.017

Hillis, D. M. 1996. Inferring complex phylogenies. Nature 383:140– 141.

Hillis, D.M. 1998. Taxonomic sampling, phylogenetic accuracy, and investigator bias. Syst. Biol. 47:3–8

Ji, Y.-J., Zhang, D.-X., He, L.-J., 2003. Evolutionary conservation and versatility of a new set of primers for amplifying the ribosomal internal transcribed spacer regions in insects and other invertebrates. Mol. Ecol. Notes 3, 581–585. https://doi.org/10. 1046/j.1471-8286.2003.00519.x.

Kalyaanamoorthy, S., Minh, B.Q., Wong, T.K.F., von Haeseler, A. & 2017. ModelFinder: Fast Model Selection for Accurate Phylogenetic Jermiin, L.S. Estimates. Nature Methodes. 14: 587-589.

Katoh, K., Misawa, K., Kuma, K. & Miyata, T. 2002. MS AFFT: a novel method for rapid multiple sequence alignment based on fast Fourier transform. Nucleic Acids Research. 33: 511–518.

Kluge, A. & Grant, T. 2006. From conviction to antisuperfluity: old and new justifications of parsimony in phylogenetic inference. Cladistics. 22: 276-288.

Kury, Adriano B., 2003. Annotated catalogue of the Laniatores of the New World (Arachnida, Opiliones). Revista Ibérica de Aracnología, volumen especial monográfico, 1: 5-337.

Kury, A.B. 2015. Classification of Opiliones. Museu Nacional/UFRJ website. Online at:

http://www.museunacional.ufrj.br/mndi/Aracnologia/opiliones.html

Kury, A. & Medrano, M. (2016) Review of terminology for the outline of dorsal scutum in Laniatores (Arachnida, Opiliones). Zootaxa. 4097(1): 130–134.

Kury, A.B. & Villareal, M.O. 2015. The prickly blade mapped: establishing homologies and chaetotaxy for macroseatae of penis ventral plate in Gonylepoidea (Arachinida, Opiliones, Laniatores). Zoological Journal of Linnean Society. 174(1), 1-46.

Larsson, A. 2014. AliView: a fast and lightweight alignment viewer and editor for large datasets. Bioinformatics. 30(22): 3276-3278. http://dx.doi.org/10.1093/bioinformatics/btu531

Lee, M. S. Y., & Palci, A. (2015). Morphological Phylogenetics in the Genomic Age. Current Biology, 25(19), R922–R929. doi:10.1016/j.cub.2015.07.009

Lewis, P.O. 2001. A Likelihood Approach to Estimating Phylogeny from Discrete Morphological Character Data. *Systematic Biology*, 50(6): 913–925. https://doi.org/10.1080/106351501753462876

Maddison, W. P. and D.R. Maddison. 2017. Mesquite: a modular system for evolutionary analysis. Version 3.31 http://mesquiteproject.org

Mello-Leitão, C. F. de, 1922. Some new Brazilian Gonyleptidae. Ann. Mag. Nat. Hist., 9(9): 329-349.

Mello-Leitão, C. F. de, 1926. Notas sobre Opiliones Laniatores sul-americanos. Revista Museu paulista, 14: 327-383.

Mello-Leitão, C. F. de, 1927b. Generos novos de Gonyleptideos (Nota previa). Mus. nac. Rio de J., 3 (2): 13-22.

Mello-Leitão, C. F. de, 193ld. Opiliões novos ou críticos. Archos Mus. nac. Rio de J., 33(3): 1 1 7- 148.

Mello-Leitão, C. F. de, 1932. Opiliões do Brasil. Revista Museu paulista, 1 7(2): 1 -505.

Mello-Leitão, C. F. de, 1934. Novos Gonyleptidae nas Cal. do Instituto Butantan. Mem. Inst. Butantan, 8: 409-417.

Mello-Leitão, C. F. de, 1935a. Alguns novos opiliões do Estado de S. Paulo e do Districto Federal. Archos Mus. nac. Rio de J., 36: 9-37.

Mello-Leitão, C. F. de, 1935b. Algumas notas sobre os Laniatores. Archivos Mus. Nac. Rio de J., 3 6(4): 87- 1 1 6.

Mello-Leitão, C. F. de, 1937a. Alguns opiliões da colecção do Instituto Butantan. Mem. Inst. Butantan, 1 1 : 275-288.

Mello-Leitão, C. F. de, 1937b. Notas sobre opiliões do Instituto Butantan. Mem. Inst. Butantan, 10: 289-295 .

Mello-Leitão, C. F. de, 1 940b. Sete gêneros e vinte e oito espécies de Gonyleptidae. Archivos Zoo/. Est. S. Paulo, 1 (1): 1 -52.

Mendes, A. C. (2011). Phylogeny and taxonomic revision of Heteropachylinae (Opiliones: Laniatores: Gonyleptidae). Zoological Journal of the Linnean Society. 163: 437–483.

Mestre, L.A.M. & Pinto-da-Rocha, R. (2004). Population dynamics of an isolated population of the harvestman *Ilhaia cuspidata* (Opiliones, Gonyleptidae), in araucaria forest (Curitiba, Paraná, Brazil). Journal of Arachnology. 32(2): 208–20.

Meyer CP. Molecular systematics of cowries (Gastropoda: Cypraeidae) and diversification patterns in the tropics. Biol J Linn Soc. 2003;79:401–459. doi: 10.1046/j.1095-8312.2003.00197.x.

Minh, B.Q., Nguyen, M.A.T. & von Haesler, A. 2013. Ultrafast approximation for phylogenetic bootstrap. Molecular Biology and Evolution. 30: 1118-1195.

Morellato, L.P.C. & C.F.B. Haddad. 2000. Introduction: the Brazilian Atlantic Forest. Biotropica 32(4b):786–792.

Nguyen, L.T., Schmidt, H.A., von Haeseler, A., & Minh, B.Q. 2015. IQ-TREE: A fast and effective stochastic algorithm for estimating maximum likelihood phylogenies. Molecular Biology and Evolution. 32:268-274

Nixon, K.C. 1999. The parsimony ratchet, a new method for rapid parsimony analysis.

Cladistics. 15: 407- 414.

Nixon, K.C. 2002. Winclada (BETA) ver. 1.00.08 New York, Published by author, Ithaca.

Palumbi, S.R., 1996. Nucleic acids, II: the polymerase chain reaction. In: Hillis, D.M., Moritz, C., Mable, B.K. (Eds.), Molecular Systematics. Sinauer Associates, Sunderland, MA, pp. 205–247.

Peres, E.A., Benedetti, A.R., Hiruma, S.T., Sobral-Souza, T., & Pinto-da-Rocha, R. (2019). Phylogeography of Sodreaninae harvestmen (Arachnida: Opiliones: Gonyleptidae): insights into the biogeography of the southern Brazilian Atlantic Forest. Molecular Phylogenetics and Evolution. doi:10.1016/j.ympev.2019.05.028

Peres, E.A., DaSilva, M.B., Antunes, M., Pinto-Da-Rocha, R., 2018. A short-range endemic species from south-eastern Atlantic Rain Forest shows deep signature of historical events: phylogeography of harvestmen Acutisoma longipes (Arachnida: Opiliones). Syst. Biodivers. 16, 171–187. https://doi.org/10.1080/14772000.2017.1361479

Pinto-da-Rocha, R. (1997) Systematic review of the Family Stygnidae Opiliones: Laniaores: Gonyleptoidea). Arquivos de Zoologia, 33 (4), 163–342. http://dx.doi.org/10.11606/issn.2176-7793.v33i4p163-342.

Pinto-da-Rocha, R. 2002. Systematic review and cladistics analysis of the Caelopyginae (Opiliones, Gonyleptidae). Arquivos Zoologia. 36:357-464.

Pinto-da-Rocha, R. & Bragagnolo, C. 2010. Systematic revision and cladistic analysis of the Brazilian subfamily Sodreaninae (Opiliones: Gonyleptidae). Invertebrate Systematics, 24, 509-538.

Pinto-da-Rocha, R., DaSilva, M.B. & Bragagnolo, C. (2005). The Faunistic similarity and historic biogeography of the harvestmen of southern and southeastern atlantic rain forest of Brazil. The Journal of Arachnology, 33, 290–299.

Pinto-da-Rocha, R., Benedetti, A.R., Vasconcelos, E. & Hara, M.R. 2012. New systematic assignments in Gonyleptoidea (Arachnida, Opiliones, Laniatores).

Zookeys. 198, 25-68.

Pinto-da-Rocha, R., Bragagnolo, C., Marques, F.P.L. & Antunes Junior, M. 2014. Phylogeny of harvestmen family Gonyleptidae inferred from a multilocus approach (Arachnida: Opiliones). Cladistics. 30: 519-539.

Prendini, L., Weygoldt, P. & Wheeler, W.C. 2005. Systematics of the *Damon variegatus* group of African whip spiders (Chelicerata: Amblypygi): evidence from behaviour, morphology and DNA. Organisms Diversity & Evolution 5: 203–236.

Puttick, M.N., O'Reilly, J.E., Tanner, A.R., Fleming, J.F., Clark, J., Holloway, L., Lozano-Fernandez, J., Parry, L.A., Tarver J.E., Pisani, D. & Donoghue P.C.J. 2017. Uncertain-tree: discriminating among competing approaches to the phylogenetic analysis of phenotype data. Proc. R. Soc. B, 284. http://doi.org/10.1098/rspb.2016.2290.

Rambaut, A. (2010) FigTree v1.3.1. Institute of Evolutionary Biology, University of Edinburgh, Edinburgh. http://tree.bio.ed.ac.uk/software/figtree/

Ramírez, M. J. (2005). Resampling measures of group support: a reply to Grant and Kluge. Cladistics, 21(1): 83–89. doi:10.1111/j.1096-0031.2004.00046.x

Resende, L.P.A., Pinto-da-Rocha, R. & Bragagnolo, C. (2012). The harvestmen fauna (Arachnida: Opiliones) of the Parque Estadual Carlos Botelho, and the Floresta Nacional de Ipanema, São Paulo, Brazil. Biota Neotropica, 12(4), 146-155. https://dx.doi.org/10.1590/S1676-06032012000400016

Reyda, F.B. & Olson, P.D. 2003. Cestodes of Peruvian freshwater stingrays. Journal of Parasitology 89: 1018–1024.

Rocha DFO, Wouters FC, Zampieri DS, Brocksom TJ, Machado G, Marsaioli AJ (2013a) Harvestmen phenols and benzoquinones: characterisation and biosynthetic pathway. Molecules 18: 11429–11451

Rosenberg, M.S. & Kumar, S. 2001 Incomplete taxon sampling is not a problem for phylogenetic inference. Proceedings of the National Academy of Sciences, 98 (19) 10751-1075. http://doi.org/10.1073/pnas.191248498.

Sánchez-Pacheco, S.J., Torres-Carvajal, O., Aguirre-Peñafiel, V., Sales Nunes, P.M., Verrastro, L., Rivas, G.A., Rodrigues, M.T., Grant, T. & Murphy, R.W. 2017. Phylogeny of *Riama* (Squamata: Gymnophthalmidae), impact of phenotypic evidence on molecular datasets, and the origin of the Sierra Nevada de Santa Marta endemic fauna. Cladistics, 34(3), 260-291. doi:10.1111/cla.12203.

Sereno, P.C. 2007. Logical basis for morphological characters in phylogenetics. Cladistics. 23(6): 565-587.

Sharma, P. & Giribet, G. 2011. The evolutionary and biogeographic history of the armoured harvestmen – Laniatores phylogeny based on the molecular markers, with the description of two new families of Opiliones (Arachnida). Invertebrate Systematics. 25:106-142.

Shultz, J.W. 1998. Phylogeny of Opiliones (Arachnida): an assessment of the "Cyphopalpatores" concept. The Journal of Arachnology, 26 (3), 257–272.

Strong, E.E. & Lipscomb, D. 1999. Character coding and inapplicable data. Cladistics.15: 363-371.

Schwarz, G. 1978. Estimating the dimension of a model. The Annals of Statistics. 6(2): 461-464.

Sundevall, C.J. 1833. Conspectus Arachnidum. 39pp. C.F. Berling, London.

Varón, A., Vinh, L.S. & Wheeler, W.C. 2010. POY version 4: phylogenetic analysis using dynamic homologies. Cladistics. 26: 72-85.

Vasconcelos. E. G. 2003. Revisão Sistemática de *Mischonyx* Bertkau, 1880 (Opiliones: Laniatores: Gonyleptidae). Dissertação de mestrado apresentada na Universidade Federal do Rio de Janeiro.

Vasconcelos, E.G. 2004. Nova espécie de *Mischonyx* Bertkau, 1880 do litoral norte do Estado de São Paulo, Brasil (Opiliones, Laniatores, Gonyleptidae). Revista Ibérica de Aracnologia. 10: 129-132.

Vasconcelos, E. G. 2005. Nova espécie de *Mischonyx* do estado do Rio de Janeiro, Brasil (Arachnida, Opiliones, Gonyleptidae). Iheringia, Sér. Zool., Porto Alegre, v. 95, n. 3,

p. 229-232

Vaschetto, L. M., González-Ittig, R. E., Vergara, J. and Acosta, L. E. (2015), High genetic diversity in the harvestman Geraeocormobius sylvarum (Arachnida, Opiliones, Gonyleptidae) from subtropical forests in north-eastern Argentina revealed by mitochondrial DNA sequences. J Zoolog Syst Evol Res, 53: 211-218. doi:10.1111/jzs.12093.

Vaidya, G., Lohman, D. J. and Meier, R. (2011), SequenceMatrix: concatenation software for the fast assembly of multi-gene datasets with character set and codon information. Cladistics, 27: 171-180. doi:10.1111/j.1096-0031.2010.00329.x

Wheeler, Q.D. 2004. Taxonomic triage and the poverty of phylogeny Phil. Trans. R. Soc. Lond. B: *Biological Sciences,* 359(1444), 571–583. http://doi.org/10.1098/rstb.2003.1452

Wheeler, W.C. 1996. Optimization Alignment: the end of multiple sequence alignment in phylogenetics? Cladistics. 12: 1-9.

Wheeler, W.C. 2001a. Homology and the optimization of DNA sequence data. Cladistics 17: 3–11.

Wheeler, W.C., 2001b. Homology and DNA sequence data. In: Wagner, G.P. (Ed.), The Character Concept in Evolutionary Biology. Academic Press, New York, pp. 303–318.

Wheeler, W.C. 2003. Iterative pass optimization of sequence data. Cladistics 19: 254–260.

Wiens, J.J. 2004. The Role of Morphological Data in Phylogeny Reconstruction, *Systematic Biology*, 53(4): 653–661. https://doi.org/10.1080/10635150490472959

Willemart, R. H. & Pellegatti-Franco, F. 2006. The spider *Enoploctenus cyclothorax* (Araneae, Ctenidae) avoids preying on the harvestmen *Mischonyx cuspidatus* (Opiliones: Gonyleptidae). The Journal of Arachnology, 34(3), 649-652. https://doi.org/10.1636/S05-70.1

Wipfler, B., Pohl, H, Yavorskaya, M.I. & Beutel, R.G. 2016. A review of methods for analysing insect structures — the role of morphology in the age of phylogenomics,

Current Opinion in Insect Science, 18: 60-68. https://doi.org/10.1016/j.cois.2016.09.004.

Wright, A.M. & Hillis, D.M. 2014. Bayesian Analysis Using a Simple Likelihood Model Outperforms Parsimony for Estimation of Phylogeny from Discrete Morphological Data. PLoS ONE 9(10): e109210. https://doi.org/10.1371/journal.pone.0109210

Attachments

Table 01: List of type specimens analyzed to compare with USP Arachnology lab material. It is present the original name and the name after Kury (2003), which synonymized most of these species with *Mischonyx*. Terminology: IBSP – Butantan Institut, São Paulo, Brasil; MNRJ – Nacional Museum of Rio de Janeiro, Rio de Janeiro, Brasil; MZSP – Zoology Museum of Universidade de São Paulo, São Paulo, Brasil; SMF – Senckenberg Natural History Museum, Frankfurt, Germany.

Original species name	Museum/Number	Type	Descriptor	Locality	Kury (2003)
Arleius incisus	IBSP 11	Holotype	Mello-Leitão, 1934	Unkown	*Mischonyx antiquus*
Cryptomeloleptes spinosus	SMF 1420	Syntype	Roewer, 1914	Teresópolis	*Geraecomorbius bresslaui*
Eduardoius granulosus	SMF 1331	Holotype	Roewer, 1916	Santos*	*Mischonyx squalidus*
Eduardouius fidelis	SME 900	Holotype	Roewer, 1913	Ilha grande	*Mischonyx cuspidatus*
Geraecormobius cheloides	MZSP 23147	Paratype	Vasconcelos, 2004	Ilhabela	*Mischonyx kaisara*
Geraecormobius spinifrons	MZSP 23696	Paratype	Vanconcelos, 2005	Casemiro de Abreu	*Mischonyx poeta*
Giltaya solitaria	MNRJ-HS 361	Holotype	Soares, 1972	Ilha de São Sebastião	*Mischonyx insulanus*
Gonyleptes antiquus	MNRJ 1408	Syntype	Mello-Leitão, 1931	Piraí	*Mischonyx fidelis*
Ilhaia cuspidata	MNRJ 1469	Holotype	Mello-Leitão, 1927	Niterói	*Mischonyx holacanthus*
Ilhaia insulana	MNRJ 1483	Holotype	Mello-Leitão *in litteris*	Niterói	*Mischonyx holacanthus*
Ilhaia intermedia	IBSP 46	Holotype	Moojen, 1934	Viçosa, MG	*Mischonyx intermedius*
Ilhaia meridionalis	MNRJ 1479	Holotype	Mello-Leitão, 1931	Piraí	*Mischonyx cuspidatus*
Mischonyx kaisara	MNRJ 42282	Holotype	Mello-Leitão, 1936	Antonina	*Mischonyx anomalus*
Mischonyx poeta	MNRJ 11392	Holotype	Mello-Leitão, 1931	Rio de Janeiro	*Mischonyx squalidus*
Pernygorna infuscata	MNRJ 11418	Holotype	Mello-Leitão, 1942	Santa Teresa	*Geraecormobius cervifrons*
Urodiabunus arlei	MNRJ 42695	Syntype	Mello-Leitão, 1936	Viçosa	*Mischonyx intermedius*
Weyhia absconsa	MNRJ 42476	Syntype	Mello-Leitão, 1935	Petrópolis	*Urodiabunus arlei*
Weyhia bresslaui	MNRJ 58236	Holotype	Mello-Leitão, 1940	Rio de Janeiro	*Geraecormobius convexus*
Weyhia clavifemur	MNRJ 1473	Holotype	Mello-Leitão, 1932	Rio de Janeiro	*Mischonyx cuspidatus*
Weyhia montis	MNRJ 1496	Holotype	Mello-Leitão, 1927	Blumenau	*Geraecormobius clavifemur*
Weyhia parva	MNRJ 41759	Holotype	Mello-Leitão, 1935	Rio de Janeiro	*Mischonyx squalidus*
Weyhia vellardi	MNRJ 1474	Holotype	Mello-Leitão, 1927	Blumenau	*Mischonyx meridionalis*
Xundrava anomala	MNRJ 1501	Holotype	Mello-Leitão, 1932	Niterói	*Mischonyx holacanthus*
Xundrava holacantha	MNRJ 42461	Holotype	Mello-Leitão, 1935	Petrópoliss	*Geraecormobius spinifrons*

Tabel 02: Sequenced genes per taxon. Out./In: Outgroup or Ingroup. Bp: Total number of base pairs sequenced. Numbers below each gene represent the base pairs sequenced for each gene. X represents the genes thar could not be sequenced.

Taxon/ LAL Voucher	**Out./ In.**	**Bp**	**12S**	**16S**	**28S**	**CAD**	**COI**	**H3**	**ITS**
Ampheres leucopheus 377	Outgroup	3742	408	386	974	639	570	309	456
Deltaspidium asperum 2201	Outgroup	3742	408	386	974	639	570	309	456
Deltaspidium orguense 0520	Outgroup	3742	408	386	974	639	570	309	456
Deltaspidium tenue 0102	Outgroup	3286	408	386	974	639	570	309	X
Gonyleptes horridus 0103	Outgroup	3103	408	386	974	X	570	309	456
Heliella singularis 1837	Outgroup	3103	408	386	974	X	570	309	456
Multumbo dimorphicus 0069	Outgroup	3103	408	386	974	X	570	309	456
Multumbo terrenus 2136	Outgroup	3742	408	386	974	639	570	309	456
Piassagera brieni 0141	Outgroup	2647	408	386	974	X	570	309	X
Promitobates ornatus 0054	Outgroup	2647	408	386	974	X	570	309	X
Pseudotrogulus telluris 2118	Outgroup	3742	408	386	974	639	570	309	456
Roeweria virescens 0081	Outgroup	2647	408	386	974	X	570	309	X
Sodreana sodreana 0056	Outgroup	3742	408	386	974	639	570	309	456
Mischonyx anomalus 0122	Ingroup	3103	408	386	974	X	570	309	456
Mischonyx anomalus 0693	Ingroup	3742	408	386	974	639	570	309	456
Mischonyx anomalus 1638	Ingroup	3742	408	386	974	639	570	309	456
Mischonyx anomalus 2953	Ingroup	3742	408	386	974	639	570	309	456
Mischonyx anomalus 3363	Ingroup	2647	408	386	974	X	570	309	X
Mischonyx antiquus 3707	Ingroup	3742	408	386	974	639	570	309	456
Mischonyx antiquus 3708	Ingroup	3742	408	386	974	639	570	309	456
Mischonyx bresslaui 0111	Ingroup	3742	408	386	974	639	570	309	456
Mischonyx bresslaui 2120	Ingroup	3742	408	386	974	639	570	309	456
Mischonyx bresslaui 2152	Ingroup	3742	408	386	974	639	570	309	456
Mischonyx bresslaui 2809	Ingroup	3334	X	386	974	639	570	309	456
Mischonyx bresslaui 3375	Ingroup	2647	408	386	974	X	570	309	X
Mischonyx clavifemur 0079	Ingroup	3742	408	386	974	639	570	309	456
Mischonyx clavifemur 0845	Ingroup	3103	408	386	974	X	570	309	456
Mischonyx insulanus 0143	Ingroup	3103	408	386	974	639	570	309	456
Mischonyx insulanus 1374	Ingroup	3742	408	386	974	X	570	309	456
Mischonyx insulanus 1455	Ingroup	3433	408	386	974	639	570	X	456
Mischonyx insulanus 2345	Ingroup	3742	408	386	974	639	570	309	456
Mischonyx insulanus 3066	Ingroup	3334	X	386	974	639	570	309	456
Mischonyx intermedius 4116A	Ingroup	2948	X	X	974	639	570	309	456
Mischonyx intermedius 4116B	Ingroup	2360	X	386	X	639	570	309	456
Mischonyx intermedius 4117A	Ingroup	1974	X	X	X	639	570	309	456
Mischonyx intervalensis 0099	Ingroup	3742	408	386	974	639	570	309	456
Mischonyx intervalensis 3709	Ingroup	3742	408	386	974	639	570	309	456
Mischonyx kaisara 3575	Ingroup	3103	408	386	974	X	570	309	456
Mischonyx minimus 3649	Ingroup	3742	408	386	974	639	570	309	456
Mischonyx parvus 3621A	Ingroup	3742	408	386	974	639	570	309	456
Mischonyx parvus 3621B	Ingroup	3742	408	386	974	639	570	309	456
Mischonyx parvus 3651A	Ingroup	3742	408	386	974	639	570	309	456
Mischonyx poeta 3650A	Ingroup	3742	408	386	974	639	570	309	456
Mischonyx poeta 3650B	Ingroup	3742	408	386	974	639	570	309	456
Mischonyx processigerus 0463	Ingroup	3742	408	386	974	639	570	309	456
Mischonyx processigerus 3648	Ingroup	3742	408	386	974	639	570	309	456
Mischonyx proletariae 2361	Ingroup	2647	408	386	974	X	570	309	X
Mischonyx reitzi 0672	Ingroup	3742	408	386	974	639	570	309	456
Mischonyx squalidus 0085	Ingroup	3742	408	386	974	639	570	309	456

Mischonyx squalidus 2026	Ingroup	3742	408	386	974	639	570	309	456
Mischoyx fidelis 4115A	Ingroup	3334	X	386	974	639	570	309	456
Mischoyx fidelis 4115B	Ingroup	2948	X	X	974	639	570	309	456

Figure 01: Likelyhood hypothesis with morphological data only. The values near the nodes are the Bootstrap values of each one. Numbers after the species name are the LAL Vouchers of each individual.

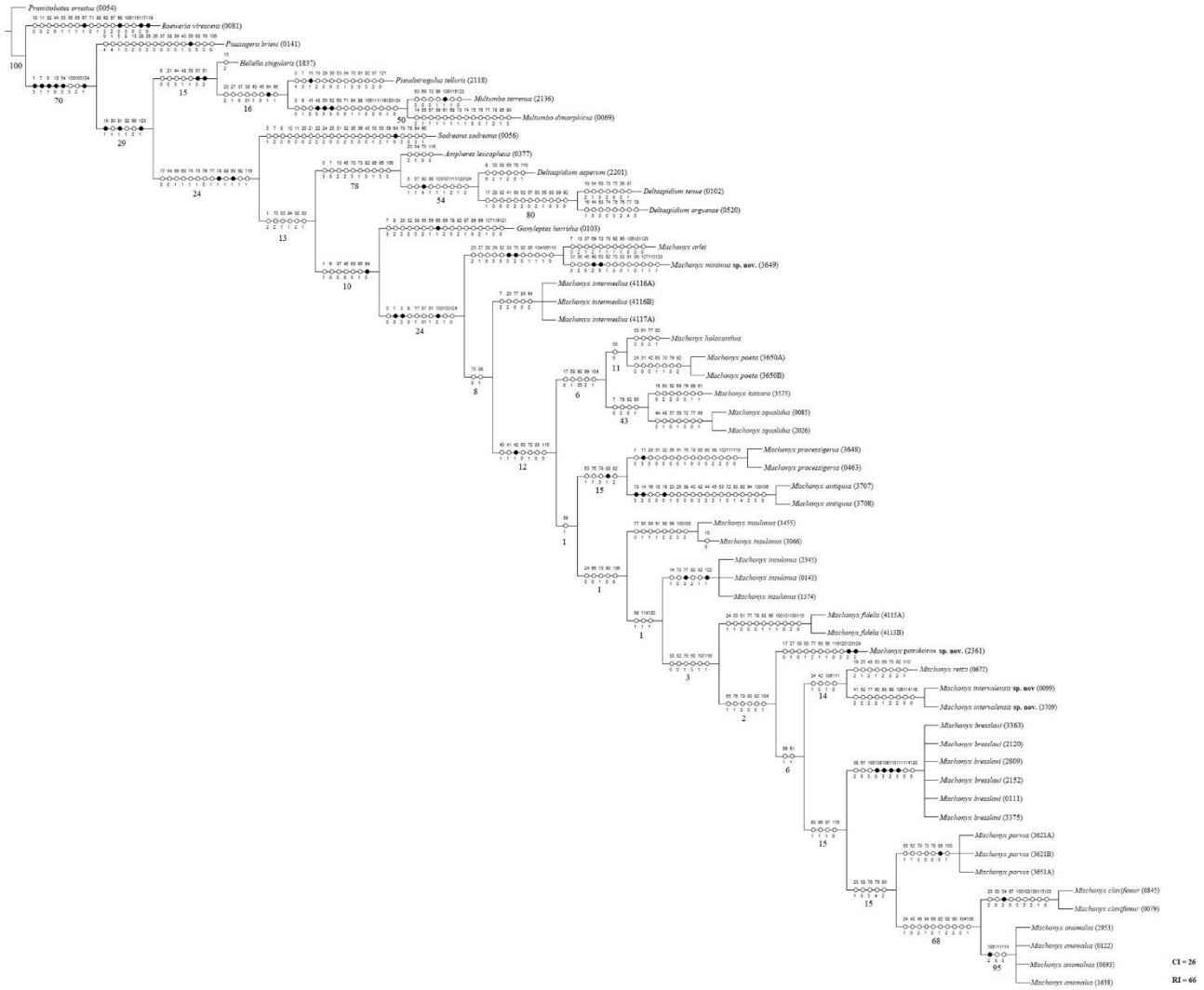

Figure 02: Strict consensus of the three most parsimonious trees with morphological data only. The values near the nodes are the Bootstrap values of each one. Numbers after the species name are the LAL Vouchers of each individual. Consistency and Retention indexes are expressed in the right bottom.

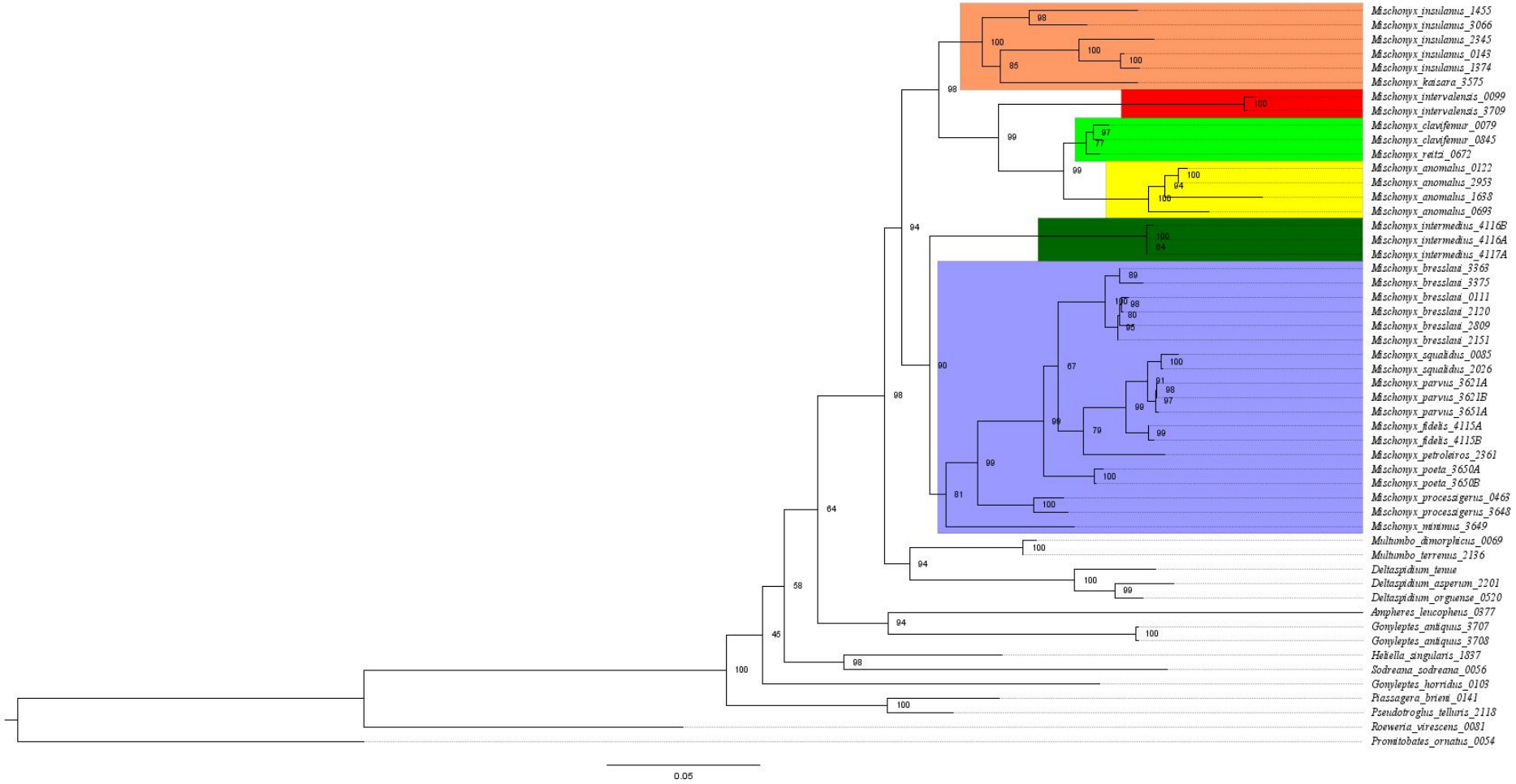

Figure 03: Likelyhood hypothesis with molecular data only. The values near the nodes are the bootstrap values of each one. Numbers after the species name are the LAL Vouchers of each individual. The colored clades are according to their location. Light green: Santa Catarina; yellow: Parana; Red: south of São Paulo; orange: north of São Paulo; blue: Rio de Janeiro; dark green: Minas Gerais.

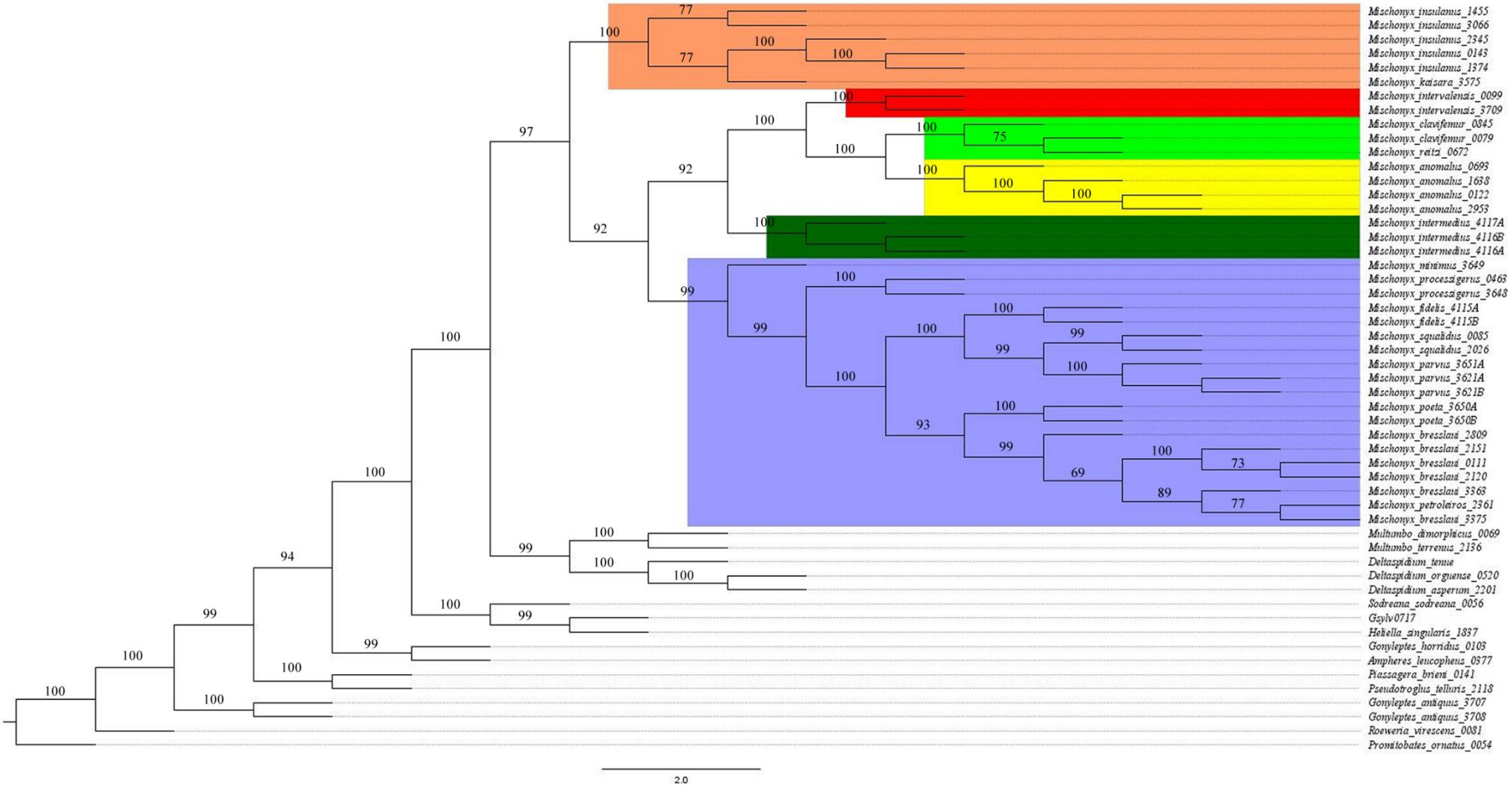

Figure 04: Parsimony hypothesis with molecular data only. The values near the nodes are the bootstrap values of each one. Numbers after the species name are the LAL Vouchers of each individual. The colored clades are according to their location. Light green: Santa Catarina; yellow: Parana; Red: south of São Paulo; orange: north of São Paulo; blue: Rio de Janeiro; dark green: Minas Gerais.

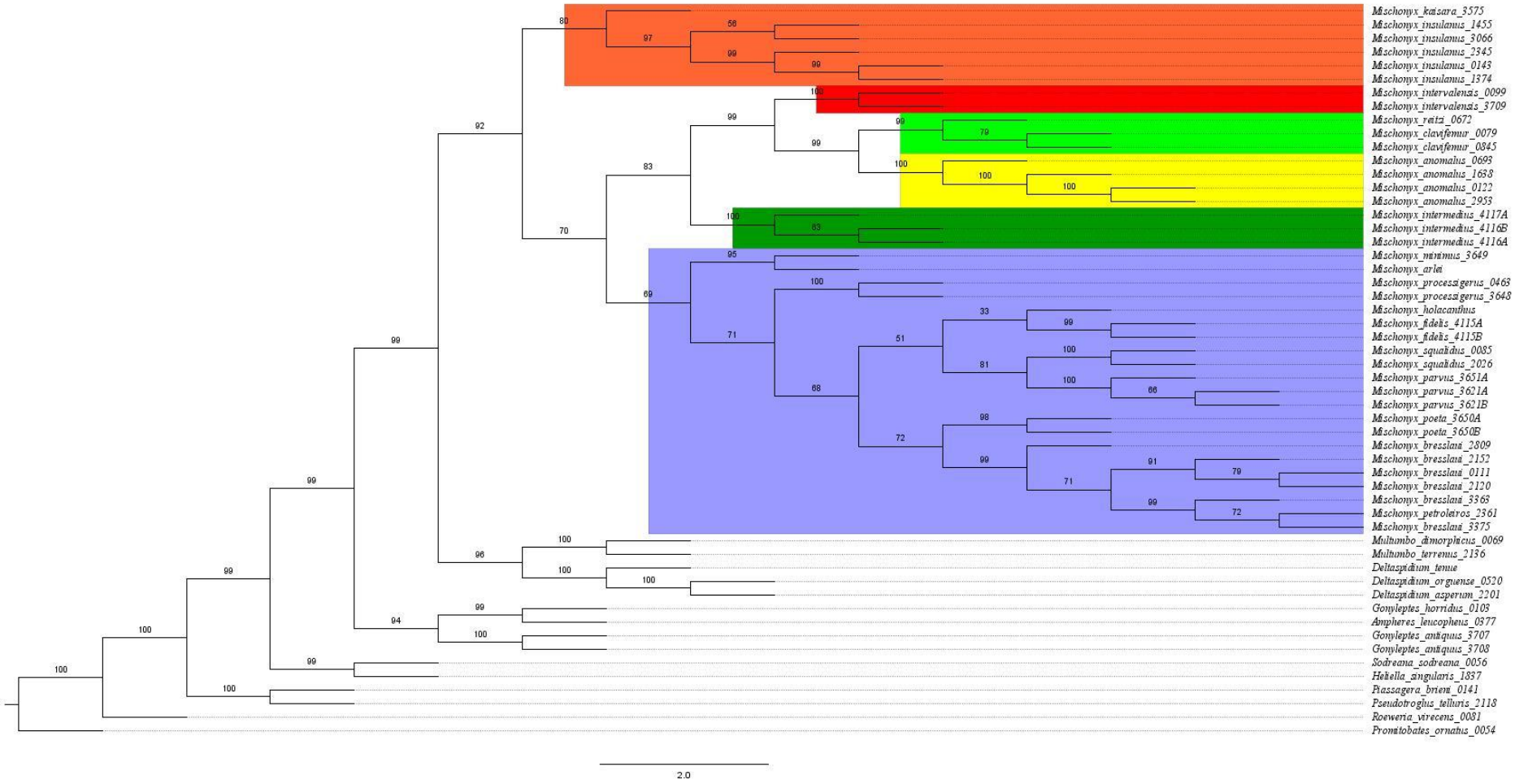

Figure 05: Total Evidence Likelyhood hypothesis. The values near the nodes are the bootstrap values of each one. Numbers after the species name are the LAL Vouchers of each individual. The colored clades are according to their location. Light green: Santa Catarina; yellow: Parana; Red: south of São Paulo; orange: north of São Paulo; blue: Rio de Janeiro; dark green: Minas Gerais.

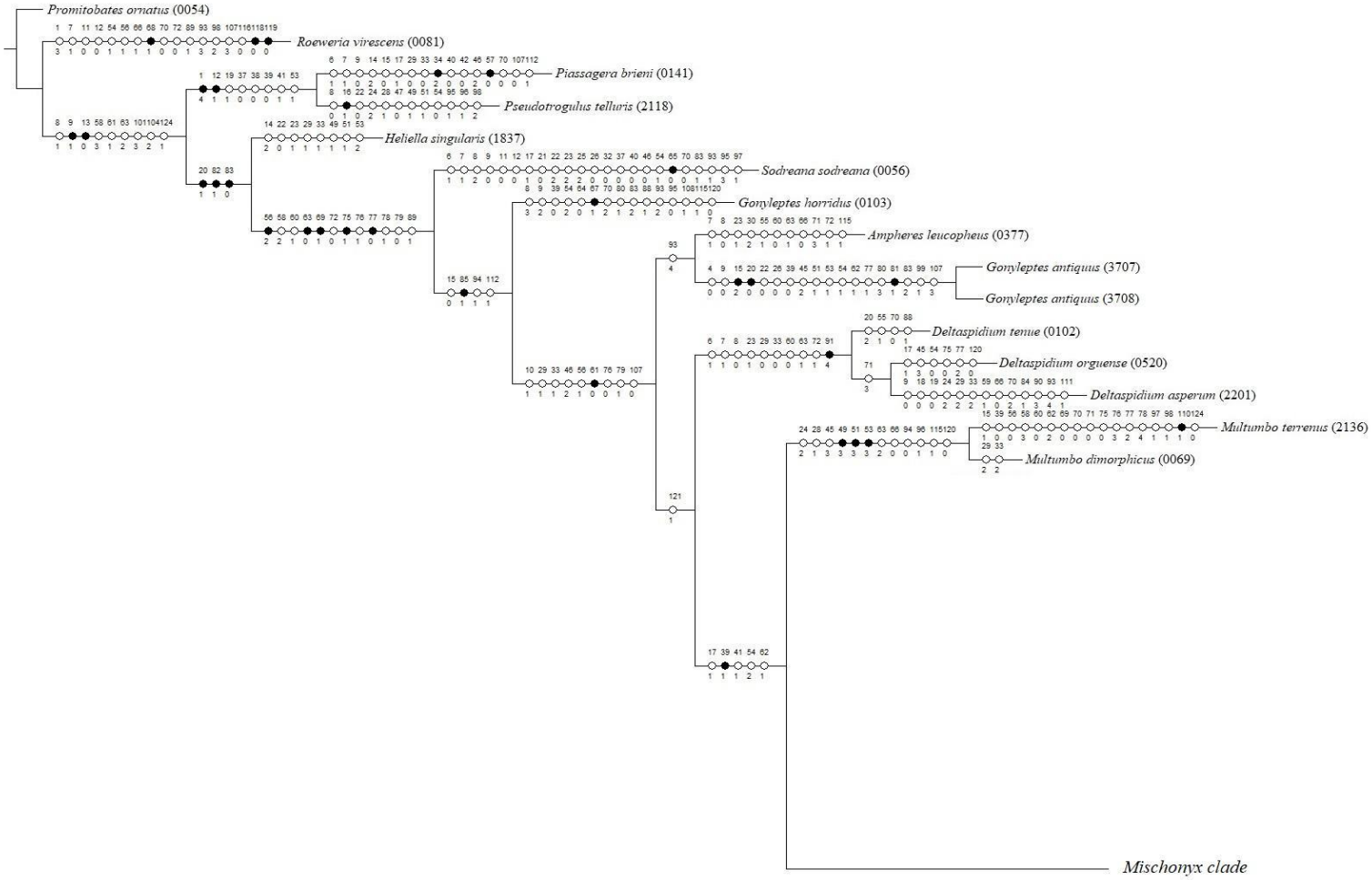

Figure 06: Total Evidence Maximum Likelyhood hypothesis with the character change plotted on each branch, representing the external group only. Numbers after the species name are the LAL Vouchers of each individual.

Figure 07: Total Evidence Maximum Likelihood hypothesis with the character change plotted on each branch, representing the *Mischonyx* clade only. Numbers after the species name are the LAL Vouchers of each individual. Consistency and Retention indexes are in the bottom right.

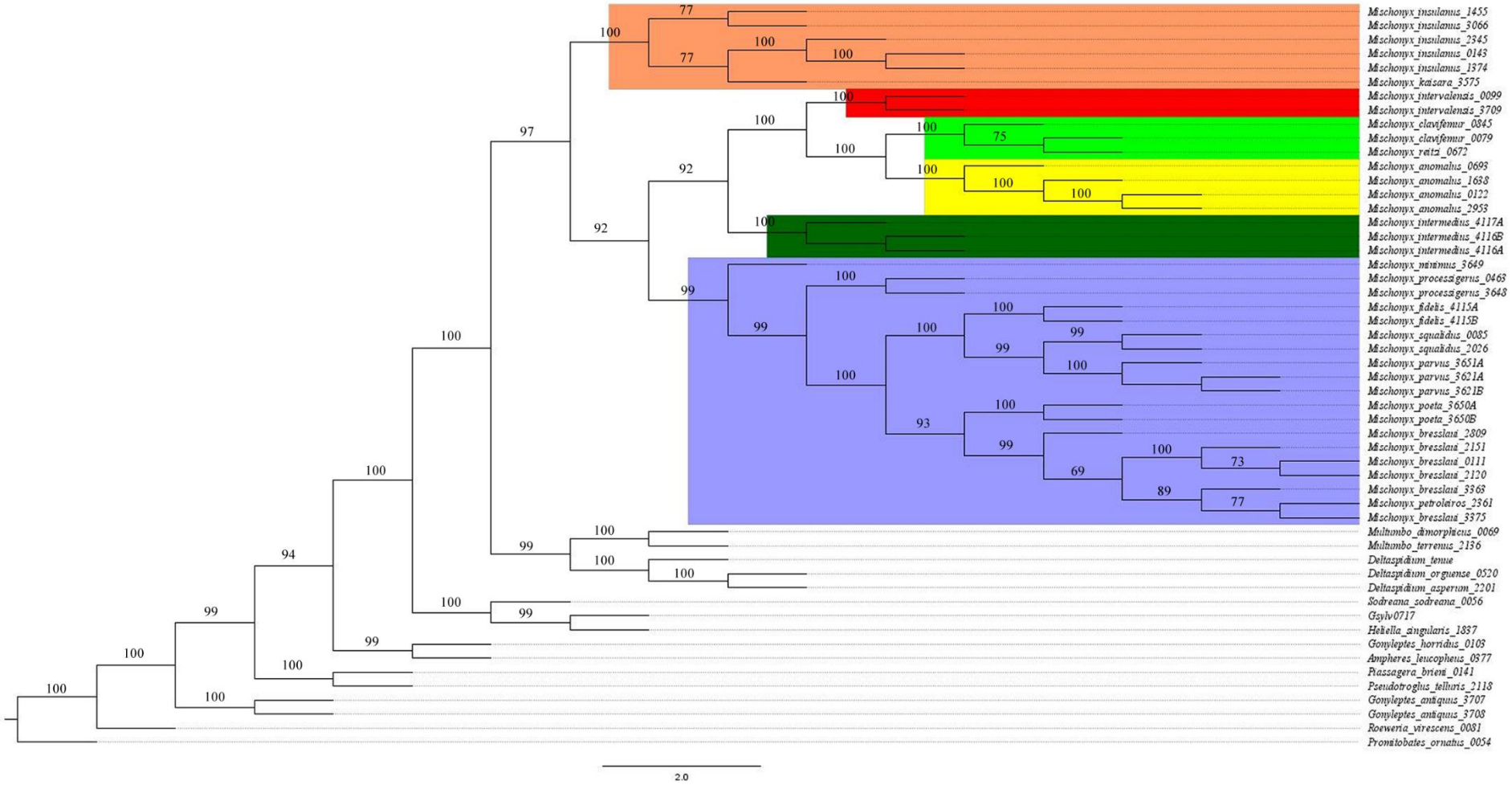

Figure 08: Total Evidence Parsimony hypothesis. The values near the nodes are the bootstrap values of each one. Numbers after the species name are the LAL Vouchers of each individual. The colored clades are according to their location. Light green: Santa Catarina; yellow: Parana; Red: south of São Paulo; orange: north of São Paulo; blue: Rio de Janeiro; dark green: Minas Gerais.

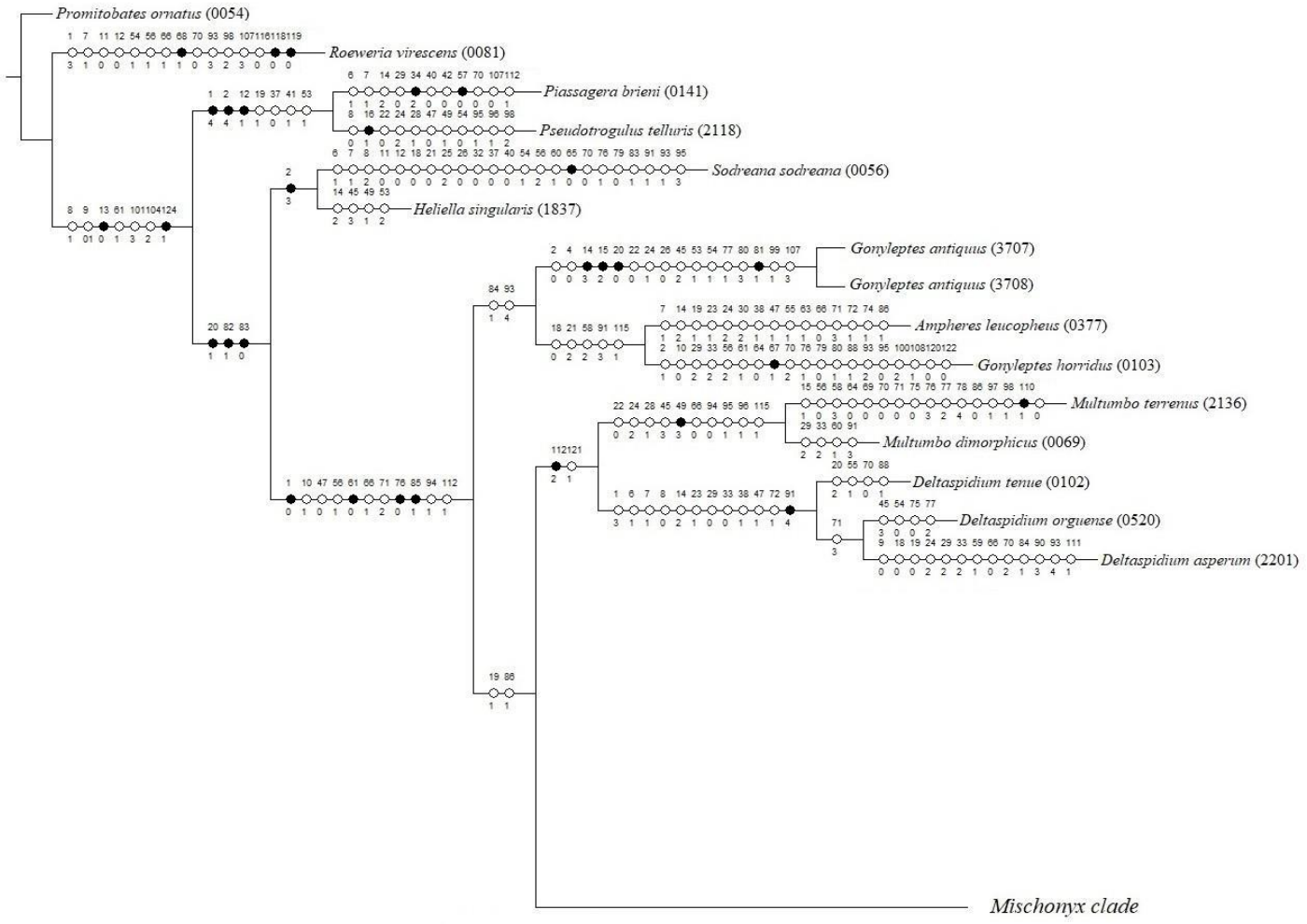

Figure 09: Total Evidence Maximum Parsimony hypothesis with characters change plotted in each node, representing only the external group. Numbers after the species name are the LAL Vouchers of each individual.

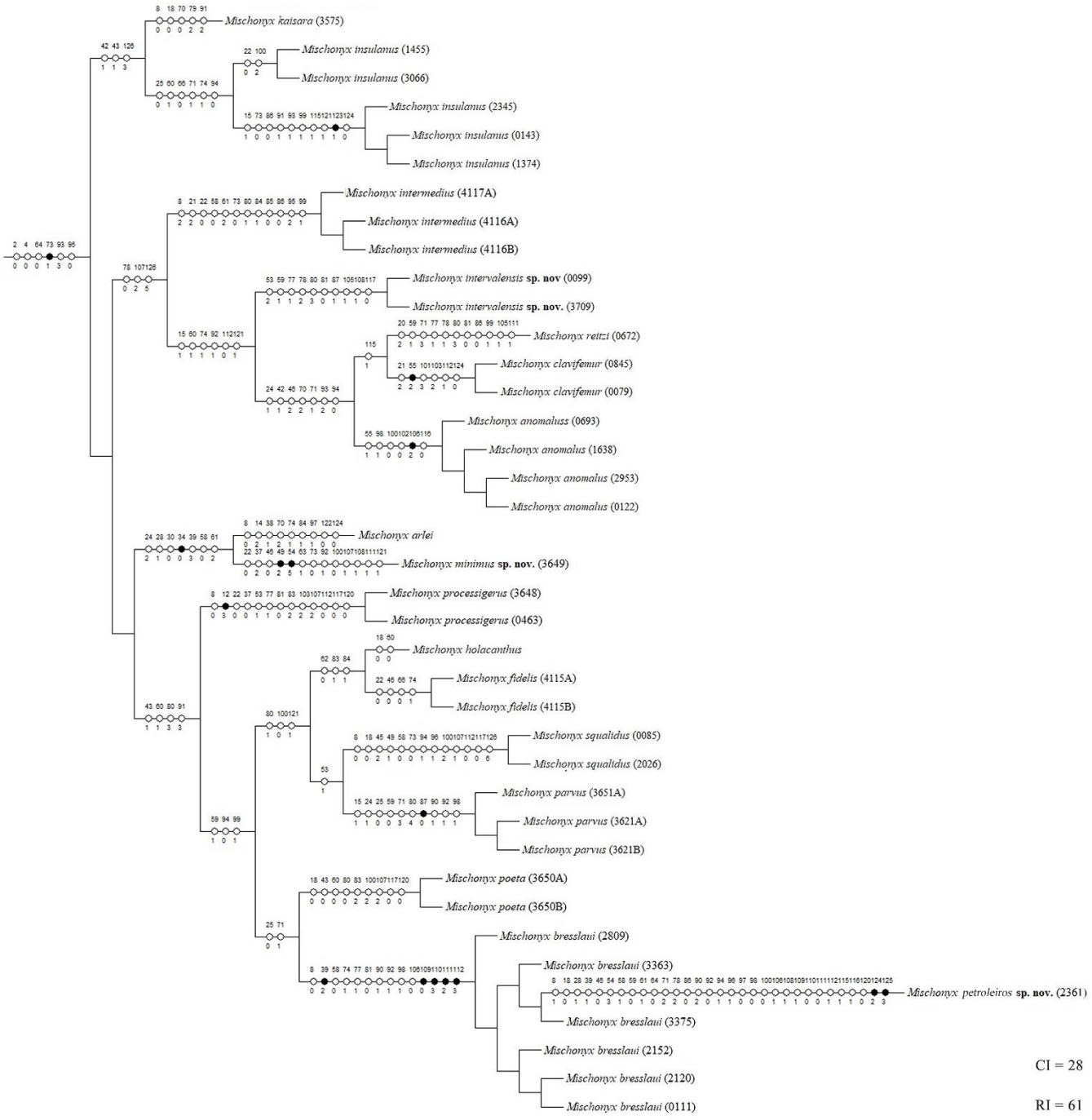

Figure 10: Total Evidence Maximum Parsimony hypothesis with characters change plotted in each node, representing *Mischonyx* internal relatioships. Numbers after the species name are the LAL Vouchers of each individual. Consistency (CI) and Retention indexes (RI) are in the bottom right.

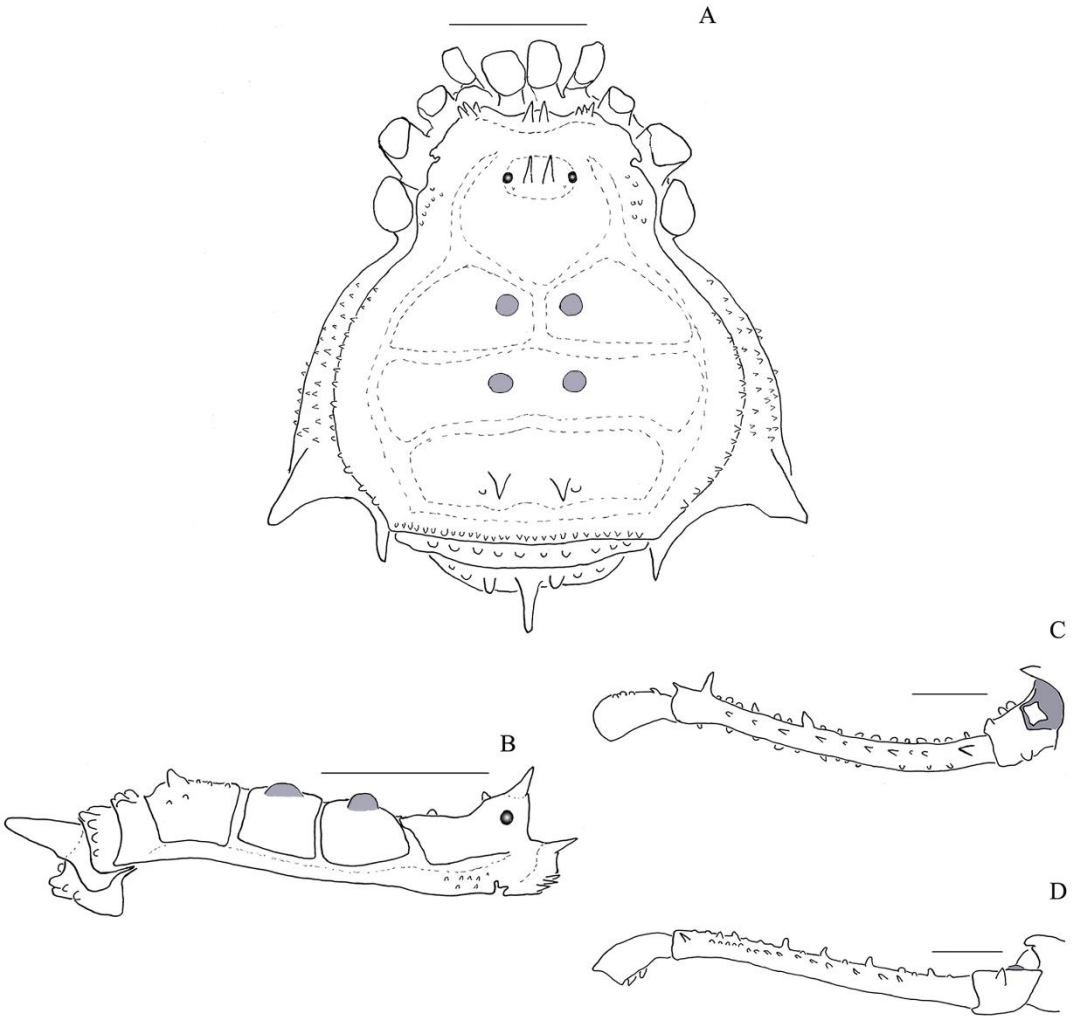

Figure 11: ***Mischonyx minimus* sp. nov.** male holotype. A, dorsal view; B, lateral view; C, dorsal view of the right leg; D, retrolateral view of the right leg. The tubercles painted in gray are whitish in ethanol. Scale bars = 1 mm.

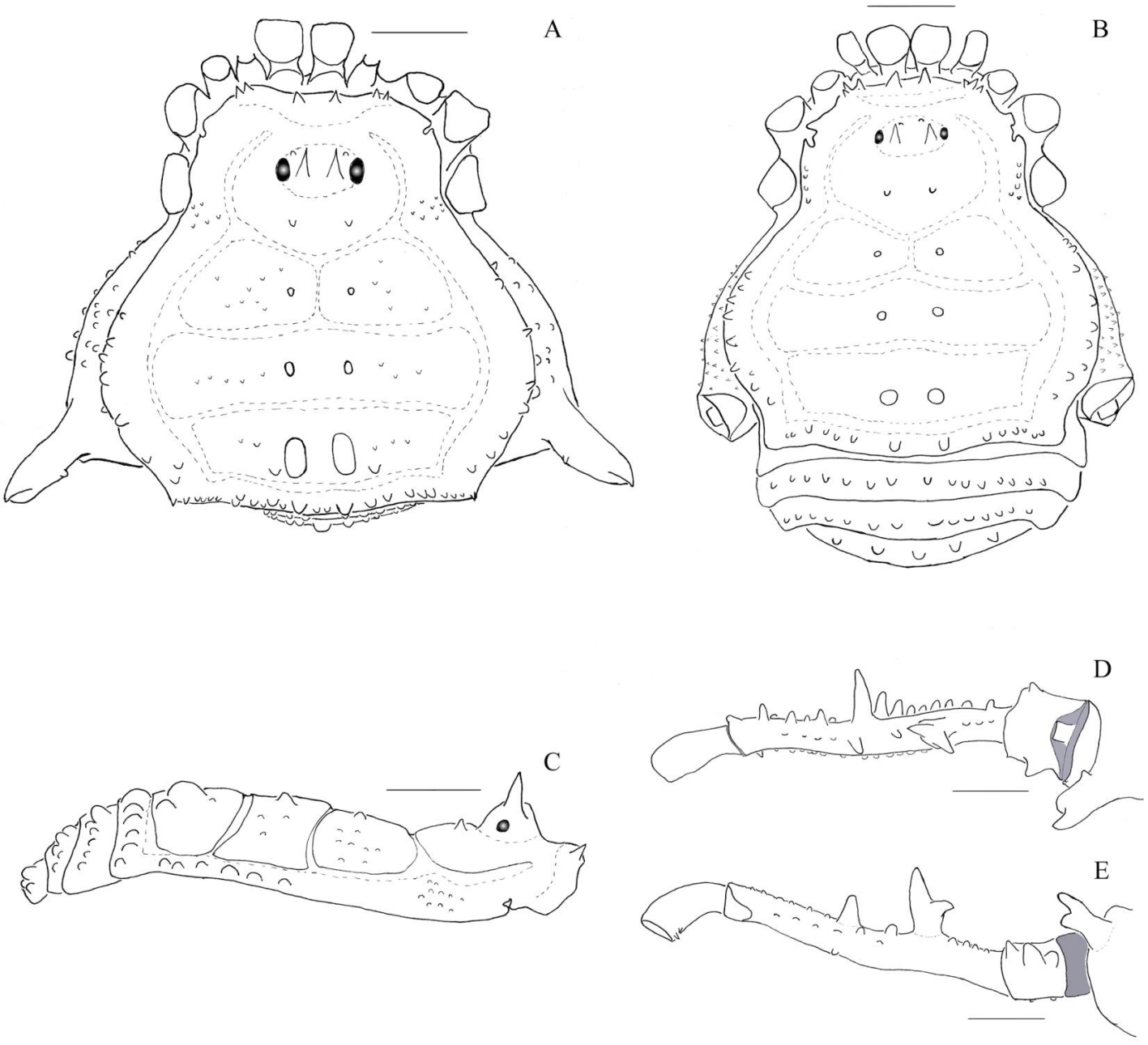

Figure 12: ***Mischonyx intervalensis* sp. nov.** A, C, Male holotype, dorsal and lateral view, respectively; B, Female paratype, dorsal view; D, E Right leg of the male holotype right, dorsal and retrolateral view, respectively. Scale bars = 1 mm.

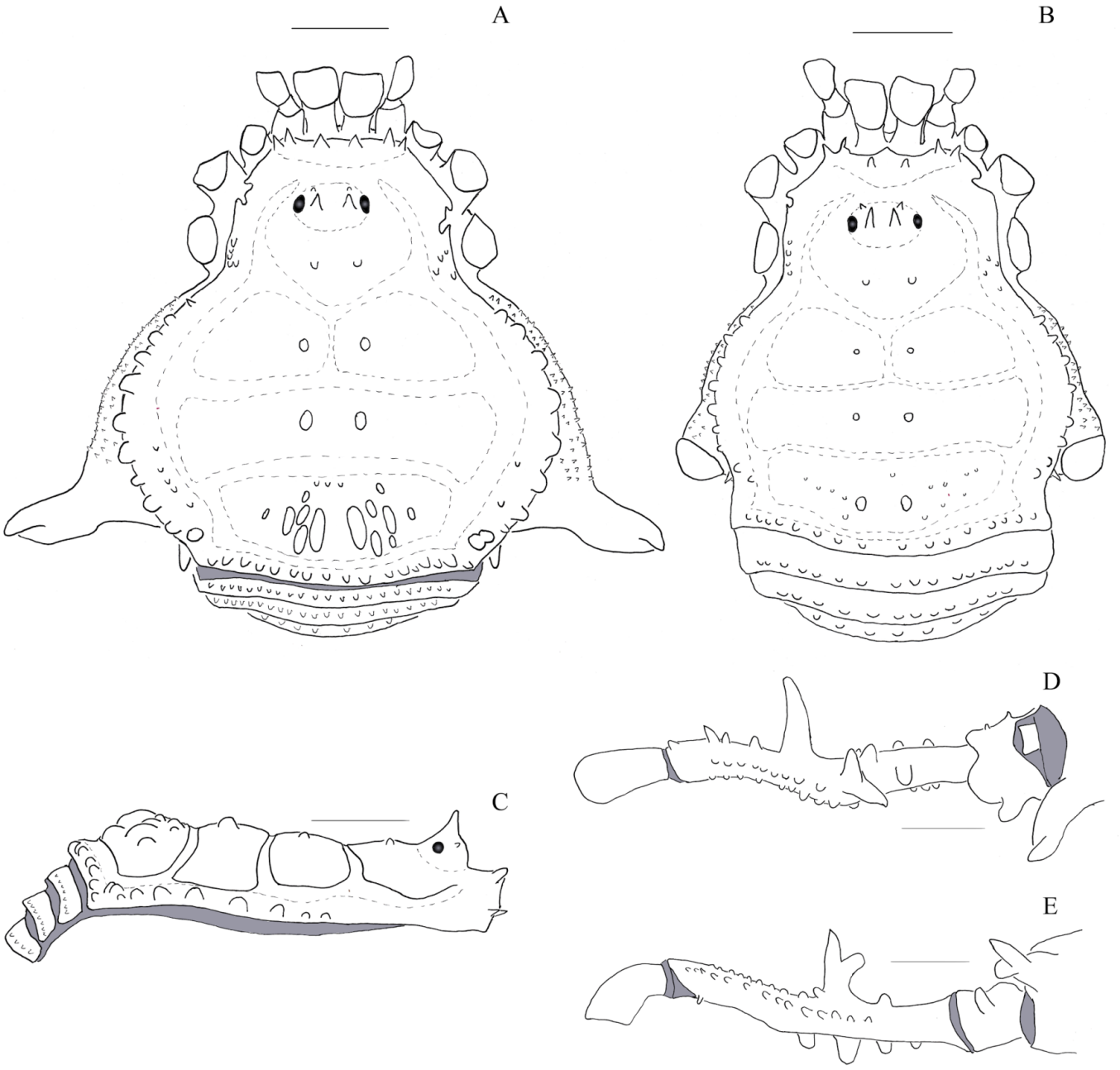

Figure 13: ***Mischonyx proletarieae*** **sp. nov.** A, C, Male holotype, dorsal and lateral view, respectively; B, Female paratype, dorsal view; D, E Right leg of the male holotype right, dorsal and retrolateral view, respectively. Scale bars = 1 mm.

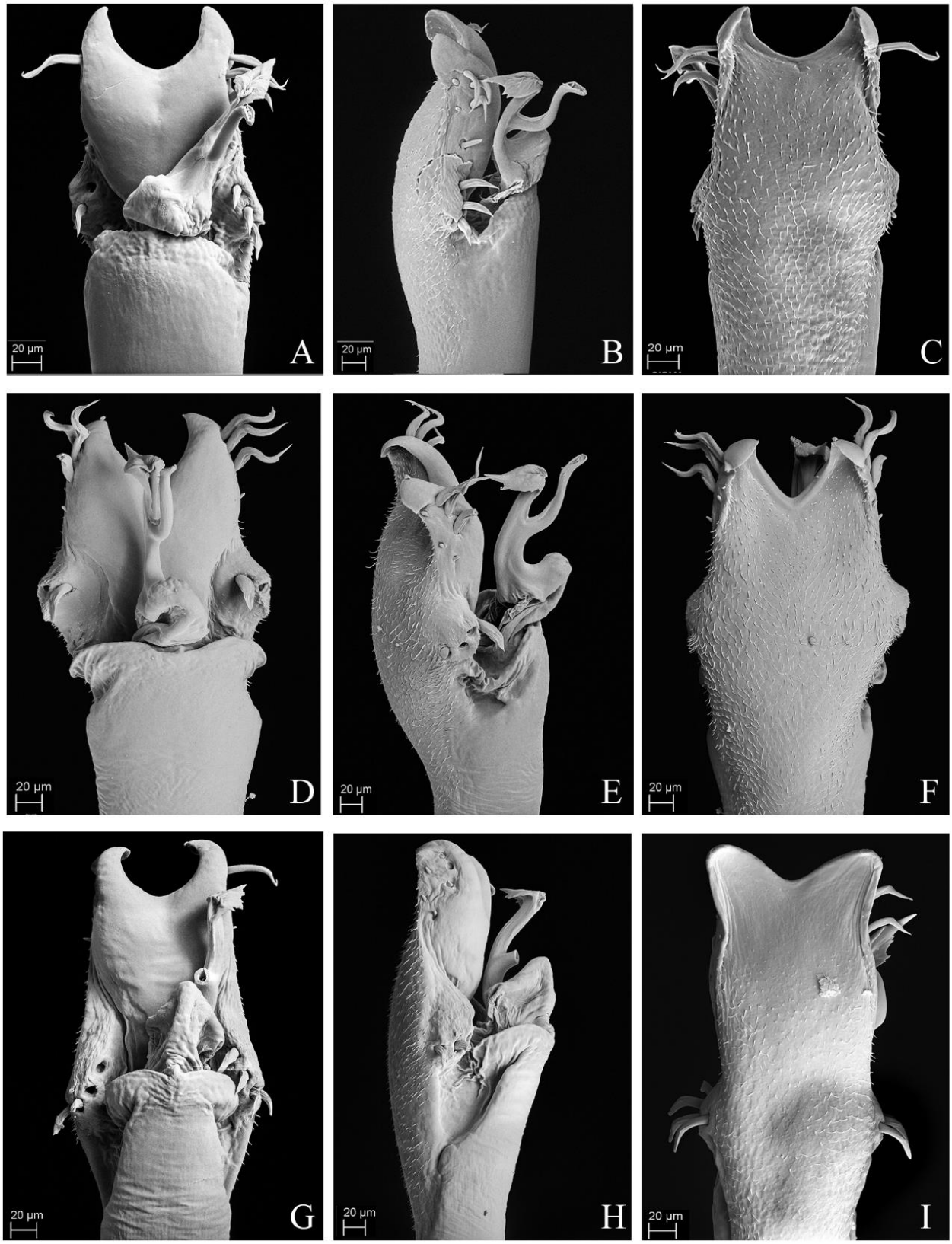

Figure 14: Penis of the new species. A – C. Dorsal, right lateral and ventral views, respectively, of the penis of *Mischonyx minimus* **sp. nov.** paratype (3649). D – F. Dorsal, right lateral and ventral views, respectively, of the penis of *Mischonyx proletariae* **sp. nov.** paratype (2361). G – I. Dorsal, right lateral and ventral views, respectively, of the penis of *Mischonyx intervalensis* **sp. nov.** paratype (0099).

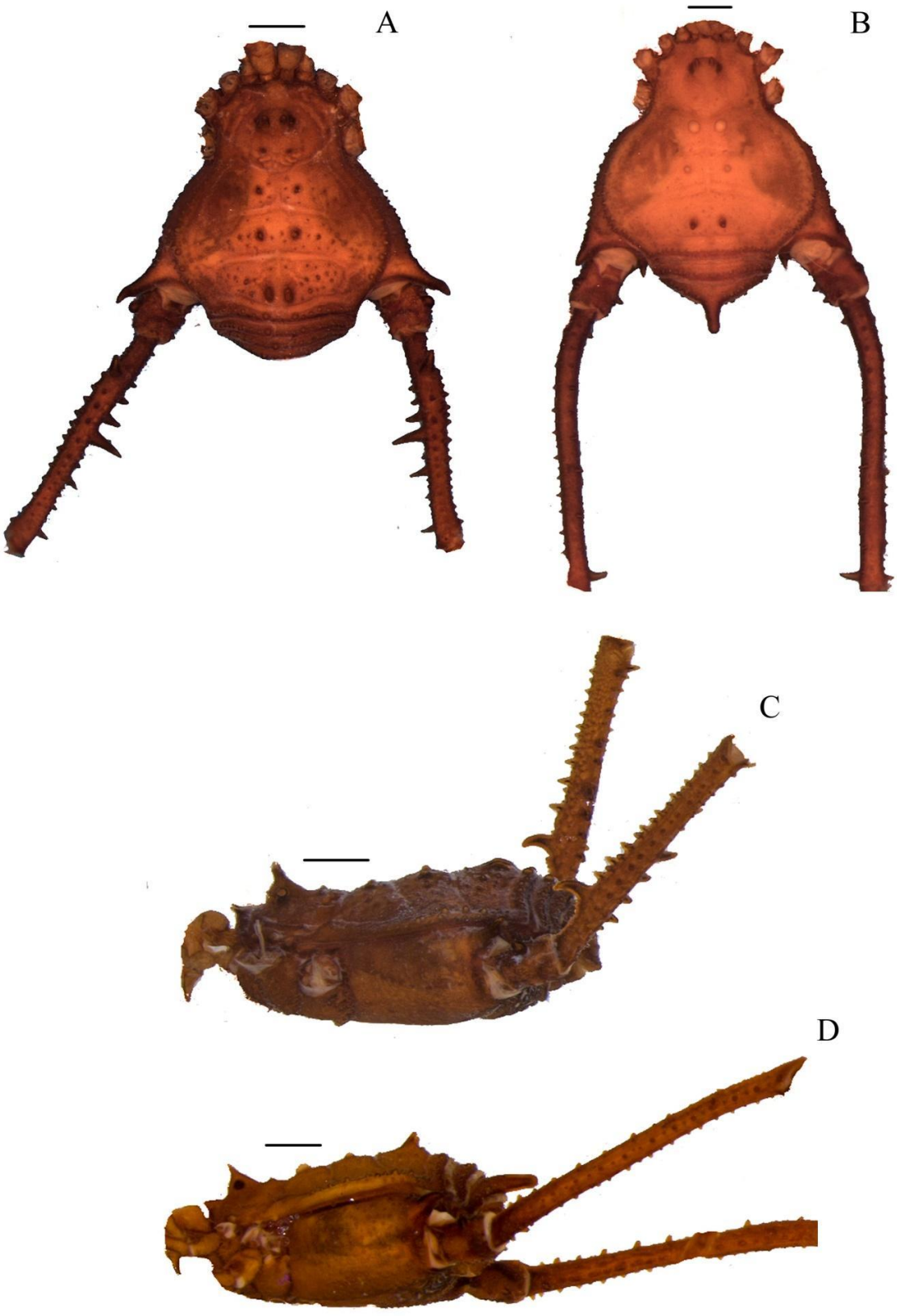

Figure 15: *Mischonyx anomalus* and *Mischonyx arlei* holotypes. A and C. *Mischonyx anomalus*, dorsal and lateral views, respectively. B and D. *Mischonyx arlei*, dorsal and lateral views, respectively. Scale bars: 1 mm.

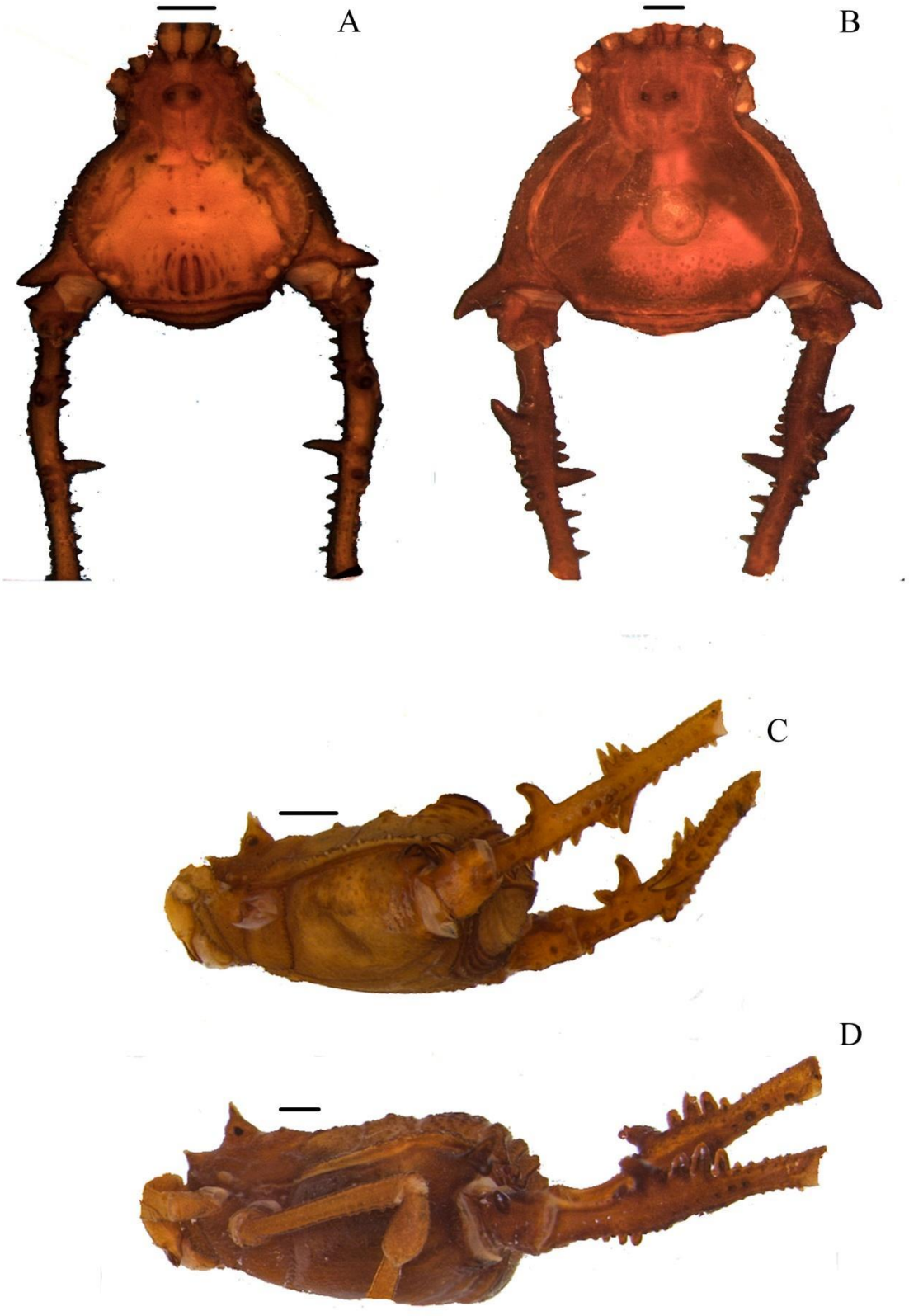

Figure 16: *Mischonyx bresslaui* and *Mischonyx clavifemur* holotypes. A and C. *Mischonyx bresslaui*, dorsal and lateral views, respectively. B and D. *Mischonyx clavifemur*, dorsal and lateral views, respectively. Scale bars: 1 mm.

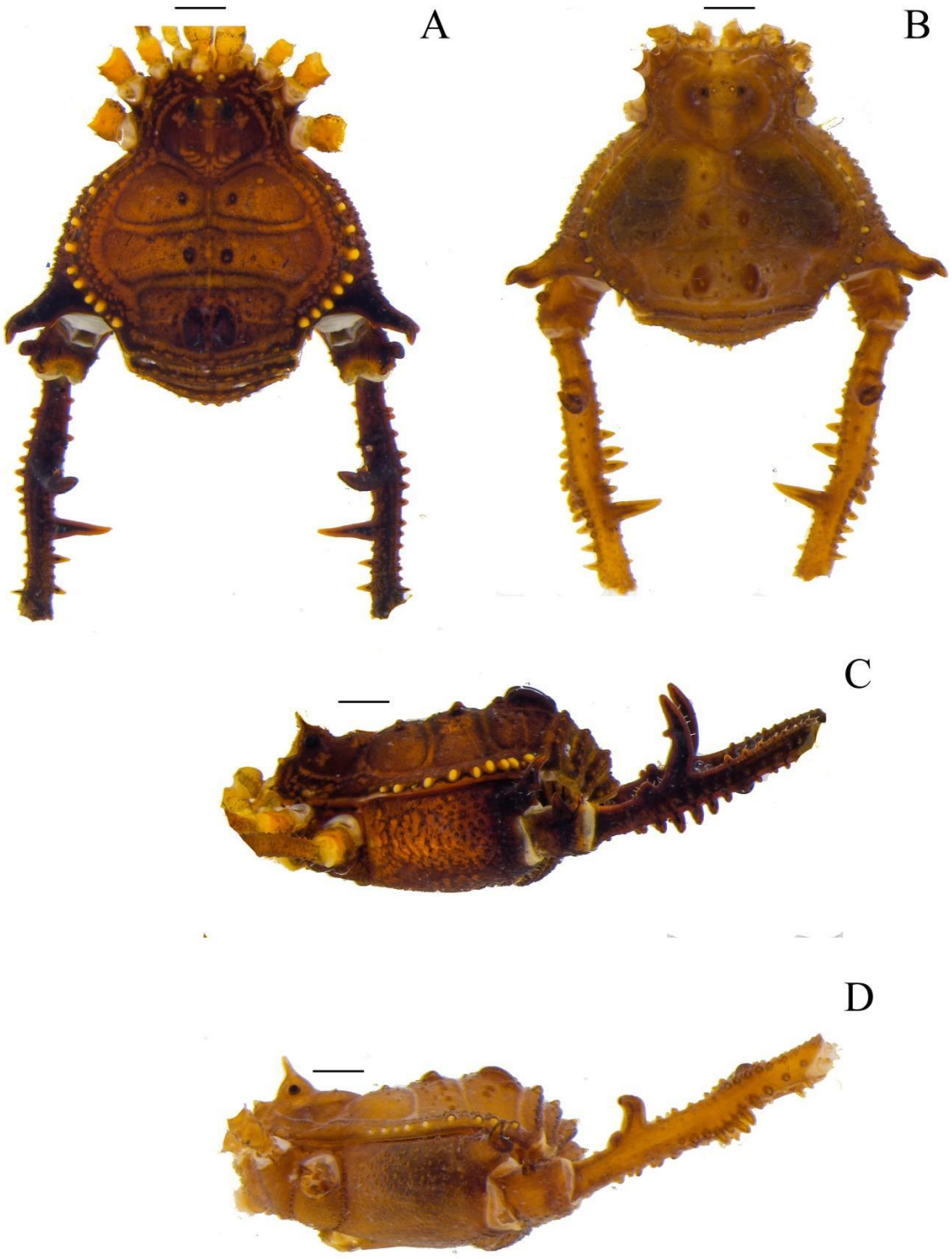

Figure 17: *Mischonyx fidelis* (4115A) and *Mischonyx holacanthus* holotype. A and C. *Mischonyx fidelis*, dorsal and lateral views, respectively. B and D. *Mischonyx holacanthus*, dorsal and lateral views, respectively. Scale bars: 1 mm.

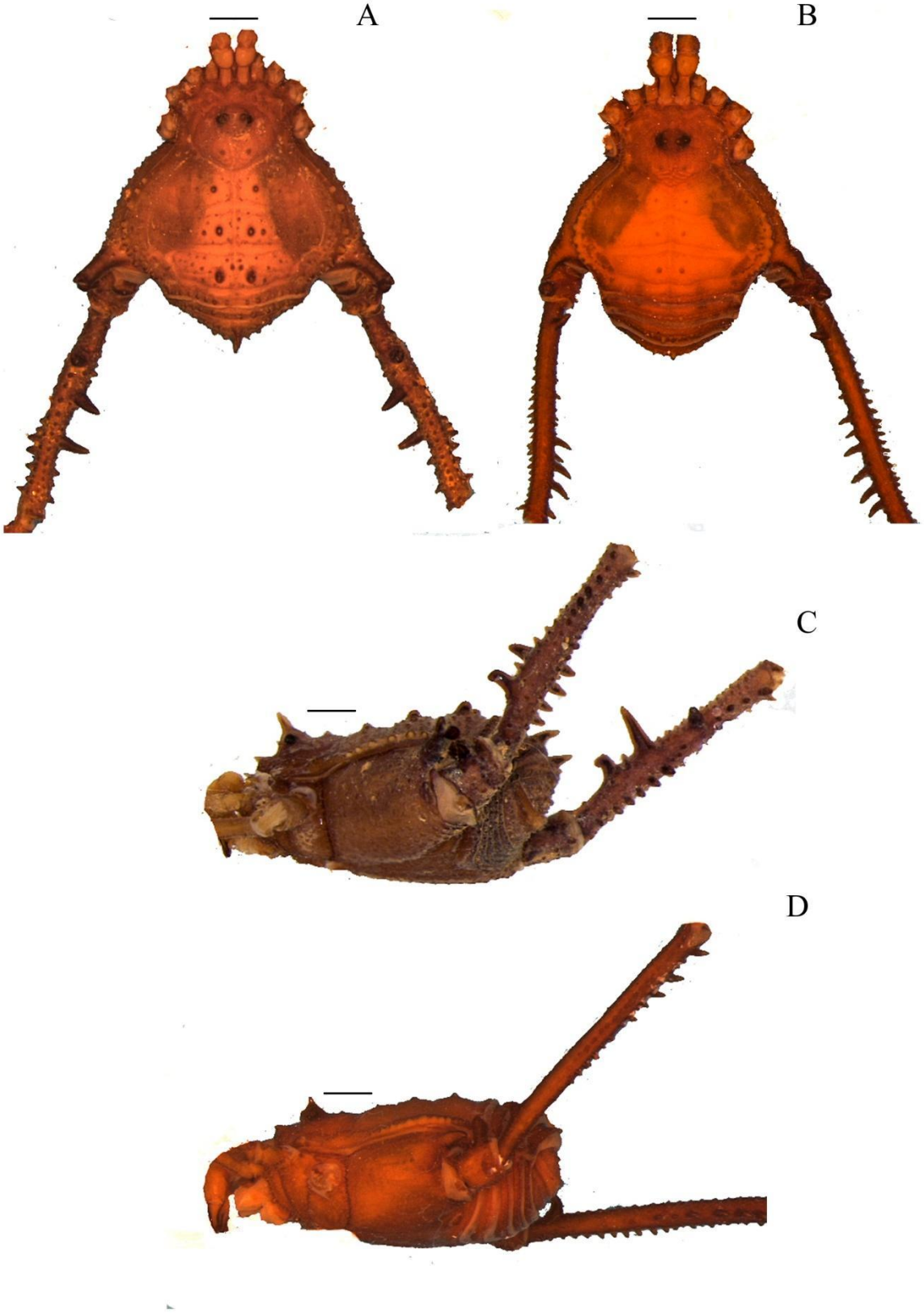

Figure 18: *Mischonyx insulanus* and *Mischonyx intermedius* holotypes. A and C. *Mischonyx insulanus*, dorsal and lateral views, respectively. B and D. *Mischonyx intermedius*, dorsal and lateral views, respectively. Scale bars: 1 mm.

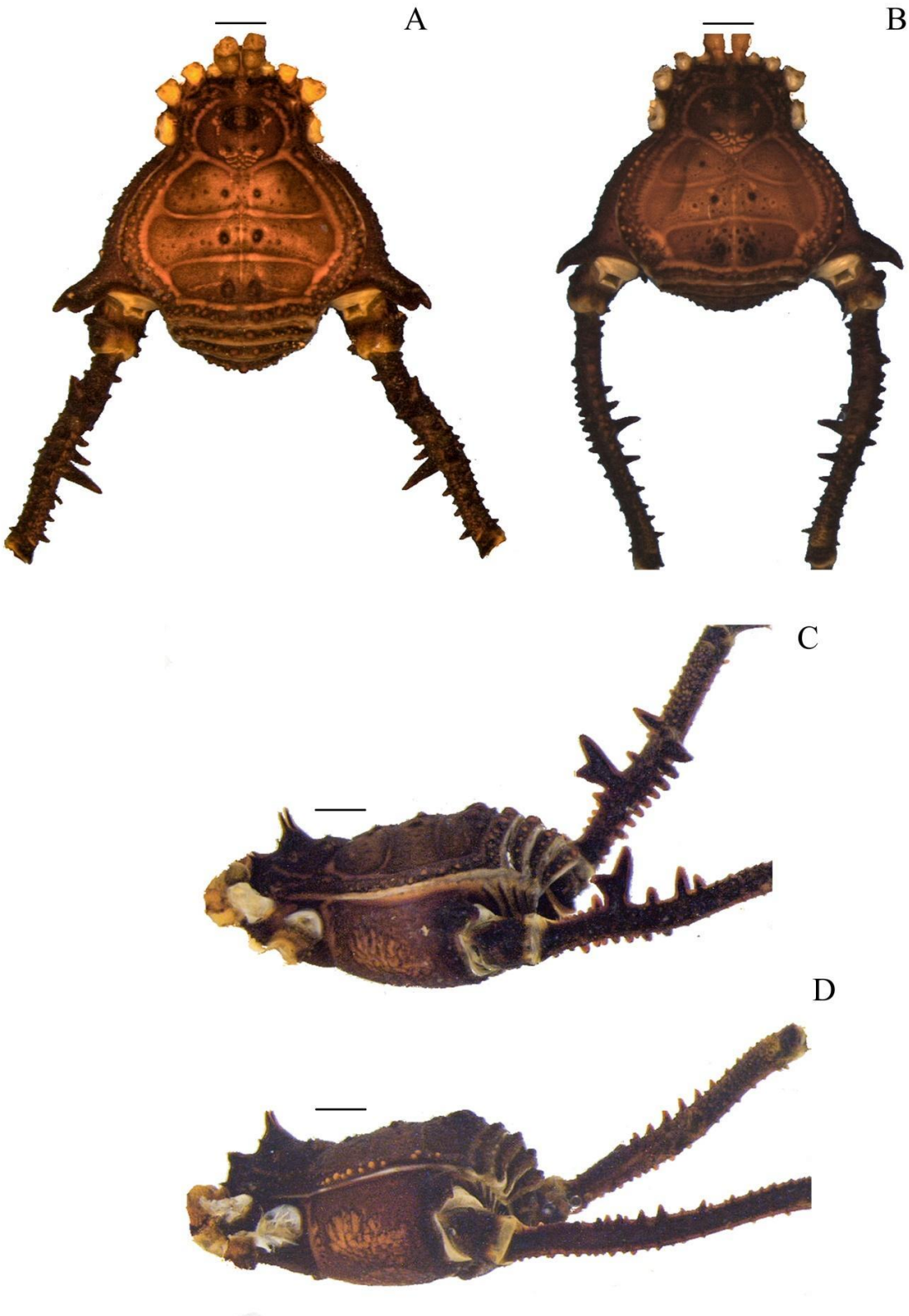

Figure 19: *Mischonyx intervalensis* **sp. nov.** and *Mischonyx kaisara* holotypes. A and C. *Mischonyx intervalensis* **sp. nov.**, dorsal and lateral views, respectively. B and D. *Mischonyx kaisara*, dorsal and lateral views, respectively. Scale bars: 1 mm.

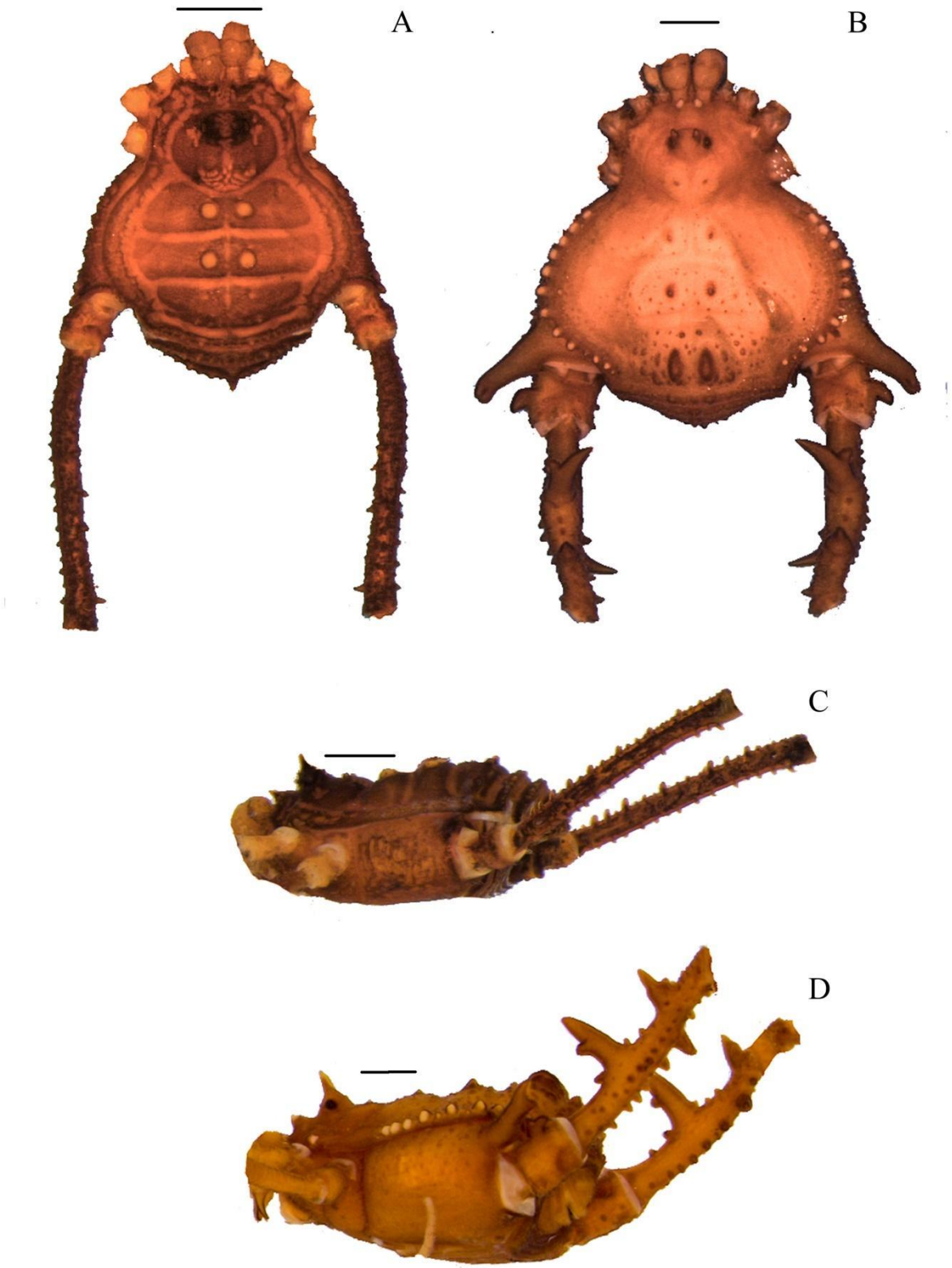

Figure 20: *Mischonyx minimus* **sp. nov.** and *Mischonyx parvus* holotypes. A and C. *Mischonyx minimus* **sp. nov.**, dorsal and lateral views, respectively. B and D. *Mischonyx parvus*, dorsal and lateral views, respectively. Scale bars: 1 mm.

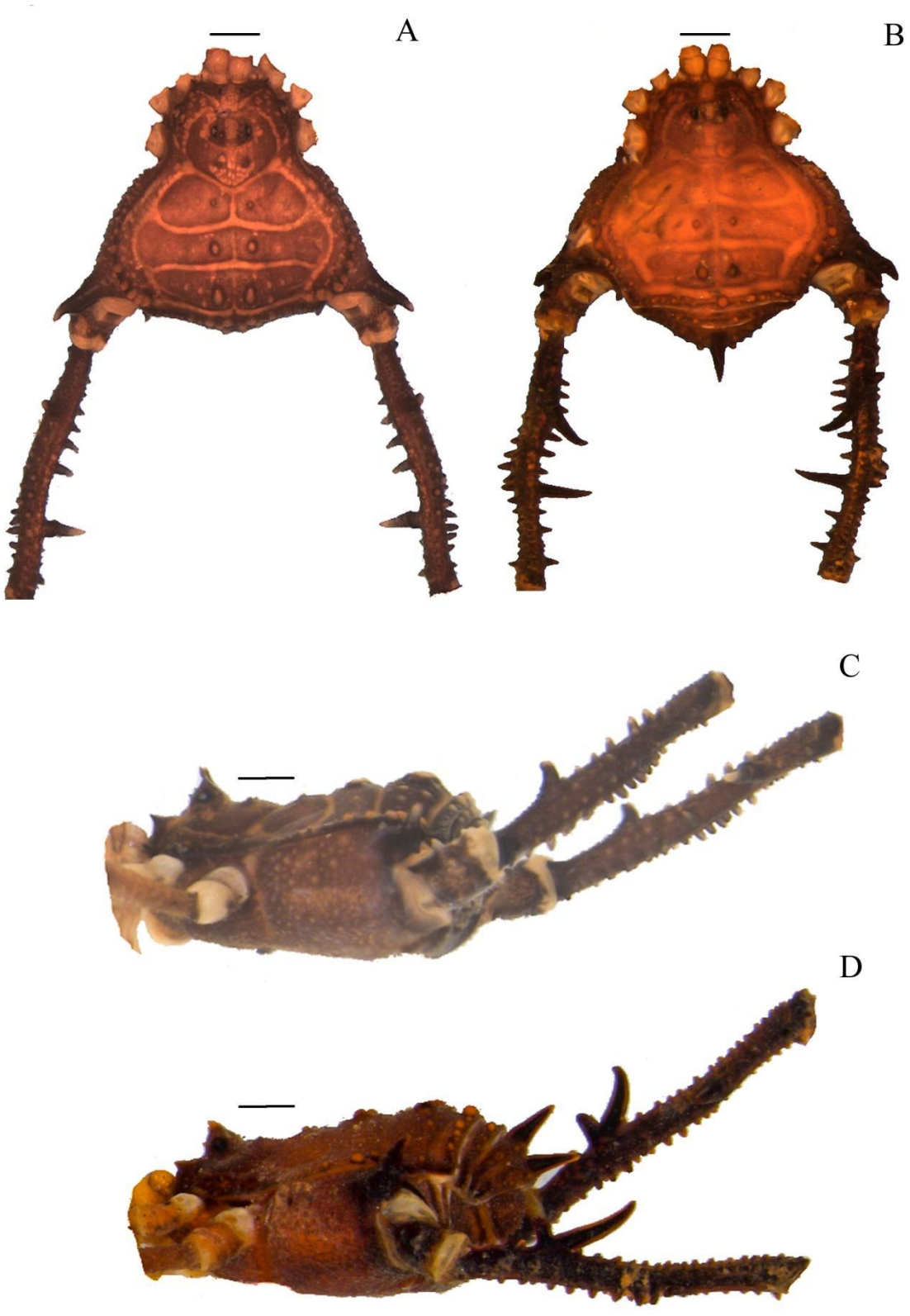

Figure 21: *Mischonyx poeta* and *Mischonyx processigerus* holotypes. A and C. *Mischonyx poeta*, dorsal and lateral views, respectively. B and D. *Mischonyx processigerus*, dorsal and lateral views, respectively. Scale bars: 1 mm.

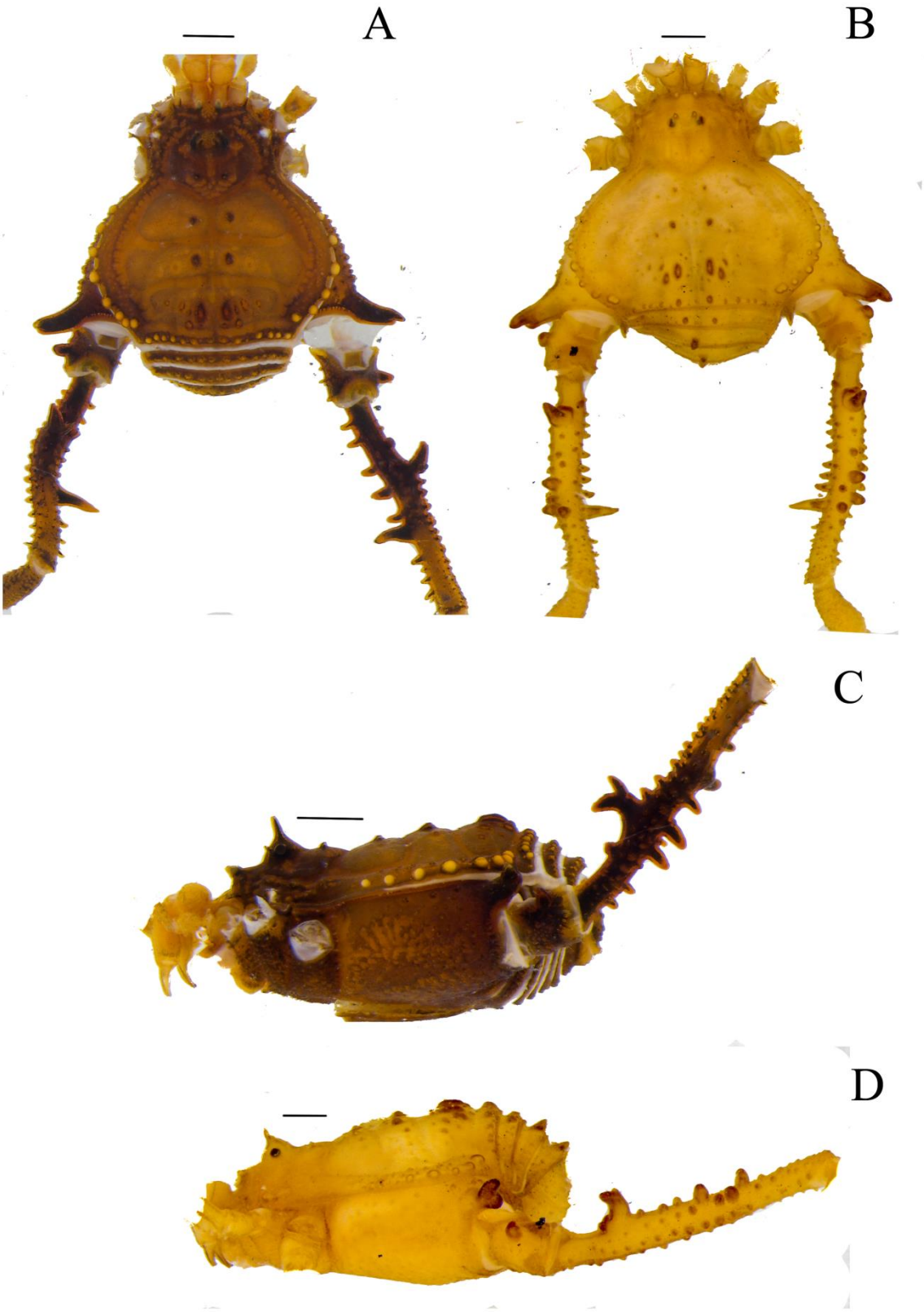

Figure 22: *Mischonyx proletariae* **sp. nov.** and *Mischonyx squalidus* holotypes. A and C. *Mischonyx proletariae* **sp. nov.**, dorsal and lateral views, respectively. B and D. *Mischonyx squalidus*, dorsal and lateral views, respectively. Scale bars: 1 mm.

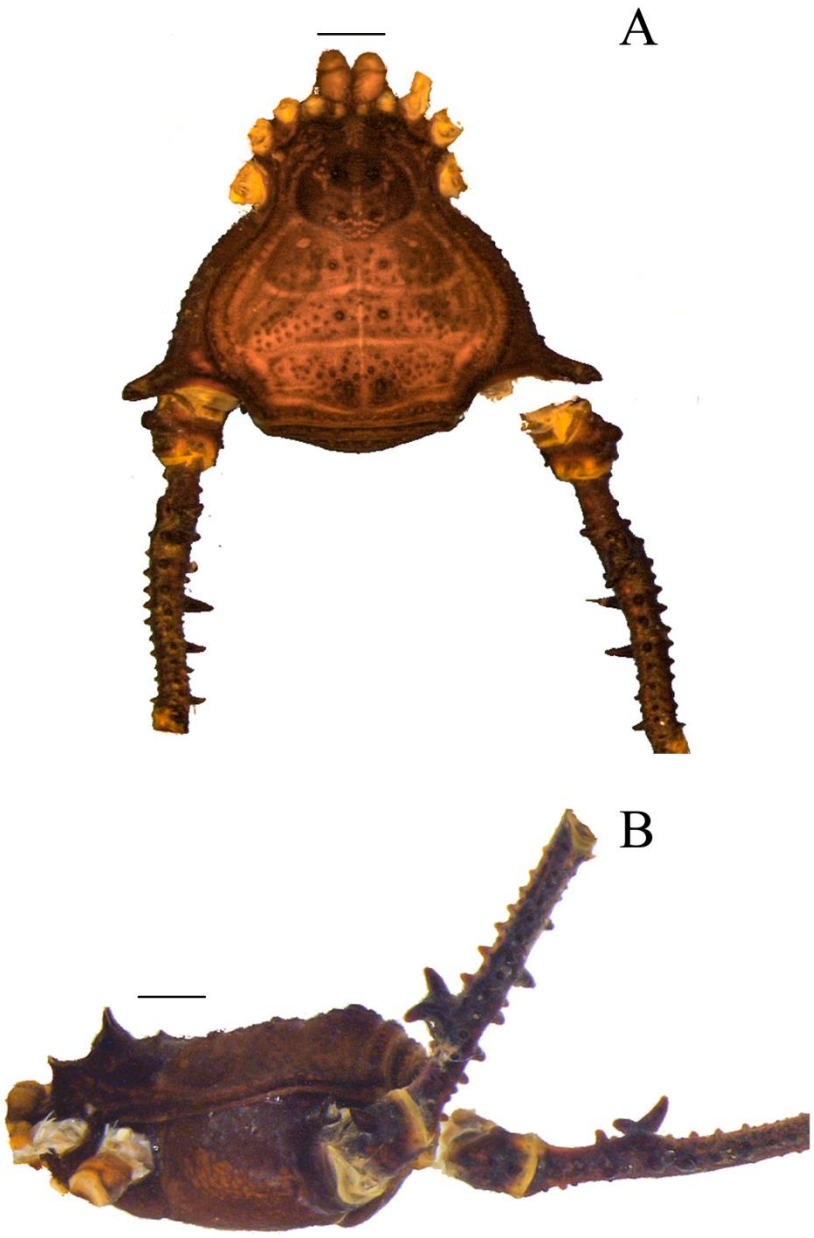

Figure 23: *Mischonyx reitzi* (0672). A. dorsal view. B. lateral. Scale bars: 1 mm.

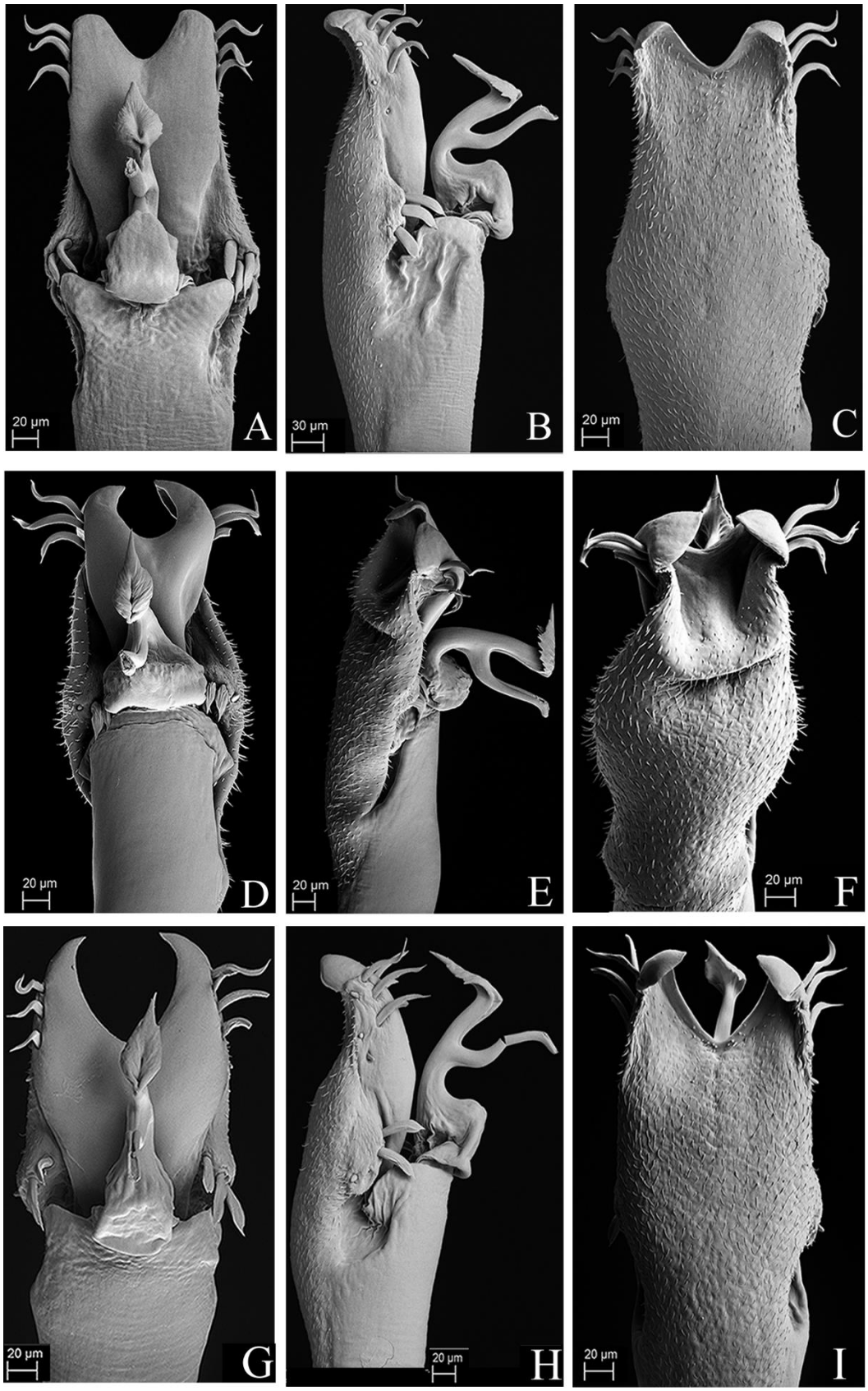

Figure 24: Penis of *Mischonyx* species. A – C. Dorsal, right lateral and ventral views, respectively, of *Mischonyx anomalus*. D – F. Dorsal, right lateral and ventral views, respectively, of the penis of *Mischonyx bresslaui*. G – I. Dorsal, right lateral and ventral views, respectively, of the penis of *Mischonyx clavifemur*.

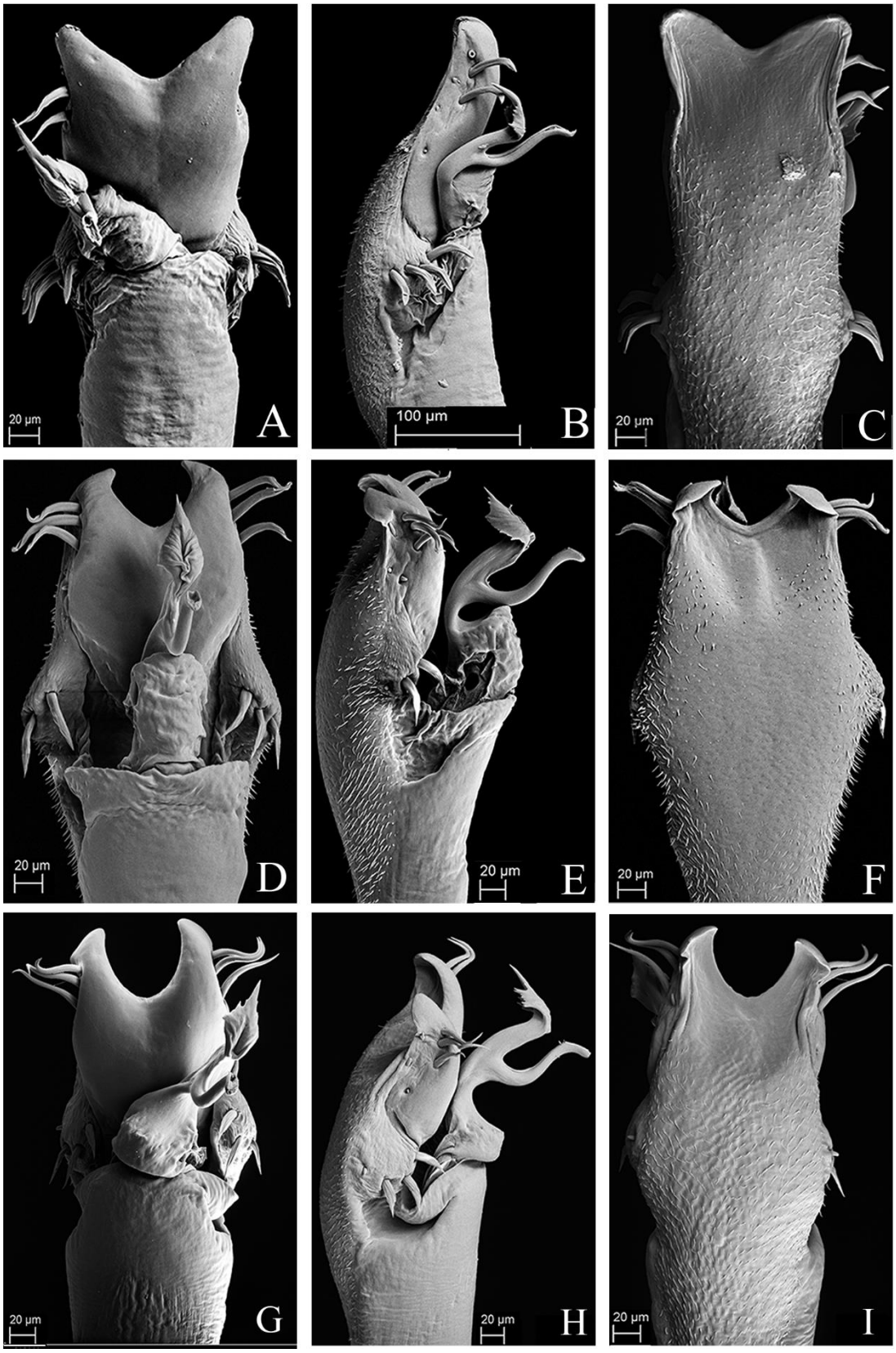

Figure 25: Penis of *Mischonyx* species. A – C. Dorsal, right lateral and ventral views, respectively, of the penis of *Mischonyx fidelis.* D – F. Dorsal, right lateral and ventral views, respectively, of *Mischonyx insulanus*. G – I. Dorsal, right lateral and ventral views, respectively, of the penis of *Mischonyx intermedius*.

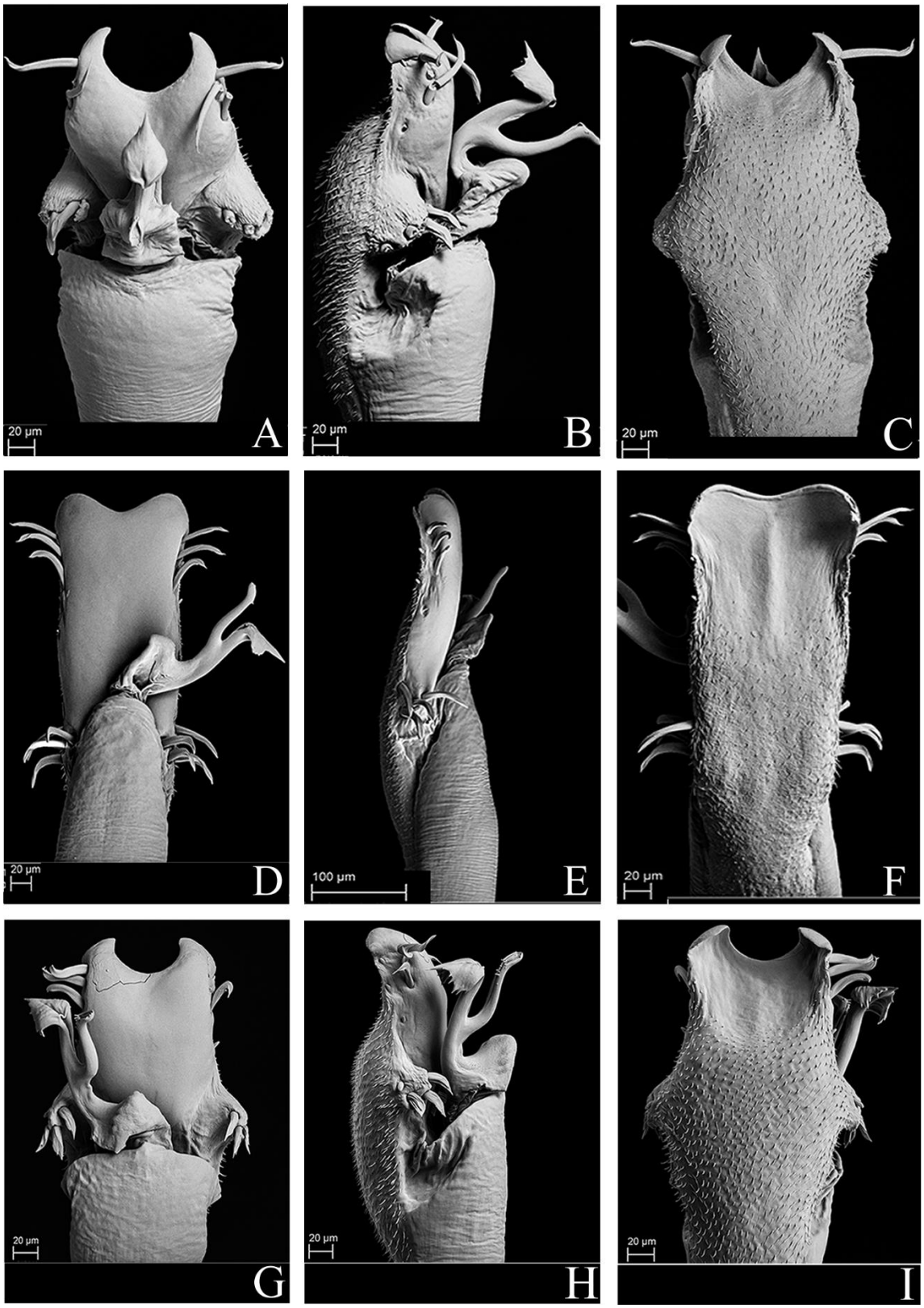

Figure 26: Penis of *Mischonyx* species. A – C. Dorsal, right lateral and ventral views, respectively, of the penis of *Mischonyx kaisara.* D – F. Dorsal, right lateral and ventral views, respectively, of the penis of *Mischonyx parvus.* G – I. Dorsal, right lateral and ventral views, respectively, of *Mischonyx poeta.*

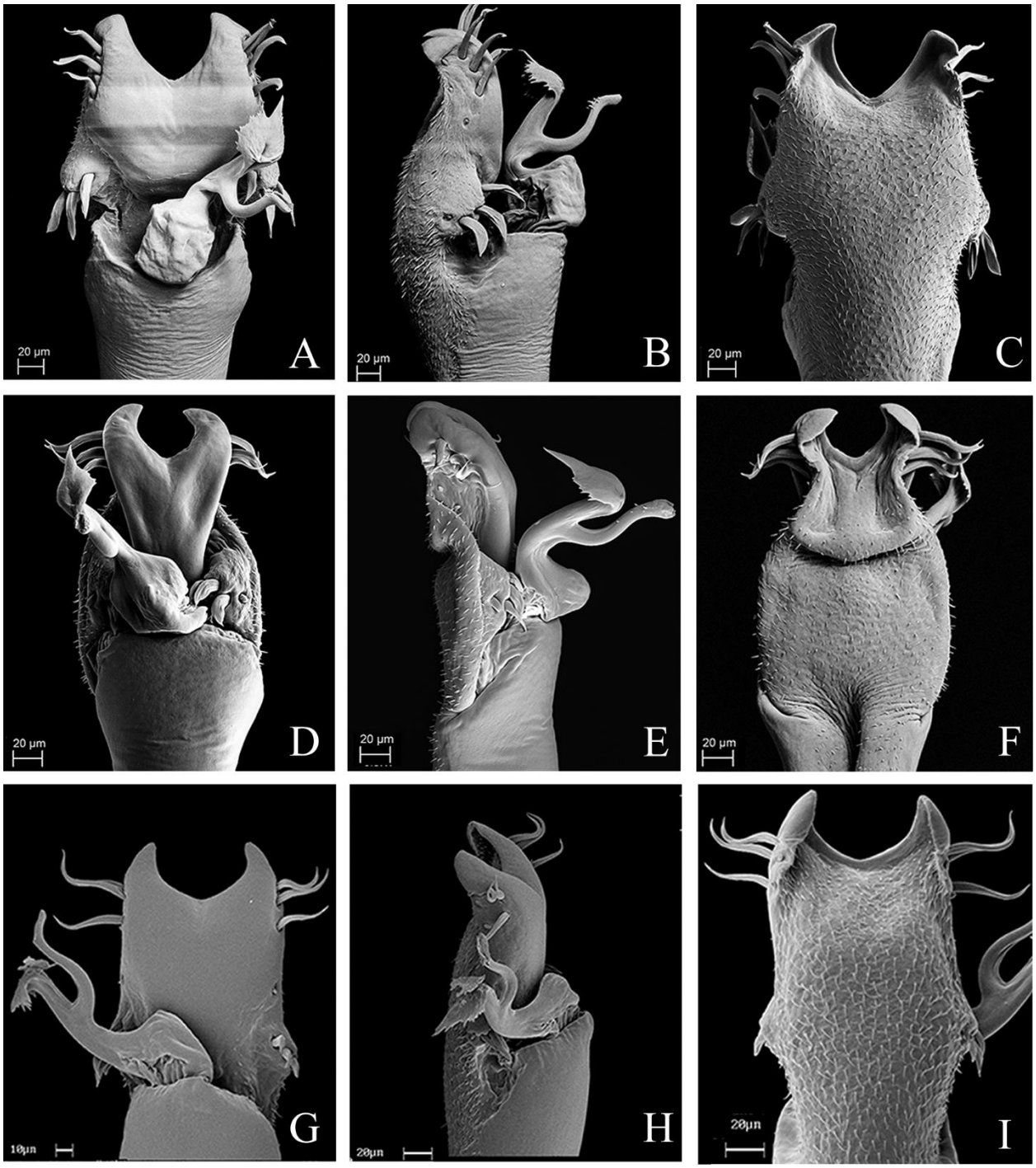

Figure 27: Penis of *Mischonyx* species. A – C. Dorsal, right lateral and ventral views, respectively, of the penis of *Mischonyx processigerus*. D – F. Dorsal, right lateral and ventral views, respectively, of the penis of *Mischonyx squalidus*. G – I. Dorsal, right lateral and ventral views, respectively, of the penis of *Mischonyx arlei.*

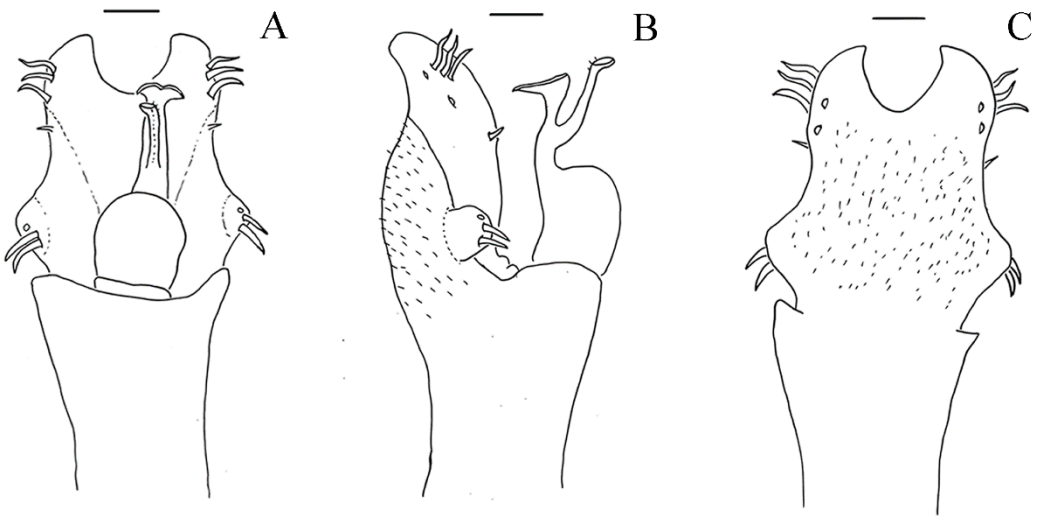

Figure 28: Penis of *Mischonyx* species. A – C. Dorsal, right lateral and ventral views, respectively, of the penis of *Mischonyx reitzi* Scale bars = 1µm.

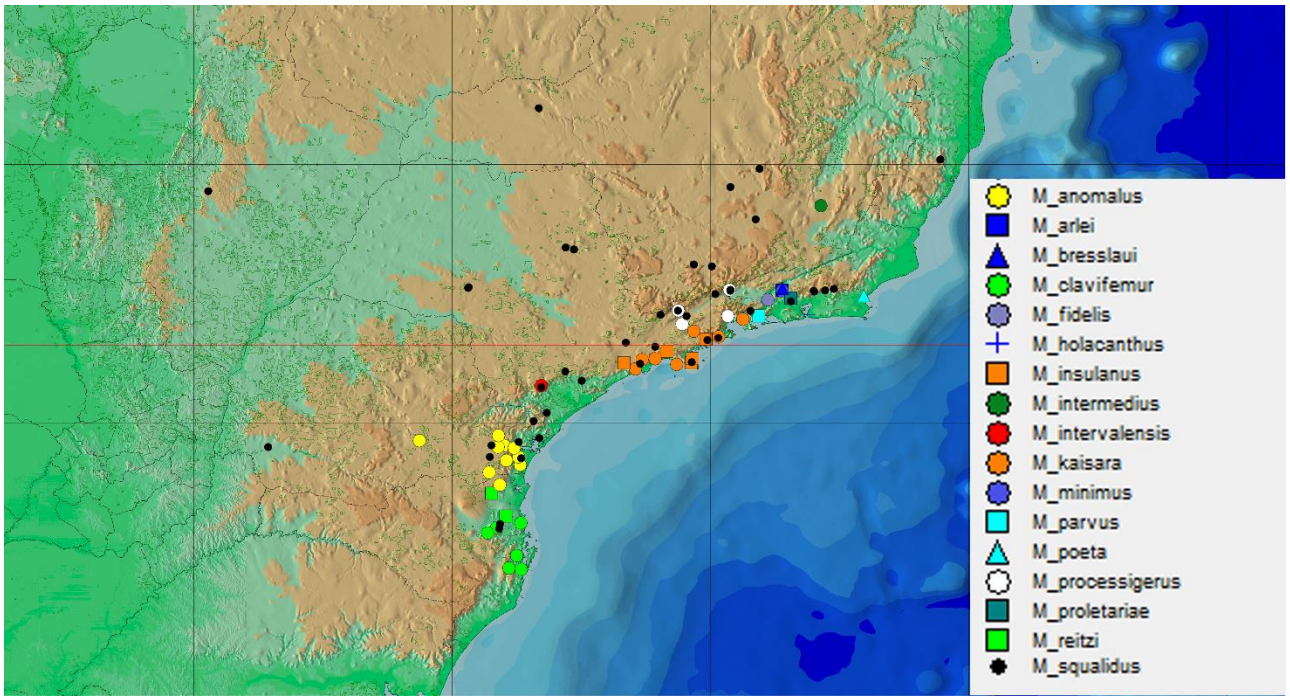

Figure 29: General geographical distribution of *Mischonyx* species. Legends are in the right of the image. The red line represent the Tropic of Capricorn and the black grid represents the full meridians and parallels.

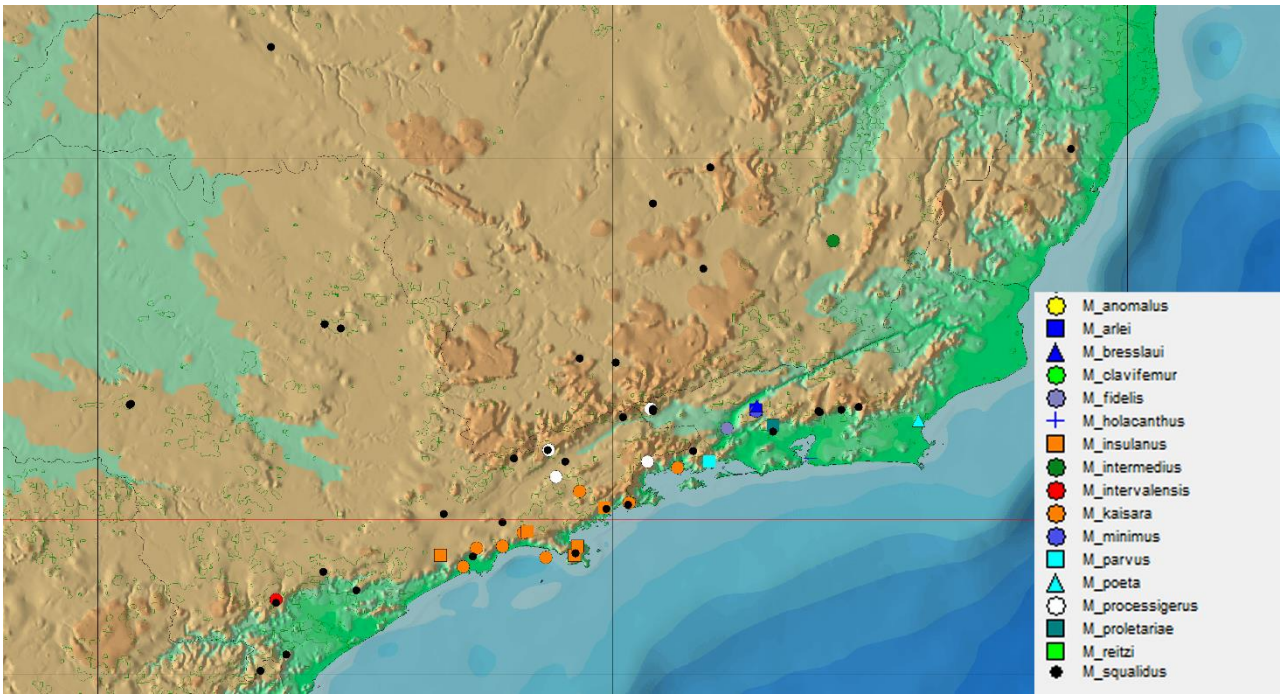

Figure 30: Geographical distribution of *Mischonyx* species from São Paulo, Rio de Janeiro e Minas Gerais states. Legends are in the right of the figure. The red line represents the Tropic of Capricorn and the black grid represents the full meridians and parallels.

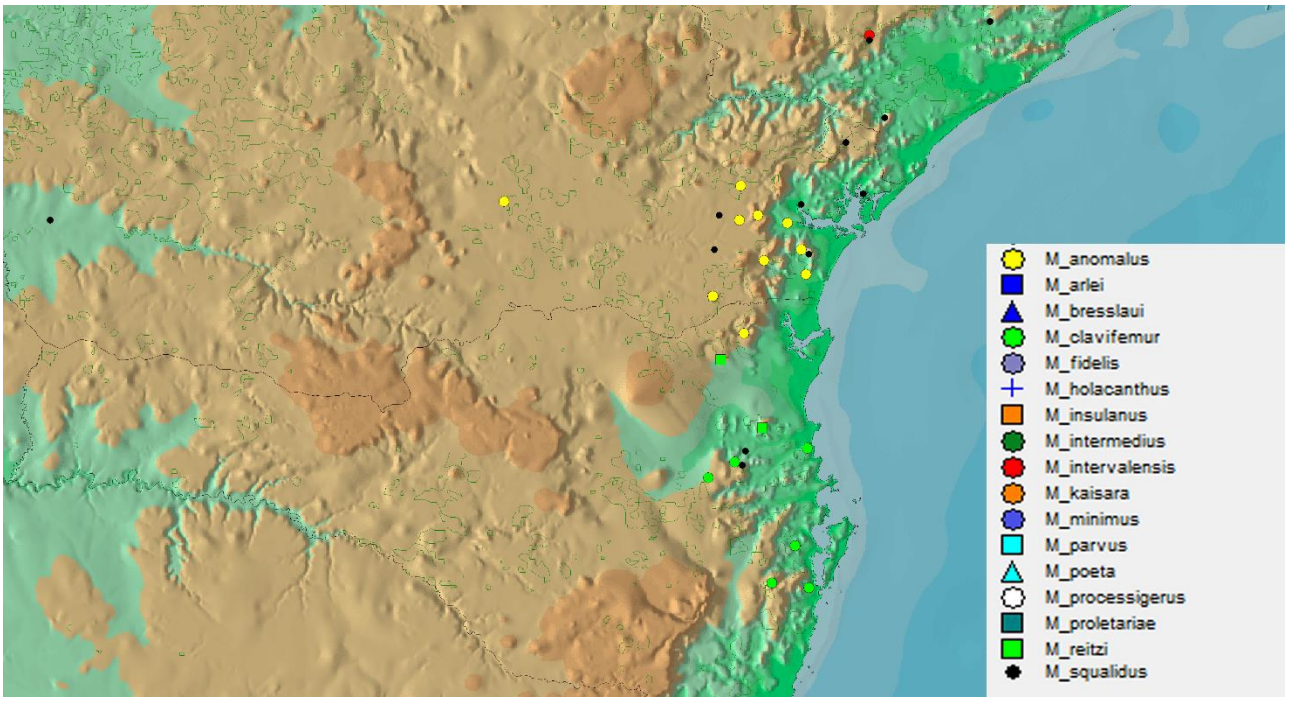

Figure 31: Geographical distribution of *Mischonyx* species from Paraná and Santa Catarina states. Legends are in the right of the figure. The black grid represents the full meridians and parallels.